PROBING THE MEMBRANE TOPOLOGY OF A DIACYLGLYCEROL ACYLTRANSFERASE TYPE I FROM *BRASSICA NAPUS*

NORA AFSANEH FOROUD
B.Sc. Biochemistry Co-op, University of Lethbridge, 2002

A Thesis
Submitted to the School of Graduate Studies
of the University of Lethbridge
in Partial Fulfilment of the
Requirements for the Degree

[MASTER OF SCIENCE]

Department of Chemistry and Biochemistry
University of Lethbridge
LETHBRIDGE, ALBERTA, CANADA

ABSTRACT

Diacylglycerol acyltransferase (DGAT), an integral membrane protein of the endoplasmic reticulum, catalyzes the final step in the *sn*-glycerol-3-phosphate pathway leading to triacylglycerol. Although DGAT has been cloned from a variety of species, including the major oilseed crop of Canada, canola (*Brassica napus)*, little is known about the structure/function of the enzyme. BnDGAT1 is the major isoform of type I DGAT (DGAT-I) in microspore-derived cell suspension cultures of *B. napus* L. cv Jet Neuf, with the possible existence of a truncated form of BnDGAT1 known as BnDGAT2. In order to gain some insight into the topology of the enzyme, type I DGAT from *B. napus* was investigated using two approaches: (1) *in vitro* translation in the presence of microsomes and (2) immunochemical analyses of microsomes isolated from cell suspension cultures, both in combination with proteolytic mapping. Difficulties were encountered with the *in vitro* translation approach, possibly due to proper incorporation of the polypeptide into microsomal vesicles. Two cytosolic regions were identified in BnDGAT1, and one cytosolic region in putative BnDGAT2, using the immunochemical approach, thus providing some insight into the topology of *B. napus* DGAT-I. The results here support and nine and eight membrane-spanning topology for BnDGAT1 and BnDGAT2, respectively.

RÉSUMÉ

La diacylglycérol acyltransférase (DGAT), une protéine membranaire intégrée dans le réticulum endoplasmique, catalyse la réaction finale de la production du triacylglycérol via la voie de synthèse du *sn*-glycerol-3-phosphate. Peu d'information est disponible au sujet de la structure et de la fonctionnalité de la DGAT. Le clonage de la DGAT a été rapporté chez plusieurs espèces différentes incluant le canola (*Brassica napus*), une espèce oléagineuse ayant un grand impact économique au Canada. La BnDGAT1, identifiée comme l'isoforme majeur de la DGAT de type I (DGAT-I), a été isolée d'une culture cellulaire en suspension de *B. napus* L. cv Jet Neuf. Un isoforme secondaire de la DGAT-I, BnDGAT2, a aussi été identifié et semble être un gène tronqué de la BnDGAT1. Deux approches complémentaires ont été utilisées avec une méthode de cartographie avec une protéase afin d'obtenir des informations topologiques de la DGAT-I de *B. napus*. La première approche était la traduction *in vitro* en présence de microsomes du gène de la DGAT et la seconde reposait sur une analyse immunochimique des microsomes isolés de la culture cellulaire en suspension. L'approche utilisant la traduction *in vitro* de la DGAT n'a pas été concluante, probablement dû à une insertion défective des polypeptides dans les microsomes. Deux régions cytoplasmiques pour la BnDGAT1 et une région cytoplasmique pour la BnDGAT2 ont été identifiées en utilisant l'approche immunochimique. Les résultats présentés supportent des topologies avec, respectivement, neuf et huit régions transmembranaires pour la BnDGAT1 et la BnDGAT2.

ACKNOWLEDGMENTS

I have many individuals to thank for their support and feedback throughout my masters program.

A special thanks to my supervisors Dr. Randall Weselake and André Laroche for your guidance and direction. Thank you for both your patience and support. I have learned a great deal from each of you and have been lucky to have the two of you for my supervisors.

I would like to thank my thesis supervisory committee members Dr. Steven Mosimann and Dr. Olga Kovalchuck for your feedback and advice. You have both served as excellent resources.

Thank you to the various labs that I have had the pleasure to work in during my thesis work. *The Weselake Research Group (University of Lethbridge)*: Chris Kazala, Tara Furukawa-Stoffer, Tracy, Brent, Shaun, Kris, Ben, John, Cory and Mike. Those of you who let me join in on the hacky-sack games. Chris for talking and troubleshooting. Cory Chesla for your friendship and 'after-hour' discussions. Mike Baker for your friendship and climbing—and more often discussions of climbing! *The Laroche Research Group (Lethbridge Research Center)*: Denise and Carolyn for showing me the locations of forgotten items in the lab. Michele Frick, you have been a fabulous resource—you are my walking encyclopedia! *The Moloney Research Group (University of Calgary)*: Dr. Maurice Moloney, for welcoming me into your lab for a summer. Nancy and Sandy for showing me around. Joenelle Alcantara for your creative suggestions and friendship. Erin Brown for your friendship. *The Thomas Research Group (University of Lethbridge)*: Dr. Jim Thomas for allowing me to use your lab space to finish up my thesis work. Cassandra Lang for essential coffee breaks and for you friendship.

Several people who were not directly involved in my research served as great resources in my study. Dr. Brent Sellinger from the University of Lethbridge, you have been an incredible resource, your feedback and suggestions have been greatly appreciated. Dr. Ben Abell from Manchester, thank you for your correspondence and feedback, you have been very helpful in the early troubleshooting of my research. Dr. Jeanne Vance from the University of Alberta, thank you for your correspondence. Dr. Thomas McKeon from the United States Department of Agriculture, for your suggestion that saved the day and your subsequent commitment to read this document!

A special thanks to Kathleen Schrage, the University of Lethbridge Graduate Studies Coordinator, for your support throughout my degree, and for your open door policy. Thank you to the School of Graduate Studies for financial support through teacher assistant positions. Thank you to the Natural Sciences and Engineering Research Council of Canada for supporting this research through a Discovery Grant to Dr. Randall Weselake.

I would also like to thank a couple of people for their influence during my undergraduate studies. Dr. Jim Thomas and Dr. Stewart Rood from the University of Lethbridge, you may not be aware of this, but your feedback during my coursework helped me through some difficult times. I thank you for this now, because I would not be completing my thesis today if it were not for each of you.

I would like to thank my friends from the University of Lethbridge. Michelle Duke for the lunch and coffee breaks, for listening and understanding. Dr. Michael Gerken for the pork, the good food, the tea (we will have to get your office a kettle) and wine. Lori Packarynuk for always laughing and listening (and the wine). Peter Dibble for your help with my electrons (and the wine).

I would like to thank my dearest friends, those whom I have grown with throughout this degree, Mandy Bondaruk and Keri Lotion (Colwell), for your love and friendship that has become so dear to me that I don't remember a time without it. ☼ Chris Huisman for your love and friendship and for always being a confidant. ☼ Deonne Parker for your love and friendship, always, and for the colour of the stars. ☼ The *dudes*, David Shaw and Aurora Fawlkner-Kilam, for your love and friendship and laughter—for always understanding. Your connection is one I cannot do without. ☼ My fabulous second family the ever endearing Glovbees: Leslie, Rick, Elysia and Meghan, for your love and friendship.

My family for the everlasting love, support and patience ◦ My dear parents, Dr. Nader Foroud and Zahra Foroud, for being the best mentors and friends, for your example and food, for your love, support and patience. For guiding me to where I have come and where I am going. You have taught me well. Your love is so grand ◦ My 'baby' sister, Rebecca Foroud for your sweetness and kindness and precious love, for your growth and your ever-growing friendship ◦ My older but wiser sister Afra Foroud for you have taught me so much and loved me so much, and I would not be this person I am, if not for your friendship ◦ My husband, Dr. Paul Hazendonk, for your ever-growing love, patience and support ◦ Your advice is tremendous ◦ Your patience is my savior ◦ Your love is my life ◦

TABLE OF CONTENTS

LIST OF FIGURES

LIST OF TABLES

LIST OF ABBREVIATIONS

A. thaliana	*Arabidopsis thaliana*
ACAT	acyl-CoA:cholesterol acyltransferase
ACC	acetyl-coenzyme A carboxylase
ACP	acyl-carrier protein
ALA	α-linolenic acid
B. campestris	*Brassica campestris*
B. napus	*Brassica napus*
B. rapa	*Brassica rapa*
BC	biotin carboxylase
BCCP	biotin carboxylase carrier protein
BKR	β-ketoacyl-acyl carrier protein reductase
BnDGAT	*Brassica napus* diacylglycerol acyltransferase
C. tincotrius	*Carthamus tincotrius*
cDNA	complementary deoxyribonucleic acid
CDP	cytidine diphosphate
CMP	cytidine monophosphate
CoA	coenzyme A
CPT	cytidine diphosphate-choline:1,2-diacylglycerol cholinephosphotransferase
CT	carboxyltransferase
DGAT	diacylglycerol acyltransferase
DGDG	digalactosyldiacylglycerol
DGTA	diacylglycerol:diacylglycerol transacylase

DHA	docosahexaenoic acid
DNA	deoxyribonucleic acid
dNTP	deoxynucleoside triphosphate
DTT	dithiothreitol
E. coli	*Escherichia coli*
EDTA	ethylenediaminetetraacetic acid
EGTA	ethylenebis(oxyethylenenitrilo)tetraacetic acid
ENR	enoyl-acyl carrier protein reductase
EPA	eicosapentaenoic acid
ER	endoplasmic reticulum
Eq	equivalent
FA	fatty acids
FabA	β-hydroxyacyl-acyl carrier protein dehydratase
FabZ	β-hydroxyacyl-acyl carrier protein dehydratase
FAD	fatty acid desaturase
FAS	fatty acid synthase
G3P	glycerol-3-phosphate
GFP	green fluorescent protein
GPAT	glycerolphosphate acyltransferase
HEAR	high erucic acid rapeseed
HDL	high-density lipoproteins
KAS	β-ketoacyl-ACP synthase
L. alba alba	*Limnanthes alba alba*

LA	linoleic acid
LEAR	low erucic acid rapeseed
LDL	low-density lipoproteins
LPA	lysophosphatidic acid
LPAAT	lysophosphatidyl acyltransferase
LPC	lysophosphatidylcholine
LPCAT	lysophosphatidylcholine acyltransferase
M. ramanniana	*Mortierella ramanniana*
MAG	monoacylglycerol
MCAT	malonyl-CoA:ACP transacylase
MD	microspore-derived
MGD	monogalactosyldiacylglycerol
mRNA	messenger ribonucleic acid
mtGPAT	mitochondrial glycerolphosphate acyltransferase
MUFA	monounsaturated fatty acid
PAGE	polyacrylamide gel electrophoresis
PMSF	phenylmethylsulfonyl fluoride
RcDGAT	*Ricinus communis* DGAT
RNC	ribosome nascent chain complex
P. pastoris	*Pichia pastoris*
PA	phosphatidic acid
PC	phosphatidylcholine
PDAT	phospholipid:diacylglycerol acyltransferase

PE	phosphatidylethanolamine
PG	phosphatidylglycerol
PI	phosphatidylinositol
PUFA	polyunsaturated fatty acid
R. communis	*Ricinus communis*
RNA	ribonucleic acid
SDS	sodium-dodecyl sulfate
SFA	saturated fatty acid
SL	sulfoquinovosyldiacylglycerol (sulfolipid)
SLO	streptolysin O
SR	signal recognition particle receptor
SRP	signal recognition particle
TAG	triacylglycerol
TEA	triethanolamine
UFA	unsaturated fatty acid

1. INTRODUCTION

Acyl-coenzyme A (-CoA):diacylglycerol acyltransferase (DGAT) is an integral membrane protein that catalyzes the final acylation step in triacylglycerol (TAG) synthesis via the Kennedy pathway (Kennedy, 1961; Weselake, 2002; 2005). DGAT is the only enzyme in the Kennedy pathway that is unique to TAG synthesis (Nykiforuk et al., 2002) and its activity may limit the flow of carbon into TAG (Stals et al., 1994). In animals this enzyme may be involved in regulating TAG storage in adipose tissues and metabolic activity (Chen and Farese Jr., 2000). In recent studies, mice lacking DGAT activity, with or without increased fat intake, have shown an increase in energy use and metabolic activity, and a decrease in total body fat (Chen and Farese, Jr., 2000). In plants, DGAT gene expression has been shown to be correlated with TAG accumulation (Katavic et al., 1995; Bouvier-Navé, 2000; Giannoulia et al., 2000; Jako et al., 2001; He et al., 2004a).

Acyl-CoA dependent DGAT activity has primarily been characterized at the endoplasmic reticulum (microsomal DGAT), although plastidal forms have also been identified (Martin and Wilson, 1983; 1984; Kaup et al., 2002). There are two known microsomal DGAT gene families: DGAT-I and DGAT-II. DGAT-I shares high sequence identity to the acyl-CoA:cholesterol acyltransferase (ACAT) gene family, and DGAT-II has no apparent homology to DGAT-I or to ACAT (Cases et al., 2001; Lardizabal et al., 2001). DGAT-I has been purified to apparent homogeneity in *Mortierella ramanniana* (Kamisaka et al., 1997). The first cloning of *DGAT-I* was reported in humans and mice in 1998 (Cases et al.), and has since been cloned from several plant (Bouvier-Navé et al.,

2000; Nykiforuk et al., 2002; He et al., 2004b) and animal tissues (Cases et al., 1998; Waterman et al., 2002). The first cloning and purification of *DGAT-II* was reported in *M. ramanniana* in 2001 (Lardizabal et al.). Partial purification of DGAT from mammalian (Polokoff and Bell, 1980; Andersson et al., 1994) and plant microsomes (Kwanyuen and Wilson, 1986) have also been reported. Two cDNAs encoding type I DGATs, *BnDGAT1* and *BnDGAT2*, have been isolated and characterized from *Brassica napus* L. cv Jet Neuf microspore derived (MD) cell suspension cultures (Nykiforuk et al., 1999a; 1999b; 2002). *BnDGAT1* and *BnDGAT2* encode deduced polypeptide of 503 and 341 amino acids with predicted molecular masses of 56.9 and 39.5 kD, respectively. BnDGAT2 is essentially a truncated version of BnDGAT1, where the first 162 residues of the N-terminus have been deleted.

Limited structural information is available for DGAT-I due to the difficulties associated with the purification of microsomal proteins. Cheng et al. (2001) have recently demonstrated that human DGAT is a tetramer formed via self-association at the N-terminus. Weselake et al. (2005; in preparation) have also demonstrated that the N-terminal portion of BnDGAT1 (residues 1-116) may also self-associate to form a tetramer. Membrane topology predictions of BnDGAT1 have identified a total of 10 putative membrane-spanning helices (TM1 through TM10), with the N-terminus in the cytosol. Two topology scenarios for BnDGAT1 are presented here: scenario 1a and 1b. In scenario 1a, TM1 to TM10 are all membrane-spanning helices, placing the C-terminus in the cytosol. In scenario 1b, TM1-TM4 and TM6-TM10 are membrane-spanning helices and TM5 is not, placing the C-terminus in the lumen of the ER. A serine residue conserved among all type I DGATs and all ACATs (Nykiforuk et al., 2002), and shown

to be essential for ACAT activity (Jako et al., 2001), is found in the cytosol in both topology scenarios. BnDGAT2 shares 96 % sequence identity with BnDGAT1. With the exception of TM1, which is found within the first 162 residues of BnDGAT1 that are absent in BnDGAT2, the same predicted spanning-membrane domains are identified in BnDGAT2. Three topology scenarios for BnDGAT2 are presented here: scenario 2a, 2b and 2c. In scenario 2a, TM2-TM10 are all membrane-spanning with the N-terminus portion corresponding to the membrane-spanning TM2 region, placing both the conserved serine residue and the C-terminus in the lumen of the ER. In scenario 2b, TM3-TM10 are membrane-spanning, where the N- and C-termini and the conserved serine residue all in the cytosol. In scenario 2c, TM3-TM4, and TM6-TM10 are membrane-spanning, where the N-terminus and the conserved serine residue are in the cytosol, placing the C-terminus in the lumen of the ER.

Two approaches are used in the current study to probe the membrane topology of BnDGAT: a molecular genetics and an immunochemical approach. In the molecular genetic approach, four clones encoding BnDGAT1 and truncations of BnDGAT1 were generated for *in vitro* transcription/translation studies to be followed by protease mapping. *In vitro* translation reactions were performed with either a rabbit reticulocyte lysate or wheat germ extract translation system in the presence of *B. napus* or rat liver microsomes prepared here, or in the presence of purchased canine pancreatic microsomes (Promega, Technical Manual No. 231). Translation reaction products were used in a protease mapping study. Immunodetection studies, using two polyclonal antibodies raised against two different regions in BnDGAT1, were performed with a protease protection assay of *B. napus* MD cell suspension culture microsome preparations. In

addition to providing evidence in support of a topology scenario of BnDGAT1 presented in this report, immunodetection studies have also lead to the putative identification of BnDGAT2 expression at the level of the protein. Previously, BnDGAT2 was only identified in the mRNA fraction from the cell suspension cultures, and while expression of the corresponding cDNA in yeast cells yielded active protein, no studies have previously been done to identify its expression in the cell suspension cultures. The results presented here may be the first evidence of BnDGAT2 putative expression at the protein level. The identification of BnDGAT2 expression and subsequent protease mapping of this truncated form of BnDGAT1 has provided some insight into the topology of this isoform.

2. LITERATURE REVIEW

2.1 Properties of Vegetable Oils

Triacylglycerol (TAG) is the major component of vegetable oils and dietary fat. TAGs are composed of saturated fatty acids (SFAs) and unsaturated fatty acids (UFAs). Other dietary lipids include phospholipids (the primary component of cellular membranes), and sterols (including cholesterol) found in animal fats. Health Canada recommends that Canadians minimize their consumption of SFAs and cholesterol (http://www.hc-sc.gc.ca). High intake of SFAs and animal fats have been associated with 80% of cancers (Breuer-Katchinski et al., 2001; Zock, 2001), and have been implicated in heart diseases (Bemelmans et al., 2000). The levels of lipoproteins in the blood are often indicators of the risk levels in cardiovascular disease. Low-density lipoproteins (LDL) are associated with an increased risk factor, while high-density lipoproteins (HDL) are more beneficial (Águila et al., 2002). Ingestion of omega-3 fatty acids (FAs), including α-linolenic acid (ALA), eicosapentaenoic acid (EPA), and docosahexanoic acid (DHA), have been shown to reduce the levels of plasma LDL (Águila et al., 2002). Nonhydrogenated vegetable oils high in UFAs, such as canola, corn, olive and soybean oil have also been shown to reduce LDL production (Nicolosi and Rogers, 1997).

A comparison of the fatty acid contents of a variety of dietary fats is presented in Figure 2.1 (Canola Council of Canada, www.canola-council.org; Flax Council of Canada, www.flaxcouncil.ca). Canola oil is one of the healthier vegetable oils available, with a low SFA content (7 % of the total acyl lipid content) and relatively high ALA content (11 %). Flax seed oil is also low in SFA content (9 %) and particularly high in ALA (57 %).

Figure 2.1 Fatty acid profiles of various dietary fats. The saturated fatty acid (SFA), polyunsaturated fatty acid (PUFA) and monounsaturated fatty acid (MUFA) contents of the major dietary fats normalized to 100 % and rounded to the unit. The PUFA component is divided here into the linoleic acid (LA) and α-linolenic acid (ALA) contents. ALA is present in trace amounts in dietary fats marked with two asterisks. Dietary fats marked with one asterisks (lard, beef tallow and butterfat) have cholesterol components of 12, 14 and 33 mg per tablespoon, respectively. This data was obtained from the Canola Council of Canada (www.canola-council.org) and from the Flax Council of Canada (www.flaxcouncil.ca).

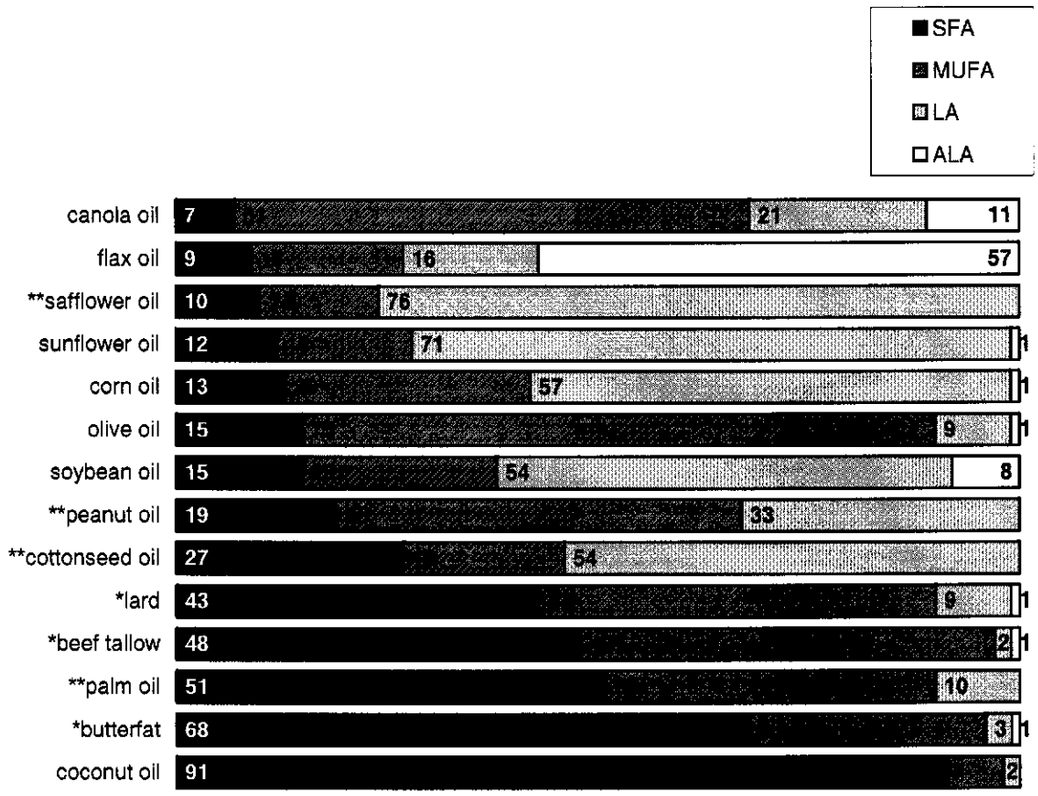
SFA
MUFA
LA
ALA
canola oil 7 21 11
flax oil 9 16 57
**safflower oil 10 76
sunflower oil 12 71 1
corn oil 13 57 1
olive oil 15 9 1
soybean oil 15 54 8
**peanut oil 19 33
**cottonseed oil 27 54
*lard 43 9 1
*beef tallow 48 2 1
**palm oil 51 10
*butterfat 68 3 1
coconut oil 91 2

After canola oil, soybean oil has the next highest ALA content (8 %) of the total acyl lipid, while the remaining sources of the major dietary fats presented in Figure 2.1 have only 1% or less ALA. Olive oil has the highest MUFA content (75 %), but also has higher SFA content (15 %). Canola is the next highest for total monounsaturated fatty acid (MUFA) content (61 %). Animal sources of dietary fats tend to have higher SFA contents in addition to a cholesterol component, while the sterol content in vegetable oils are negligible.

Canola oil is a popular vegetable oil grown primarily in Western Canada, as well as various regions in North America, Australia, Europe and Asia (Canola Council of Canada). Canola oil is extracted from the seeds of *Brassica napus* and *Brassica rapa* (formerly *Brassica campestris*). The seed oil is used as a dietary product in salad and cooking oils, and in margarine, shortening, mayonnaise and other food products. The oil is also used in the industry in cosmetics, industrial lubricants, and biodiesels (Canola Council of Canada). The meal remaining after seed oil extraction is used in feed for cattle, swine, poultry and other farm animals (Canola Council of Canada).

Canola oil is derived from rapeseed oil, a crop grown in Asia and Europe for thousands of years. The common name for *B. rapa* is Polish rapeseed, and was established in Canada by a Polish farmer in 1936. Another variety, *B. napus*, or Argentine rapeseed, was introduced in Canada in the 1940s (Canola Council of Canada). In early years, *B. napus* dominates the canola industry, but greater yields from *B. rapa* cultivation has led to a moving trend towards the cultivation of *B. rapa* in the last ten years.

Traditionally, rapeseed oils are high in erucic acid (ranging from 28 to 40 % in *B.*

napus; Stefansson et al., 1961) and high in glucosinolates (80 μM g^{-1} in 1975; Dupont et al., 1989). Glucosinolates are a group of thioglucosides that reduce the quality of feed due to toxicity levels (Jezek et al., 1999). Erucic acid is a long chain FA that has been associated with smooth muscle lesions (Bodak and Hatt, 1975; Engfeldt and Brunius, 1975a; 1975b; Knauf and Facciotti, 1995). The seed oil of high erucic acid rapeseed (HEAR) contains 25-50% erucic acid (Dupont et al., 1989). In 1961, low erucic acid rapeseed (LEAR) varieties were identified in Canada, with only 5% erucic acid in the seed oil (Stefansson et al., 1961; Dupont et al., 1989). Selective breeding of LEAR led to the development of canola in 1974 (Dupont et al., 1989). Today, canola oil, by definition, is guaranteed to contain less than 2% erucic acid, and the solid component of the seed is guaranteed to contain less than 30 μmol total glucosinolate per gram of air-dry, oil-free solids (Canola Council of Canada). Every year, 4-5 million hectares of canola is cultivated in Canada, bringing 2.5 billion dollars at Canada's Farm Gate (Canola Council of Canada). Increasing our understanding of how seed oil is produced may allow us to develop strategies for increasing or modifying seed oil content. As much as a 1% increase in the seed oil content of canola could mean an additional $35 million to the canola oil extraction and processing industry in Canada (Canola Council of Canada). Although the seed oil content of canola has increased through selective breeding, it may be possible to further enhance the seed oil content through genetic engineering (Jako et al., 2001).

2.2 Lipid Biosynthesis in Plants

Lipids are the fundamental components of cellular membranes and they are the major

form of energy store (Harwood, 1996). Some lipids have metabolic functions including cellular signaling (Harwood, 1996; Martelli et al., 2004). Lipids also form the waxy surface layer of plant tissues, providing these tissues with a waterproof barrier and protection against environmental stresses (Post-Beittenmiller, 1996). FAs, hydrocarbon chains with a carboxylate group at one end, are the simplest form of lipids. There are different types of FAs differentiated by both the length of the hydrocarbon chain and by the number and location of double bonds. SFAs are saturated with hydrogen and therefore have no double bonds. UFAs can be monounsaturated (MUFA) with only one double bond, or polyunsaturated (PUFA) with two or more double bonds. The general structure of a few FAs is presented in Figure 2.2A, and a list of FA names, abbreviations and chain lengths is presented in Table 2.1.

Glycerolipids, the primary form of plant lipids, are composed of a glycerol molecule with FA groups esterified to the three carbon stereochemical positions of the glycerol backbone (Figure 2.2B; Frentzen, 1993). There are two major forms of glycerolipids. The first of these are the polar membrane lipids: glycodiacylglycerols found in prokaryotic membranes and in the plastidal membranes of plant cells, and phosphodiacylglycerols found in extraplastidal membranes of plant cells. The structures of some of the major glycodiacylglycerols and phosphodiacylglycerols found in plant membranes are presented in Figures 2.2C and 2.2D, respectively. All membrane lipids have FA groups at the *sn*-1 and *sn*-2 positions, and a polar head group at the *sn*-3 position (Frentzen, 1993). The second form of glycerolipids is the non-polar acylglycerols, including TAGs, which are storage lipids. TAG molecules have a FA group esterified at each of the three stereochemical positions of the glycerol backbone (Figure 2.2B,

Figure 2.2 The chemical structure of lipids. ***A.*** Fatty acids (FAs) are composed of hydrocarbon chains with a carboxylic acid at C_1. Stearic acid is an 18-carbon chain saturated with hydrogen. Biological unsaturated fatty acids (UFAs) are primarily found in the *cis* configuration. Oleic acid is a monounsaturated 18-carbon FA with a *cis* double bond introduced at C_9. The two polyunsaturated 18-carbon FAs presented here, linoleic and linolenic acid, have *cis* double bonds introduced at the C_9 and C_{12}. Linoleic acid has a third a *cis* double bond at C_{15}. ***B.*** Glycerolipids are composed of a glycerol (left) molecule with FA groups esterified to the glycerol backbone at one or more of the stereochemical positions (*sn*-1, *sn*-2 and *sn*-3). Triacylglycerol (TAG; right) has three FAs esterified at all three positions. Diacylglycerol have FAs at the *sn*-1, and *sn*-2 positions, and monoacylglycerol have one FA at the *sn*-1 position (not shown). ***C, D.*** Membrane lipids have FAs esterified at the *sn*-1, and *sn*-2 positions and a polar head group at *sn*-3. There are two types of membrane lipids, glycodiacylglycerols (***C***) found in plastid membranes, and phosphodiacylglycerols (***D***) found in extraplastidal membranes. Glycodiacylgycerols include monogalactosyldiacylglycerol (MGD), digalactosyldiacylglycerol (DGDG), and sulfoquinovosyldiacylglycerol (sulfolipid; SL). Phosphodiacylglycerols include phosphatidylglycerol (PG), phosphatidylcholine (PC), phosphatidylethanolamine (PE) and phosphatidylinositol (PI). FA (***A***) and glycerolipid structures (***C*** and ***D***) were adapted from Browse (1998), and TAG structure (***B***) was adapted from Mathews and van Holde (1996).

A.

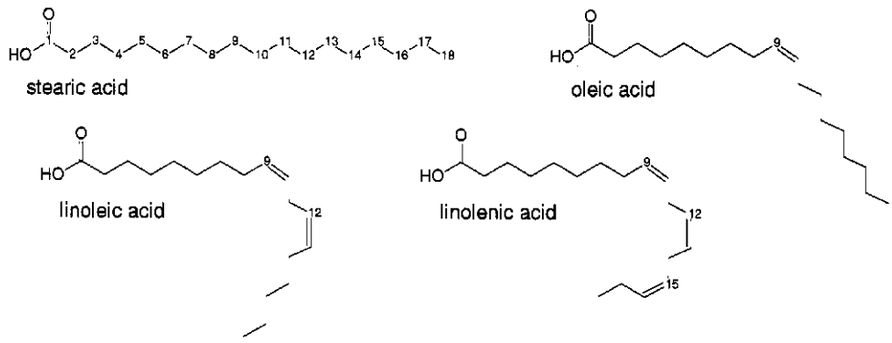
stearic acid
oleic acid
linoleic acid
linolenic acid

B.

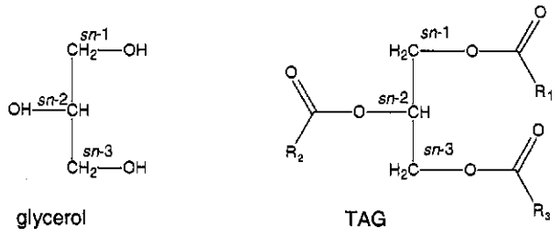
sn-1
sn-2
sn-3
glycerol
TAG

C.

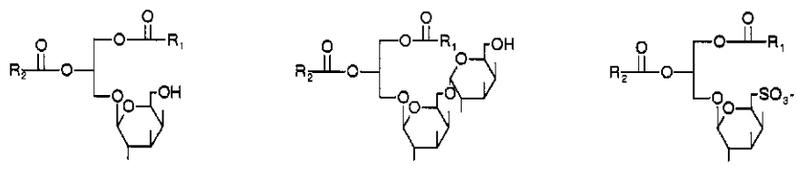
MGD
DGDG
SL

D.

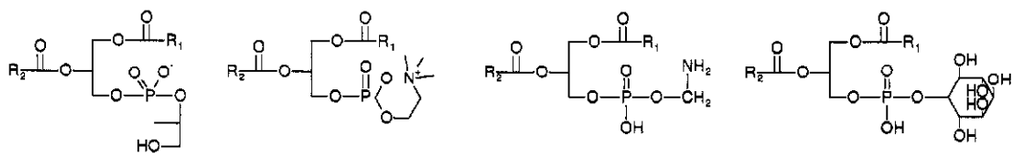
PG
PC
PE
PI

Table 2.1 Common fatty acids. The common names and abbreviations of some of the major fatty acids are presented here. The number before the colon represents the number of carbons and the number after the colon represents the number of double bonds. The superscript numbers following the delta sign indicate the carbon-number(s) where the double bond is introduced. For example, $18{:}1^{\Delta 9,12}$ has one double bond between carbon-9 and carbon-10, and a second double bond between carbon-12 and carbon-13. Sometimes a lower case *c* or *t* are written prior to the delta sign, indicated whether or not the double bonds are in *cis* or *trans* configuration, respectively. Most unsaturated fatty acids have double bonds in the *cis* configuration, and often the *c* is omitted in the abbreviated name.

Common name	Abbreviation
Capric acid	10:0
Lauric acid	12:0
Myristic acid	14:0
Palmitic acid	16:0
Palmitoleic acid	$16{:}1^{\Delta 9}$
Stearic acid	18:0
Oleic acid	$18{:}1^{\Delta 9}$
Linoleic acid	$18{:}2^{\Delta 9,12}$
Linolenic acid	$18{:}3^{\Delta 9,12,15}$
Arachidic acid	20:0
Arachidonic acid	$20{:}4^{\Delta 5,8,11,14}$
Behenic acid	22:0
Erucic acid	$22{:}1^{\Delta 11}$
Lignoceric acid	24:0
Cerotic acid	26:0

Frentzen, 1993). Sections 2.3 and 2.4 provide a review of FA biosynthesis and TAG bioassembly in plants, respectively.

2.3 Fatty Acid Biosynthesis

FA biosynthesis occurs in the plastid of plant cells through the activity of several highly conserved dissociable enzymes that are collectively called type II fatty acid synthase (FAS II). FAS II is often referred to as the prokaryotic FA biosynthetic machinery, since FAS II is also found in bacteria. FA biosynthesis in animals and yeast occurs via the activity of type I FA synthase (FAS I). FAS I is composed of two large multifunctional subunits of a single enzyme. A diagram of FAS II biosynthesis in the plastid is presented in Figure 2.3, and a summary of the FAS II enzymes is presented in Table 2.2.

The first committed step, in fatty acid synthesis is catalyzed by acetyl-coenzyme A (-CoA) carboxylase (ACC; Davies et al., 2000). The level of ACC activity in developing seeds may have a substantial effect on the amount of FA formed (Davies et al., 2000). ACC catalyzes the formation of malonyl-CoA in a two-step reaction involving three functional domains of multisubunit ACC (Alberts and Vagelos, 1968; Alberts et al., 1969): (*i*) biotin carboxylase (BC), (*ii*) biotin carboxylase carrier protein (BCCP), and (*iii*) carboxyltransferase (CT). In the first step of the reaction, BC catalyzes the energy dependent carboxylation of the biotin component of BCCP, using bicarbonate as a substrate (for a review see Cronan Jr. and Waldrop, 2002). In the second step, CT catalyzes the carboxyl transfer from BCCP to acetyl-CoA, forming malonyl-CoA. The malonyl group is then transferred from the CoA molecule to an acyl-carrier protein (ACP) in a reaction catalyzed by malonyl-CoA:ACP transacylase (MCAT; Ruch and

Figure 2.3 Plastidal fatty acid biosynthesis. Fatty acid (FA) biosynthesis occurs in the plastid (gray background) of plant cells. The enzymes of FA synthesis (acetyl-coenzyme A (-CoA) carboxylase (ACC), malonyl-CoA:ACP transacylase(MCAT), β-ketoacyl-ACP synthase (KAS), β-ketoacyl-acyl carrier protein (-ACP) reductase (BKR), β-hydroxyacyl-ACP dehydratase (FabA and FabZ) and enoyl-ACP reductase (ENR)) are presented in bold font.

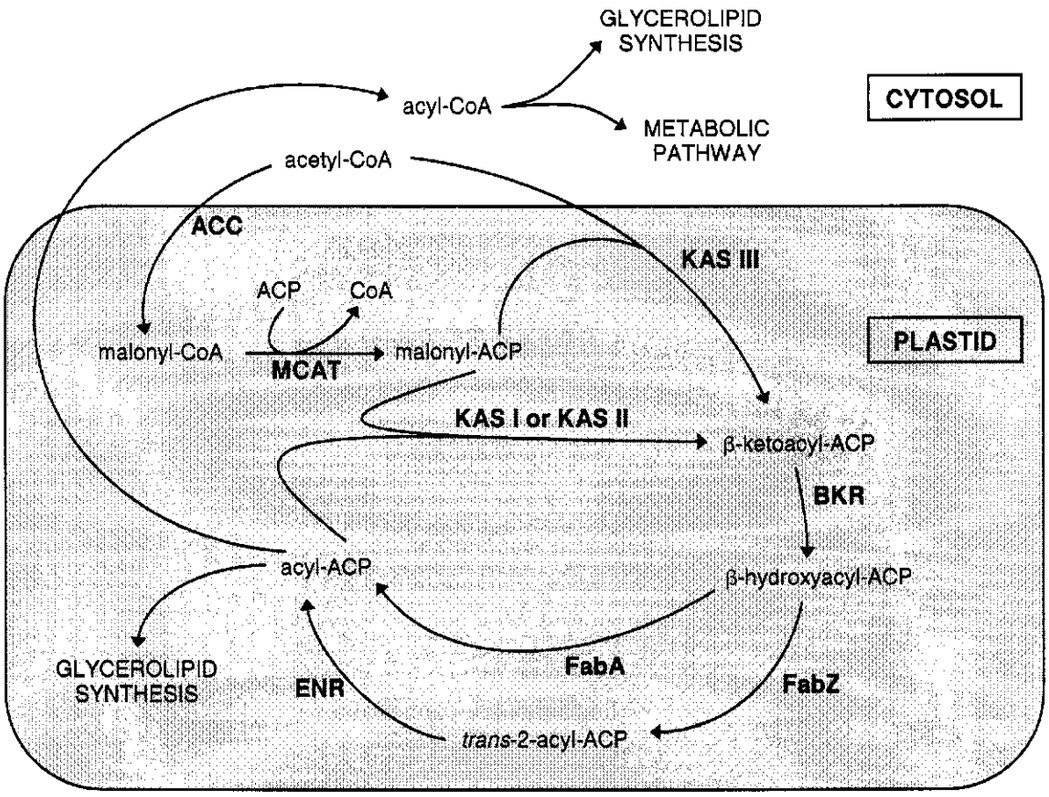
GLYCEROLIPID
SYNTHESIS
CYTOSOL
acyl-CoA
METABOLIC
PATHWAY
acetyl-CoA
ACC
KAS III
ACP
CoA
malonyl-CoA
MCAT
malonyl-ACP
PLASTID
KAS I or KAS II
β-ketoacyl-ACP
BKR
acyl-ACP
β-hydroxyacyl-ACP
GLYCEROLIPID
SYNTHESIS
ENR
FabA
FabZ
trans-2-acyl-ACP

Table 2.2 The enzymes of fatty acid synthase type II.

Enzyme	Acronym	EC	Co-factor	Substrates	Products
Acetyl-CoA Carboxylase	ACC	6.4.1.2	ATP, Mg^{2+}	acetyl-CoA, HCO^{3-}	malonyl-CoA
biotin carboxylase carrier protein	BCCP				
biotin carboxylase	BC				
carboxyltransferase	α-CT				
carboxyltransferase	β-CT				
Malonyl-CoA:ACP Transacylase	MCAT	2.3.1.39		malonyl-CoA, ACP	malonyl-ACP, CoA
β-Ketoacyl-ACP Synthase	KAS III	2.3.1.41		malonyl-ACP, acetyl-CoA	β-ketoburyl-ACP
	KAS I			malonyl-ACP, C_2 to C_{14}-acyl-ACP	C_4 to C_{16}-acyl-ACP
	KAS II			malonyl-ACP, C_{14} to C_{16}-acyl-ACP	C_{16} to C_{18}-acyl-ACP
β-Ketoacyl-ACP Reductase	BKR	1.1.1.100	NAD(P)H	β-ketoacyl-ACP	β-hydroxacyl-ACP
β-Hydroxacyl-ACP Dehydratase	FabZ			β-hydroxyacyl-ACP	*trans*-2-acyl-ACPs
	FabA			*trans*-2-acyl-ACPs	*cis*-3-acyl-ACPs
Enoyl-ACP Reductase	ENR		NADH	*trans*-2-acyl-ACPs	acyl-ACPs
			NADPH	*trans*-2-acyl-ACPs	acyl-ACPs
			NADH	*trans*-2-acyl-ACPs	acyl-ACPs

Vagelos, 1973; Simon and Slabas, 1998). Together, malonyl-ACP and acetyl-CoA, enter the first cycle of FA elongation. In the remaining cycles of FA elongation, malonyl-ACP reacts with the C_n acyl-ACP (instead of acetyl-CoA) products of previous FA elongation cycles. FA elongation involves four separate reactions: condensation, reduction, dehydration and a second reduction (for review see Ohlrogge and Browse, 1995; Harwood, 1996). The condensation step is catalyzed by β-ketoacyl-ACP synthase (KAS) to produce β-ketoacyl-ACP. Three major KAS isoforms have been identified. KAS III is involved in the first cycle of elongation (Jackowski and Rock, 1987; Lai and Cronan, 2003), and is the only condensing enzyme that accepts acetyl-CoA substrates in the place of an acyl-ACP. KAS I catalyzes the next set of condensation reactions using short-chain acyl-ACPs up to C_{14}-acyl-ACP (Greenspan et al., 1969). KAS II catalyzes the final set of condensation reactions using C_{14}- to C_{16}-acyl-ACP substrates (D'Agnolo et al., 1975). β-ketoacyl-ACP is then reduced to a β-hydroxyacyl-ACP by β-ketoacyl-ACP reductase (BKR). β-hydroxyacyl-ACP undergoes dehydration, catalyzed by β-hydroxyacyl-ACP dehydratase (FabZ), to produce *trans*-2-acyl-ACP. *trans*-2-acyl-ACP then undergoes the second reduction step, catalyzed by enoyl-ACP reductase, to release a C_{n+2}-acyl-ACP. Together with a malonyl-ACP molecule, C_{n+2}-acyl-ACP re-enters the elongation cycle. Acyl-ACP products of elongation, continue to cycle through elongation until the appropriate acyl-ACP of appropriate chain length is released. The major products of FAS II in most plants are 16:0- and 18:1-ACPs (Ohlrogge and Browse, 1995; Harwood, 1996).

The acyl-ACPs generated in the plastid can either be released into the acyl-ACP pool in the plastid for synthesis of acylglycerols in the plastid, or they can be released into the acyl-CoA pool in the cytosol. FAs released into the cytosol are 'freed' from

ACP via the activity of acyl-ACP hydrolase, and then esterified to a CoA molecule at the plastidal envelope through the activity of an acyl-ACP thioesterase (Johnson et al., 2002). Further elongation of acyl-CoA can occur at the endoplasmic reticulum (Domergue et al., 1999; Puyaubert et al., 2001).

There are several pathways in the synthesis of plant UFAs. In the plastid, UFAs can be generated during FA elongation through the activity of a β-hydroxyacyl-ACP dehydratase isoform (FabA) with the ability to isomerize *trans*-2-decanoyl-ACP to produce *cis*-3-decanoyl-ACP (Brock et al., 1967). Bypassing the last step in the FA elongation cycle, isomerization products immediately move into the next cycle where KAS I initiates UFA elongation. Alternatively, acyl-ACP products can be desaturated through the activity of soluble acyl-ACP desaturases found in the plastid stroma (for review see Harwood, 1996). The most common acyl-ACP desaturase is $^{\Delta 9}$18:0-ACP desaturase, although other desaturases, including a $^{\Delta 9}$16:0-ACP desaturase from *Doxantha unguis-cati* (Cahoon et al., 1998), have been identified in plants with high contents of unusual or uncommon UFAs. Acyl-CoA desaturases, involved in the dehydrogenation of acyl-CoAs in the cytosol, have also been identified in plants (Cahoon et al., 2000). Once FAs have been incorporated into glycerolipids, further desaturation can occur through the activity of membrane bound fatty acid desaturases (FADs), which are localized in the plastid envelope (Kachroo et al., 2003) and in the endoplasmic reticulum (McCartney et al., 2004). FAD2 associated with the ER membrane and FAD6 associated with the plastid envelope are common $^{\Delta 12}$18:1-FADs responsible for the generation of $^{\Delta 9,12}$18:2 (Jin et al., 2001; Martinez-Rivas et al., 2001; Pirtle et al., 2001). Unusual FADs, including FADX from tung which is responsible for the conversion of

Figure 2.4 Type II fatty acid biosynthesis pathways and proposed catalytic or binding mechanisms. Dashed lines indicate hydrogen-bonds, small arrows indicate electron transfer and bold font indicates the name of the molecule the text is associated with. The pathways presented here were adapted from the references indicated for each pathway. ***Reaction 1.*** FA biosynthesis is initiated by the activity of a dissociable enzyme, ACC, with three subunits: BCCP, BC and CT. Biotinylated BCCP has a biotin group covalently linked via the valeric carboxyl group to the N^{ζ} of lysine (reviewed in Jitrapakdee and Wallace, 2003). In the proposed mechanism, the N1' proton of the biotin uerido ring is donated to an active site base of the BC domain. The resulting enolate ion, possibly stabilized by a BC amino acid residue, transfers an electron to the carboxyphosphate intermediate formed through interactions of bicarbonate and γ-phosphate of ATP (Blanchard et al., 1999) and the carboxyl group forms a bond with biotin's N1' (Thoden et al., 2000). Carboxybiotin-BCCP, phosphate and ADP are released (Blanchard et al., 1999). BCCP caries the carboxylated biotin to the active site of CT, and the carboxyl group is transferred to acetyl-CoA, forming malonyl-CoA. ***Reaction 2.*** MCAT is involved in the transfer the malonyl group of malonyl-CoA to ACP forming malonyl-ACP, the major substrate for FA elongation. In a mechanism proposed for *Streptomyces coelicolor* MCAT (Keatinge-Clay et al., 2003), His201 abstracts a proton from Ser97, which attacks the thioester carbonyl of malonyl-CoA, forming a tetrahedral intermediate. The CoA molecule is protonated by His201, and released. ACP reprotonates H201, and a second tetrahedral intermediate is formed between the S97, the malonyl group and ACP. Finally, malonyl-ACP is released through the reprotonation of S97 by H201.

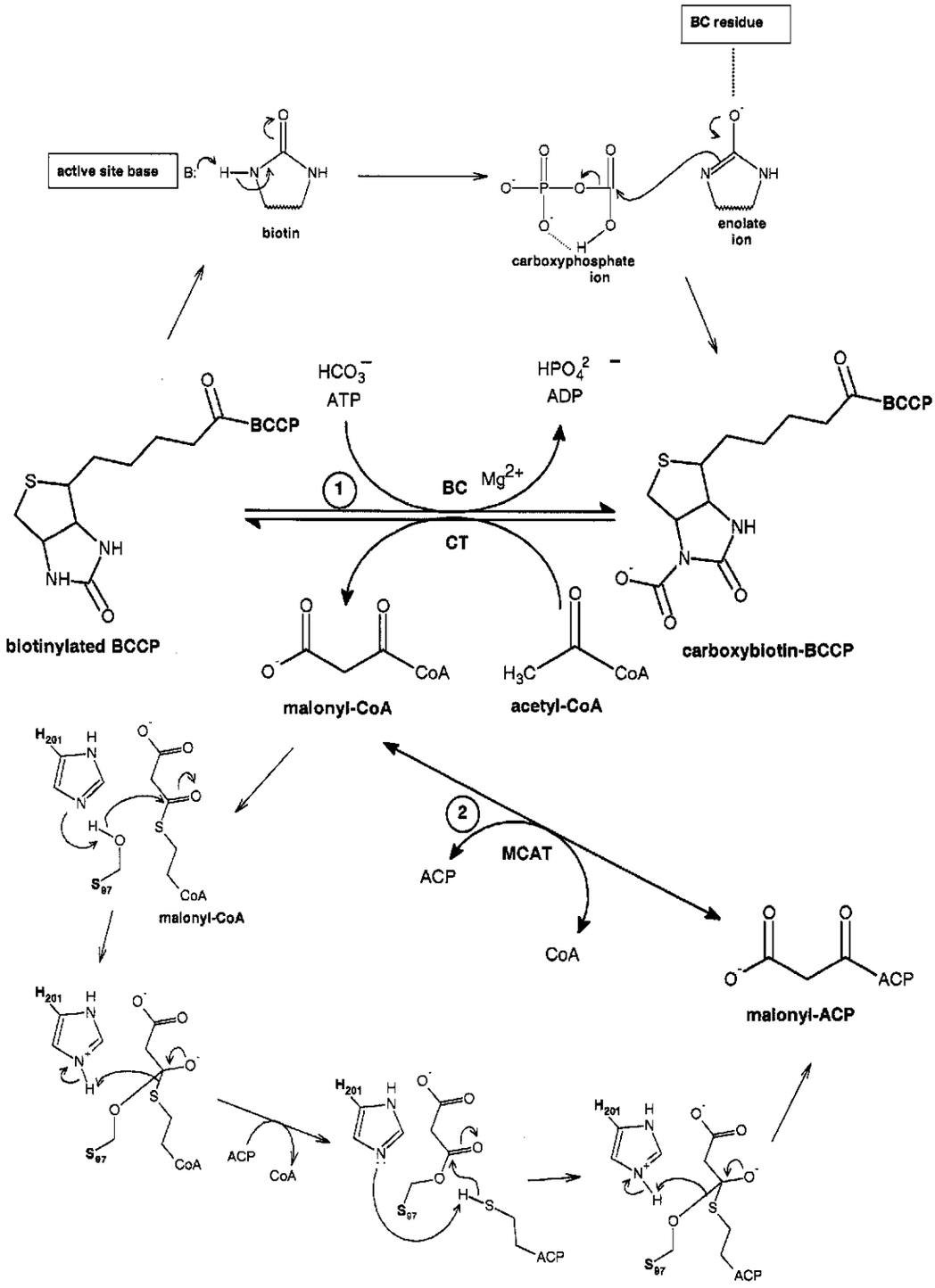
BC residue
active site base
biotin
carboxyphosphate ion
enolate ion
BCCP
ATP
ADP
BC
CT
biotinylated BCCP
carboxybiotin-BCCP
malonyl-CoA
acetyl-CoA
MCAT
ACP
CoA
malonyl-ACP

Figure 2.4 (Continued) ***Reaction 3.*** The first step of elongation is catalyzed by KAS. In the first cycle of elongation the KAS III isoform catalyzes the two-carbon addition of acetyl-CoA using malonyl-ACP as a carbon source. The reaction catalyzed by KAS enzymes is the cysteine-mediated Claisen condensation reaction, which occurs in three steps. In the first step of the proposed mechanism for *Escherichia coli* KAS III, the deprotonated C112 residue attacks the carboxyl group of acetyl-CoA forming an oxyanion hole tetrahedral intermediate stabilized by the backbone amide of Gly306. The CoA molecule is released, leaving a thioester at C112 and acetyl-CoA. In the second step, a malonyl-ACP is decarboxylated. In step three, decarboxylated malonyl-ACP attacks the carbonyl carbon of the thioester formed in step one, and is followed by a condensation reaction releasing β-ketoburyl-ACP (Qiu et al., 1999). The remaining cycles of elongation are initiated by the remaining KAS isoforms, KAS I, II and IV. The reaction mechanism of these isoforms is likely similar to the KAS III reaction, using acyl-CoA in the place of acetyl-CoA, and releasing a C_{n+2} β-ketoacyl-ACP. ***Reaction 4.*** The next step is the first reduction step in the elongation cycle, catalyzed by BKR. In the proposed mechanism, S138 of *E. coli* BKR forms a hydrogen bond with the thioester carbonyl of β-ketoacyl-ACP stabilizing the substrate (Oppermann et al., 2003). K155 effectively lowers the pKa of the Y151-OH via hydrogen bonding with the 2'-OH of the NADPH ribose group. Y151 transfers a proton to the keto moiety of β-ketoacyl-ACP (Jörnvall et al., 1995), N110 interacts with the K155 residue through a water molecule (Filling et al., 2002), and β-hydroxyacyl-ACP is released (Jörnvall et al., 1995).

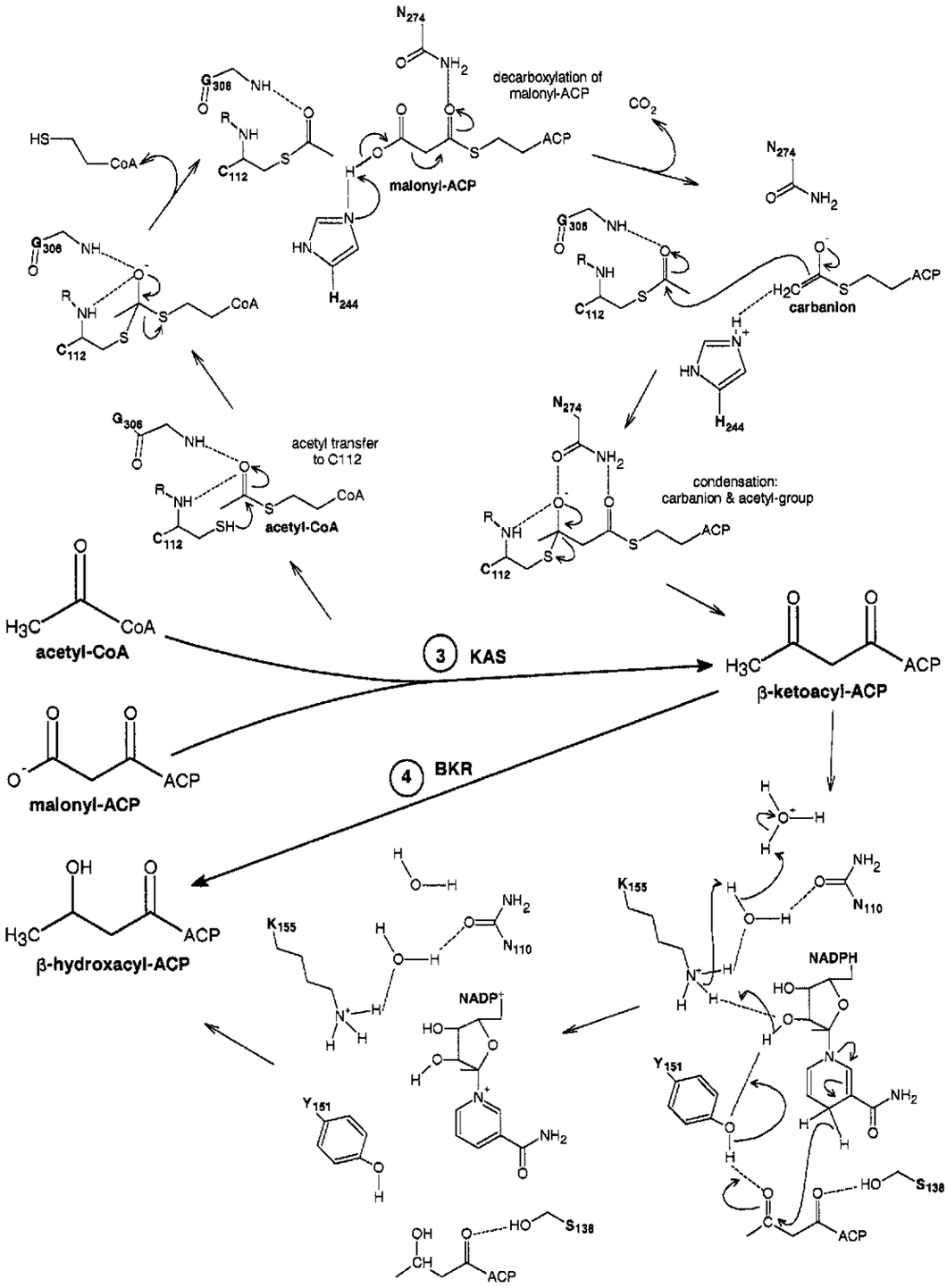
decarboxylation of malonyl-ACP
malonyl-ACP
carbanion
condensation: carbanion & acetyl-group
acetyl transfer to C112
acetyl-CoA
3 KAS
β-ketoacyl-ACP
4 BKR
malonyl-ACP
β-hydroxacyl-ACP
NADPH
NADP+

Figure 2.4 (Continued) ***Reaction 5.*** β-hydroxyacyl-ACP is dehydrated into *trans*-2-acyl-ACP via FabA or FabZ activity. In the proposed binding mechanism for *E. coli* FabA, which also catalyzes the isomerization of *trans*-2-decanoyl-ACP to form *cis*-3-decanacyl-ACP, the carbonyl group of β-hydroxydecanoyl-ACP interacts with the backbone amide of G79, and the hydroxyl group of β-hydroxydecanoyl-ACP interacts with the protonated side chain of D87'. Upon *trans*-2-decanoyl-ACP formation, the H70 side chain is protonated. The carboxyl group of D84' and the amide backbone of C80 interact with a water molecule. During isomerization the carbonyl group of *trans*-2-decanoyl-ACP interacts with the backbone amide of G79, and carbon-2 of the *trans*-2-acyl-ACP intermediate transfers an electron to the protonated side chain of H70 (Leesong et al., 1996). Finally *cis*-3-decanoyl-ACP bypasses reaction 6, proceeding immediately to reaction 3 to undergo another cycle of elongation, thus initiating UFA biosynthesis. In tissues where C_{10} FAs are prominent, *cis*-3-decanoyl-ACP may be released into the acyl-ACP pool. The *trans*-2-acyl-ACP produced by FabZ, possibly through a similar mechanism as the dehydration step in FabA activity, proceeds to reaction 6. ***Reaction 6.*** The final step in the elongation cycle is catalyzed by ENR. In the proposed catalytic mechanism for *B. napus* ENR, the nicotinamide's carbon-3 proton of NADH attacks the double bond of *trans*-2-enoyl-ACP reductase forming an enolate anion intermediate, which is stabilized by the positively charged nitrogen of K206. Y198 donates a proton to the enolate anion, producing an enol, which tautomerizes and releases acyl-ACP. Acyl-ACP will either proceed back to reaction 3, the first step in another cycle of elongation, or will be released into the acyl-ACP pool in the plastid. The acyl-ACP pool serves as a substrate for various reactions, including acylglycerolipid bioassembly.

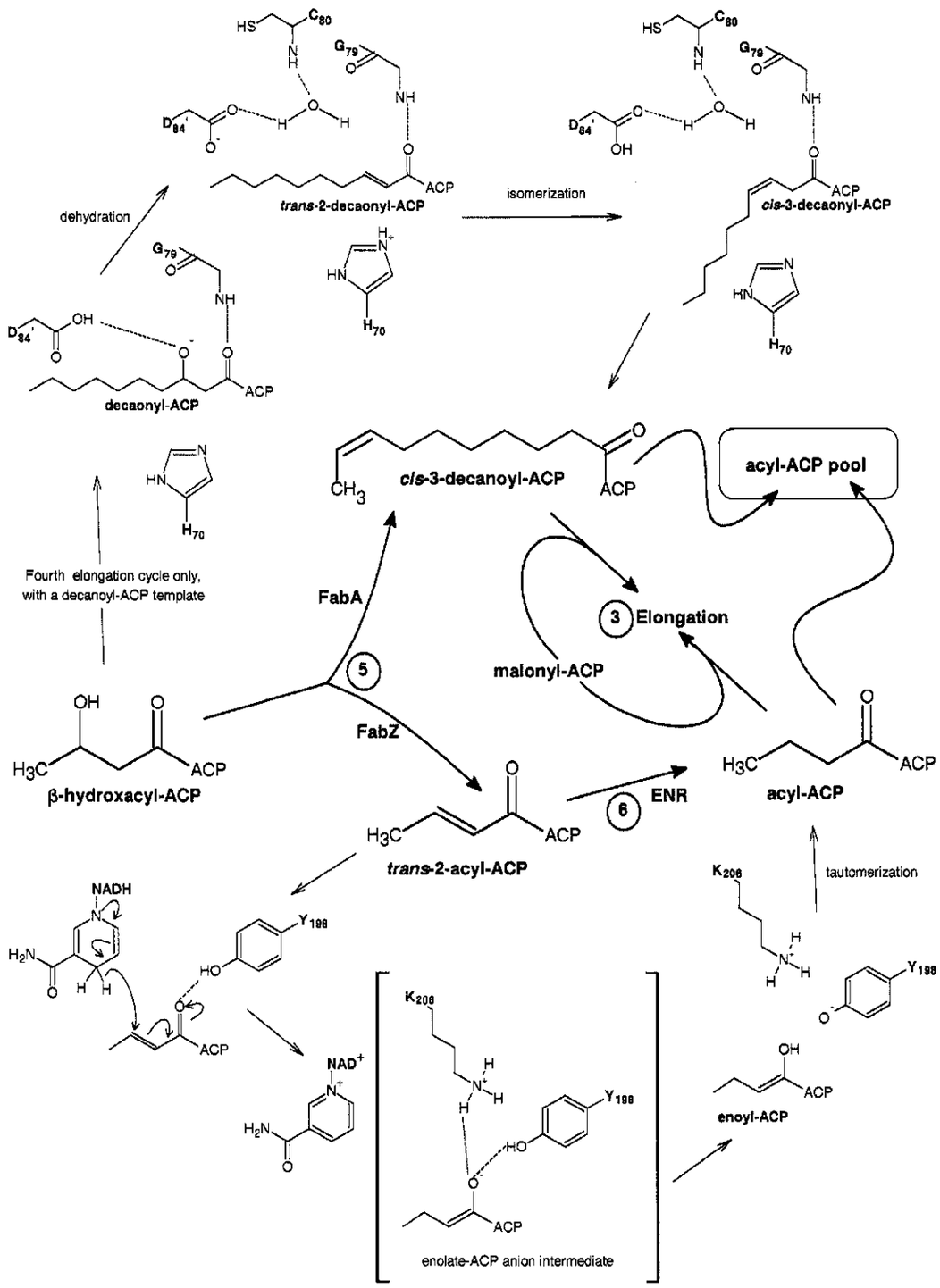
dehydration
trans-2-decaonyl-ACP
isomerization
cis-3-decaonyl-ACP
decaonyl-ACP
cis-3-decanoyl-ACP
acyl-ACP pool
Fourth elongation cycle only,
with a decanoyl-ACP template
FabA
3 Elongation
malonyl-ACP
5
FabZ
β-hydroxacyl-ACP
6
ENR
acyl-ACP
trans-2-acyl-ACP
tautomerization
NADH
NAD+
enolate-ACP anion intermediate
enoyl-ACP

linolenic acid to α-eleostearic acid have been identified in the synthesis of unusual fatty acids (Dyer et al., 2002).

The structures of most FAS II enzymes have been determined (Athappilly and Hendrickson, 1995; Rafferty et al., 1995; Leesong et al., 1996; Davies et al., 2000; Fisher et al., 2000), and residues involved in substrate binding and catalytic activity have been identified and catalytic mechanisms have been proposed (Figure 2.4). Bacterial sources of the FAS II enzymes are better characterized than those from plant sources. Since the two multifunctional enzymes of the animal FAS I system are so different from the dissociable enzymes of the FAS II systems, and since FA biosynthesis is essential for cell growth and survival, FAS II inhibitors have been a target for antibiotic development. With regards to the plant systems, a knowledge of how these enzymes function can further our understanding in the mechanisms of FA accumulation in oilseeds. A better understanding of the system may provide us with the means to modify the seed oil content or to improve oil yield in crops.

2.4 Triacylglycerol Biosynthesis

FA esterification to glycerol involves the activity of four enzymes in the Kennedy pathway (Kennedy, 1961; for reviews see Coleman and Lee, 2004; Weselake, 2005). The primary site of glycerolipid bioassembly is the endoplasmic reticulum (ER). Membrane lipid synthesis also occurs in the plastid and mitochondria, with acyltransferases of the Kennedy pathway found in both of these organelles. Plastidal acyltransferases use acyl-ACP substrates, while mitochondrial and microsomal acyltransferases use acyl-CoA substrates. The first enzyme in the Kennedy pathway,

glycerolphosphate acyltransferase (GPAT), catalyzes the addition of an acyl group to the *sn*-1 position of glycerol-3-phosphate (G3P). The resulting molecule, *sn*-1 acyl-lysophosphatidyl(LPA) undergoes a second acyl addition at the *sn*-2 position, in the presence of lysophosphatidylacyltransferase (LPAAT), to produce phosphatidic acid (PA). PA phosphatase catalyzes the release of inorganic phosphate from phosphatidic acid to produce *sn*-1,2 DAG. Microsomal acyl-CoA:diacylglycerol acyltransferase (DGAT) catalyzes the final acylation step at the *sn*-3 position of *sn*-1,2 DAG to form TAG (Stymne and Stobart, 1987). DGAT is the only enzyme in the Kennedy pathway unique to TAG biosynthesis (Stymne and Stobart 1987; Weselake et al. 1993; Bao and Ohlrogge, 1999; Nykiforuk et al., 2002).

Several additional reactions outside of the Kennedy pathway have been identified in microsomal preparations involving transacylation between different glycerolipids. Among these transacylase activities, TAG formation has been observed in at least two reactions outside of DGAT activity. One of these is through the transfer of acyl groups between two molecules of DAG catalyzed by diacylglycerol:diacylglycerol transacylase (DGTA) to produce monoacylglycerol (MAG) and TAG. This reaction has been observed in *Carthamus tincotrius* L. (safflower) seeds (Stobart et al., 1997) and in rat intestinal microsomes (Lehner and Kuksis, 1993). The second transacylation reaction in TAG formation occurs between the membrane lipid PC and DAG catalyzed by phospholipid:diacylglycerol acyltransferase (PDAT) to produce lysophosphatidylcholine (LPC) and TAG. PDAT activity has been observed in various plant and yeast microsomal preparations (Dahlqvist et al., 2000).

PA is a key intermediate in different glycerolipid synthetic pathways; it is a

precursor for the synthesis of both membrane lipids and TAGs (Stymne and Stobart, 1987). In plastidal membrane lipid synthesis, PA can be directly converted to phosphatidylglycerol (PG), or converted to diacylglycerol (DAG) and then to the sulfolipid (SL) or monogalactosyldiacylglycerol (MGD), and from MGD to digalactosyldiacylglycerol (DGDG). In ER membrane lipid synthesis, PA can be directly converted to phosphatidylinositol (PI) or phosphatidylglycerol (PG), or converted to DAG and then to phosphatidylethanolamine (PE) or phosphatidylcholine (PC; Browse, 1998).

PC plays an important role in the FA composition of TAG. While the primary products of FA synthesis in the plastid are 16:0-ACP and 18:1-ACP, other FA groups, including 18:2 and 18:3 are often found esterified to TAG. Further desaturation of 18:1 occurs primarily through the activities of 18:1- and 18:2-PC desaturases. PC synthesis is catalyzed by a cytidine diphosphate (CDP)-choline:1,2-diacylglycerol cholinephosphotransferase (CPT), which transfers the phosphocholine group of CDP-choline to the *sn*-3 position of DAG, releasing cytidine monophosphate (CMP). CPT will also catalyze the reverse reaction (for review see Weselake, 2002). PC can also be generated from LPC through the activity of acyl-CoA:lysophosphatidylcholine acyltransferase (LPCAT). LPCAT transfers the acyl group from the acyl-CoA pool to the *sn*-2 position of LPC, releasing a CoA molecule. LPCAT will also catalyze the reverse reaction to generate LPC. A diagram of TAG biosynthesis in plants is presented in Figure 2.5, and a summary of the major enzymes in TAG biosynthesis is presented in Table 2.3.

Positional distribution of the FAs on the glycerol backbone is both dependent

Figure 2.5 Triacylglycerol biosynthesis in plants. Triacylglycerol (TAG) is synthesized by four enzymes of the Kennedy pathway, including glycerolphosphate acyltransferase (GPAT), lysophosphatidylacyltransferase (LPAAT), phosphatidic acid (PA) phosphatase, and diacylglycerol acyltransferase (DGAT) and takes place in the ER of plant cells. Some of the early steps in the Kennedy pathway also take place in the plastid of plant cells. The first two steps are acyl-additions at the *sn*-1 and -2 positions of glycerol through GPAT and LPAAT, respectively. PA is a major substrate for both membrane lipid and diacylglycerol (DAG) syntheses, and DAG is a major substrate for both membrane lipid and TAG syntheses. Membrane lipids include phosphatidylglycerol (PG), phosphatidylcholine (PC), phosphatidylethanolamine (PE), phosphatidylinositol (PI), monogalactosyldiacylglycerol (MGD), digalactosyldiacylglycerol (DGDG) and sulfolipid (SL). TAG can also be formed through the reversible activities of diacylglycerol:diacylglycerol transacylase (DGTA) or phospholipid:diacylglycerol acyltransferase (PDAT). This figure was adapted from Weselake (2005) and Browse (1998).

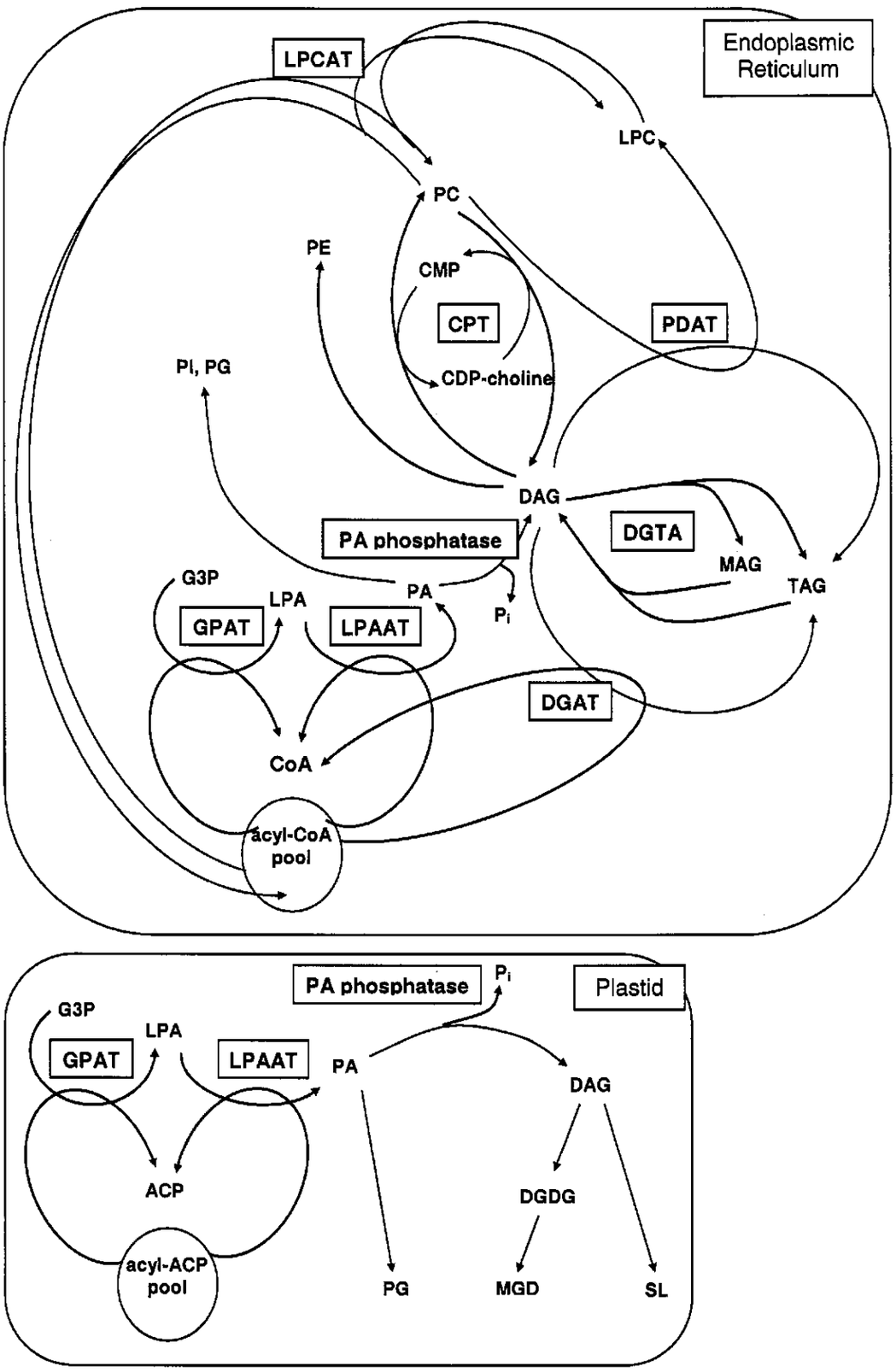
Endoplasmic Reticulum
LPCAT
LPC
PC
PE
CMP
CPT
PDAT
CDP-choline
PI, PG
DAG
PA phosphatase
DGTA
MAG
TAG
G3P
LPA
PA
Pi
GPAT
LPAAT
DGAT
CoA
acyl-CoA pool
PA phosphatase
Pi
Plastid
G3P
LPA
GPAT
LPAAT
PA
DAG
ACP
DGDG
acyl-ACP pool
PG
MGD
SL

Table 2.3 The enzymes of triacylglycerol biosynthesis.

Enzyme	*Acronym*	*EC*	*Substrates*	*Products*
Glycerolphosphate Acyltransferase	GPAT	2.3.1.15	*sn*-glycerol-3-phophate (G3P), acyl-CoA	*sn*-1-acyl-lysophosphatidyl(LPA), CoA
1-Acylglycerol-3-Phosphate Acyltransferase	LPAAT	2.3.1.51	*sn*-1-acyl-lysophospha-tidic acid (LPA), acyl-CoA	phosphatidic acid (PA), CoA
Phosphatidic Acid Phosphatase	PP	3.1.3.4	phosphatidic acid (PA)	diacylglycerol (DAG), P_i
Diacylglycerol Acyltransferase	DGAT	2.3.1.20	diacylglycerol (DAG), acyl-CoA	triacylglycerol (TAG)
Diacylglycerol: diacylglycerol transacylase	DGTA		diacylglycerol (DAG)	monoacylglycerol (MAG), triacylglycerol (TAG)
Phospholipid:diacylglycerol acyltransferase	PDAT	2.3.1.158	diacylglycerol (DAG), phosphatidylcholine (PC)	lysophosphatidylcholine (LPC), triacylglycerol (TAG)
Cholinephosphotransferase	CPT	2.7.8.2	diacylglycerol (DAG), cytidine diphosphate (CDP)-choline	cytidine monophosphate (CMP), phosphatidylcholine (PC)
Lysophosphatidylcholine acyltransferase	LCPAT	2.3.1.23	lysophosphatidylcholine (LPC), acyl-CoA	phosphatidylcholine (PC), CoA

on the species and on the localization of acyltransferase activity. The plastidal, mitochondrial, and microsomal acyltransferases all have different substrate specificities, thus leading to different FA compositions for the glycerolipids of the plastid, mitochondria, ER and plasma membranes. Membrane lipids also differ in the polar head group found at the *sn*-3 position (see section 2.2). The major glycodiacylglycerols found in plastidal membranes and the phosphodiacylglycerols found in extraplastidal plant membranes are presented in Figure 2.2C and 2.2D. The following section provides a review of the properties of the acyltransferases of the Kennedy pathway.

2.5 Properties of Acyltransferases Involved in Mainstream Triacylglycerol Biosynthesis.

2.5.1 Glycerolphosphate Acyltransferase. The first step of glycerolipid synthesis involves the transfer of an acyl group to the *sn*-1 position of glycerol-3-phosphate (G3P), a reaction catalyzed by glycerolphosphate acyltransferase (GPAT; for review see Murata and Tasaka, 1997). There are two forms of mammalian GPAT, both are membrane-spanning enzymes that use acyl-CoA substrates: (*i*) microsomal GPAT, which is located in the endoplasmic reticulum, and (*ii*) mitochondrial GPAT (mtGPAT), located on the outer mitochondrial membrane. In plants there is a third form of GPAT, (*iii*) soluble GPAT is located in the plastid where it utilizes acyl-ACP substrates in the place of acyl-CoA. GPAT has been cloned and purified from various tissues. Due to the difficulties involved in the solubilization of membrane bound proteins, soluble GPAT is the better characterized form of GPAT. Soluble GPAT has been cloned from a variety of plants

including spinach (Bertrams and Heinz, 1981) and squash (Ishizaki et al., 1988). Soluble GPAT purification from squash was reported in 1987 (Nishida et al.), and the crystal structure was recently deduced (Turnbull et al., 2001). Mouse liver mtGPAT was first cloned in 1991 (Shin et al.), and a second isoform has recently been identified (Lewin et al., 2004). Rat liver mtGPAT has been cloned (Ganesh Bhat et al., 1999), and purified (Vancura and Haldar, 1994), and membrane topology studies have been published (see section 2.8.3; Balija et al., 2000; Gonzalez-Baró et al., 2001). No plant mtGPAT cloning has been reported yet. Microsomal GPAT, the least well-characterized form of GPAT particularly at the molecular level, has been partially purified from oil palm (Manaf and Harwood, 2000) and *M. ramanniana* var. *angulispora* (Mishra and Kamisaka, 2001), and more recently cloned from *Arabidopsis* (Zheng et al., 2003).

GPAT is the first committed step in glycerolipid synthesis. Declercq et al. (1982) have shown that the *in vivo* concentration of G3P in rat hepatocytes is saturating for GPAT. Together with the supply of FAs, GPAT activity has been shown to control the overall flux of glycerolipid synthesis in rat hepatocytes (Stals et al., 1992; 1994). Transgenic *A. thaliana* expressing safflower or *E. coli* GPAT led to an 8 to 29 % increase in seed oil-content (Jain et al., 2000).

GPAT substrate specificity is species-dependent. Selective and non-selective forms of GPAT have been identified in various plants. In general, soluble and microsomal GPATs are non-selective (Murata and Tasaka, 1997). Manaf and Harwood (2000) found that oil palm microsomal GPAT showed a preference for 16:0-CoA substrates. Soluble pea GPAT was shown to be selective for 18:1-CoA substrates (Weber et al., 1991). Recent studies identified a residue involved in the substrate selectivity of a

squash soluble GPAT. An L261F mutation in the binding cleft changed the specificities from this non-selective enzyme to one selective for 18:1-ACP (Slabas et al., 2002).

2.5.2 LysophosphatidylAcyltransferase. Acylation at the *sn*-2 position of LPA to PA is catalyzed by LPAAT, also known as 1-acylglycerol-3-phosphate acyltransferase (AGAT). As is the case with GPAT, there are three forms of LPAAT in plants (Frentzen, 1993). The two membrane bound eukaryotic forms include (*i*) microsomal LPAAT and (*ii*) mitochondrial LPAAT, which are both acyl-CoA acceptors. The prokaryotic form, (*iii*) plastidal LPAAT uses acyl-ACP substrates, and in contrast to plastidal GPAT, is a membrane bound enzyme. Plastidal LPAATs are selective for C_{16}-acyl-ACPs, while cytoplasmic LPAATs do not show a preference in chain length, uses both C_{16}-and C_{18}-acyl-CoAs equally. Cytoplasmic LPAATS show a preference towards unsaturated acyl-CoA and LPA substrates (reviewed in Bourgis et al., 1999).

LPAAT was solubilized from coconut endosperm in 1995 (Davies et al.), and partial purification of the enzyme followed shortly afterwards (Knutzon et al., 1995). There are no reports of LPAAT purification to homogeneity. Microsomal and plastidal LPAATs have been cloned from several sources. A plastidal *LPAAT* cDNA has been isolated from *B. napus* (Bourgis et al., 1999). Five *LPAAT* genes have been identified in *Arabidopsis*, one of these encodes a plastidal LPAAT the remaining four encode microsomal LPAATs (Kim and Huang, 2004). Microsomal LPAATs have been cloned from several tissues including coconut endosperm (Knutzon et al., 1995), meadowfoam (Lassner et al., 1995), human tissues (Eberhardt et al., 1999) and from bovine and ovine mammary glands (Mistry and Medrano, 2002).

LPAAT activity is determined by the supply of LPA, which is the product of GPAT activity (Stals et al., 1994). Zou et al. (1997) have shown that overexpression of an *sn*-2 acyltransferase from yeast increased oil content in *Arabidopsis* and *B. napus*. On the other hand, transgenic expression of *Limnanthes alba alba* (meadowfoam) LPAAT in HEAR varieties of *B. napus* did not affect the seed oil yield (Lassner et al., 1995). Transgenic HEAR seeds did, however, show a change in the *sn*-2 content of the seed oil. While HEAR varieties of *B. napus* accumulate erucic acid at the *sn*-1 and *sn*-3 positions of TAG, erucic acid is not present at the *sn*-2 position. Meadowfoam is also high in very-long-chain FAs, and its LPAAT is selective for erucic acid for *sn*-2 esterification of LPA. Transgenic HEAR lines expressing meadowfoam LPAAT was successful in accumulating erucic acid at the *sn*-2 position in the seed oil (Lassner et al., 1995).

2.5.3 Diacylglycerol Acyltransferase. The final step in TAG biosynthesis is catalyzed by a membrane bound acyl-CoA dependent DGAT localized in the ER. DGAT activity has been observed on both sides of the ER membrane (Owen et al., 1997). Acyl-CoA:DGAT activity has also been identified in the chloroplast (Martin and Wilson, 1983; 1984; for review see Weselake, 2005) and appears to be up-regulated during leaf senescence (Kaup et al., 2002). Phospholipid dependent DGAT activity (PDAT), catalyzing the acyl-CoA independent formation of TAG, has also been identified in yeast and plants (Dahlqvist et al., 2000). In 1998, Cases et al. reported the first cloning of acyl-CoA:DGAT from humans and mice (Cases et al., 1998). DGAT has since been cloned from several plant species including *A. thaliana*, tobacco (Bouvier-Navé et al. 2000), *B. napus* (Nykiforuk et al., 1999a; 1999b; Brown et al., 2000; Nykiforuk et al., 2002), olives

(Giannoulia and Hatzopoulos, 2004), soybean (Zhang et al., 2004) and castor bean (He et al., 2004b). Until recently, all identified acyl-CoA:DGATs shared high sequence identity and similar hydropathy plots with the acyl-CoA:cholesterol acyltransferase (ACAT) gene family. A second DGAT gene family, DGAT-II, was identified in the oleaginous fungus *M. ramanniana*, with homologues in other organisms including *B. napus*. DGAT-II has no apparent homology to the ACAT family (Lardizabal et al., 2001). Purification of DGAT-I and –II to apparent homogeneity has been achieved using *M. ramanniana* as an enzyme source (Kamisaka et al., 1997; Lardizabal et al., 2001, respectively) and the enzyme has been partially purified from microsomes of both mammalian and plant source, including rat liver (Polokoff and Bell, 1980; Andersson et al., 1994) and soybean cotyldons (Kwanyuen and Wilson, 1986). Little et al. (1994) reported the solubilization of DGAT from membranes of microspore-derived embryos and from cell suspension cultures of *B. napus* (BnDGAT) using a 2 M NaCl and 1% (w/v) octanoyl-*N*-methyl-glucamide (MEGA-8), pH 8.0 at a detergent to protein ration of 2:1. Optimum activity of the solubilized enzyme was observed at pH 7, similar to the optimum activity in the particulate form of BnDGAT. The specific activity of solubilized BnDGAT was 2.4-fold and 1.6-fold greater than the particulate form of BnDGAT from MD embryos and cell suspension cultures, respectively (Little et al., 1994).

DGAT is the only enzyme in the Kennedy pathway that is unique to TAG biosynthesis (Stymne and Stobart, 1987; Weselake et al. 1993; Bao and Ohlrogge, 1999; Nykiforuk et al., 2002). DGAT plays an important role in the regulation of TAG synthesis and may limit the flow of carbon into TAG (Stals et al., 1994; Mayorek et al., 1989). By observing the levels of transcript during development in olive tissues,

Giannoulia et al. (2000) showed that DGAT gene expression is correlated with TAG accumulation. In other studies, expression of various sources of DGAT in yeast and tobacco resulted in an increase in TAG production (Bouvier-Navé, 2000), and seed-specific overexpression of *A. thaliana* DGAT resulted in an increase in seed oil content (Jako et al., 2001). *A. thaliana* mutants deficient in DGAT-I showed the opposite response, a decrease in the seed-oil content, as well as a change in the FA content of TAG (Katavic et al., 1995).

Mammalian DGAT-I is involved in the regulation of TAG storage in adipose tissues and in the regulation of metabolic activity (Chen and Farese Jr., 2000). In recent studies, mice lacking DGAT-I activity, with or without increased fat intake, have demonstrated increased use of energy, increased metabolic activity and decreased total body fat (Chen and Farese Jr., 2000).

Two cDNAs encoding type I DGATs have been isolated from *B. napus* L. cv Jet Neuf microspore derived (MD) cell suspension cultures (Nykiforuk et al., 2002). Northern blotting has shown that transcripts encoding both forms of DGAT are expressed in MD cultures, and both activities have been observed in *Pichia pastoris* transformed with cDNAs encoding these enzymes (Nykiforuk et al., 2002). This was the first report of DGAT cloning from a major oilseed crop (Nykiforuk et al., 2002). *BnDGAT1* encodes a deduced polypeptide of 503 amino acids, with predicted a molecular mass of 56.9 kD and isoelectric point of 8.4. *BnDGAT2* encodes a deduced polypeptide of 341 amino acids, with a predicted molecular mass of 39.5 kD and isoelectric point of 8.9. BnDGAT2 is essentially a truncated version of BnDGAT1, where the first 162 residues of the N-terminus have been deleted, sharing 96 % sequence identity in the remaining

residues.

Several residues or stretches of residues have been identified as possible active or binding sites in type I BnDGAT. Six stretches of amino acid residues, highly conserved among all type I DGATs identified, are present in BnDGAT1 and BnDGAT2, these are BnDGAT1 residues 274-280, 311-316, 335-341, 364-368, 372-381 and 392-399 (Nykiforuk et al., 2002). An invariant serine residue present in all identified DGATs and ACATs, and shown to be essential for ACAT activity (Cases et al., 1998) is found at residue 251 of BnDGAT1 adjacent to a tyrosine/kinase phosphorylation signature (Nykiforuk et al., 2002). Several studies have suggested that mammalian DGAT is inactivated by tyrosine kinase phosphorylation (Haagsman et al., 1981; Rodriguez et al., 1992; Lau and Rodriguez, 1996). A point mutation of the tyrosine in question to phenylalanine yielded a fully active mouse DGAT (Yu et al., 2002). Microsomal DGAT from *B. napus* cell suspension cultures, on the other hand, did not appear to be susceptible to deactivation by phosphorylation (Byers et al., 1999).

Lipidex-1000 binding assays revealed an acyl-CoA binding site at the N-terminus of BnDGAT1, predicted to be within the identified acyl-CoA binding signature in residues 99-116 (Nykiforuk et al., 2002). This signature is absent in all other DGATs identified to date, including BnDGAT2 and it is therefore believed that this sequence is not required for proper membrane folding or enzyme activity. The N-terminal segment of BnDGAT1 may have a regulatory function (Nykiforuk et al., 2002). Lipidex-1000 binding assays of the soluble N-terminus of BnDGAT1 showed a greater affinity for 22:1-CoA than for 18:1-CoA (Weselake et al., 2004). *B. napus* comes from an oilseed crop that is high in 22:1, and was generated through breeding of LEAR (see section 2.1).

The breeding process eliminated elongase activity required for converting 18:1-CoA to 22:1-CoA (Katavic et al., 2002). It is therefore not surprising that BnDGAT1 interacts effectively with 22:1-CoA. There may be other acyl-CoA binding sites, however, in BnDGAT1. *BnDGAT2* cDNA, which lacks the N-terminal portion found in BnDGAT1, was isolated from cell suspension cultures. BnDGAT2 may be specific to the cell suspension cultures and caused by mutations due to the genetic instability associated with maintaining plant lines in cell suspension (Weselake et al., 2004), or it may be specific to the pollen of *B. napus*, since the cell suspension cultures are derived from pollen microspores. No studies have been done to determine whether or not BnDGAT2 is present in the original LEAR crops or in *B. napus* plants that are not derived from cell suspension cultures. If the other acyl-CoA binding signatures of BnDGAT1 and BnDGAT2 have a preference for 18:1-CoA over 22:1-CoA, and if BnDGAT2 is not found in the original LEAR crop, then their may be evolutionary reasons for the absence of the N-terminal portion of BnDGAT1 in BnDGAT2.

2.6 Biogenesis of Membrane Proteins

Cellular membranes, at the simplest level, can be thought of as a bilayer of polar lipids. The major membrane lipids are phospholipids, consisting of a polar phosphate head group at the *sn*-3 position of a glycerol backbone and FA chains esterified to each of the *sn*-1 and *sn*-2 positions (see section 2.2; Figure 2.2). The hydrophobic fatty acid chains interact with one another forming a hydrophobic core of the membrane, and the phosphate groups interact with one another forming the outside and inside hydrophilic surfaces of the membrane (Figure 2.6; Lodish et al., 1995; Lommerse et al., 2004). Two

Figure 2.6 Cellular membrane composition. Phospholipids form the basic unit of cellular membranes with a phosphate head group and two fatty acid (FA) chains. The hydrophobic FA chains interact with one another and the hydrophilic phosphate head groups (light gray) interact with one another. Two layers of phosholipids interact via the hydrophobic portions, forming the hydrophobic core of the membrane phospholipid bilayer, and the hydrophilic portions interact with the cytoplasm and explasm. Biological membranes interact with two types of proteins, integral proteins (black) that span the bilayer one or more times, and peripheral proteins (dark gray) that associate with the hydrophilic surface of the cytopasmic or exoplasmic face. Proteins and lipids may be glycosylated on the exoplasmic side of the membrane. This figure was adapted from Lodish et al. (1995).

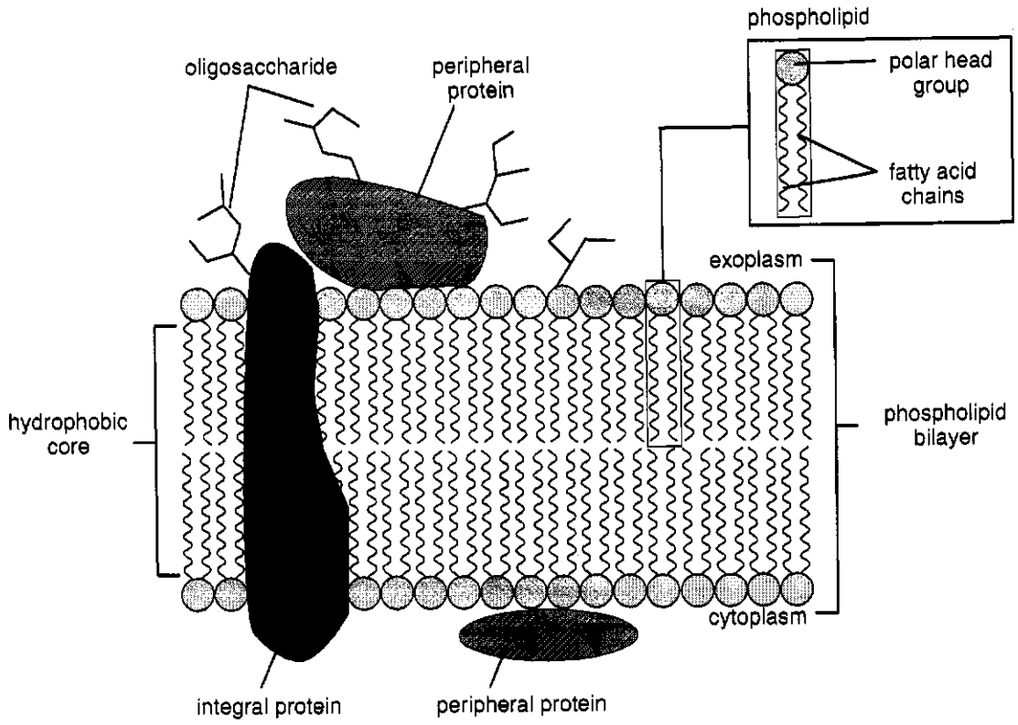
phospholipid
polar head group
fatty acid chains
oligosaccharide
peripheral protein
exoplasm
hydrophobic core
phospholipid bilayer
cytoplasm
integral protein
peripheral protein

types of proteins interact with biological membranes: peripheral membrane proteins interact with the surface of the membrane, and integral membrane proteins interact both with the hydrophobic core of the membrane and with the hydrophilic surfaces on the inside and/or outside of the membrane (Lodish et al., 1995; Lommerse et al., 2004). There are three types of integral membrane proteins: monotopic proteins have a hydrophilic portion exposed only to one side of the membrane; bitopic proteins span the membrane only once, with their hydrophilic N- and C- termini on opposite sides of the membrane; and polytopic proteins span the membrane two or more times, with hydrophilic portions exposed on both sides of the membrane (Blobel, 1980). Two classes of transmembrane proteins have been identified: class I proteins have transmembrane helices 17-25 amino acids long, and class II are 16-stranded β-barrel structures, which have only been identified in the bacteria outer porins (Tusnády and Simon, 1998).

Translation of cytosolic proteins occurs on cytosolic ribosomes bound to cytoskeletal fibers in the cytoplasm. Translation of secretory and integral membrane proteins and of endoplasmic reticulum (ER) associated proteins occurs on ribosomes that are associated with the ER (Figure 2.7). The initial steps in the translation of secretory and integral membrane proteins are similar. The nascent chains of secretory and integral membrane proteins target the ribosome nascent chain complex (RNC) to the ER by a topogenic sequence (sequences involved in targeting translation/translocation of secretory and integral membrane proteins) called the *signal sequence*. The signal sequence of secretory proteins is a short transient sequence that appears at the N-terminus of the

Figure 2.7 Translation of secretory and integral membrane proteins. The first five steps in translation of secretory and integral membrane proteins are similar. mRNA translation occurs on ribosomes. The emergence of a signal sequence from the nascent polypeptide targets the binding of a signal recognition particle (SRP), which halts translation and targets the nascent chain to the ER (step 1). SRP interacts with an SRP receptor (SR) at the ER membrane and targets the ribosome nascent chain complex (RNC) to the translocon where translation continues (step 2). The signal sequence is removed co-translationally through the activity of a signal peptidase (step 4). The nascent chain is co-translationally glycosylated through the activity of oligosaccharyltransferase, and molecular chaperones aid in protein folding. Upon completion of secretory protein translation (step 5a) newly synthesized proteins are released into the lumen of the ER. During translation of integral membrane proteins (step 5b) the emergence of the first membrane-spanning domain behaves as a signal sequence and targets the protein to the ER for translation. In this case the signal sequence is usually a permanent sequence that is not removed by signal peptidase. When the signal sequence emerges a chaperone will create a barrier between the translocon and the lumen. Emerging cytosolic loops enter the cytosol via a small gap at the ribosome-translocon interface. The next membrane-spanning region is a stop-transfer sequence, which halts translation and allows integration of the transmembrane helix into the lipid bilayer. The next membrane-spanning domain is a second signal sequence and is followed by another stop-transfer sequence. Co-translational insertion continues in this way until the full-length protein has been synthesized. This figure was adapted from Lodish et al. (1995), Kalies and Hartmann (1998) and Johnson and van Waes (1999).

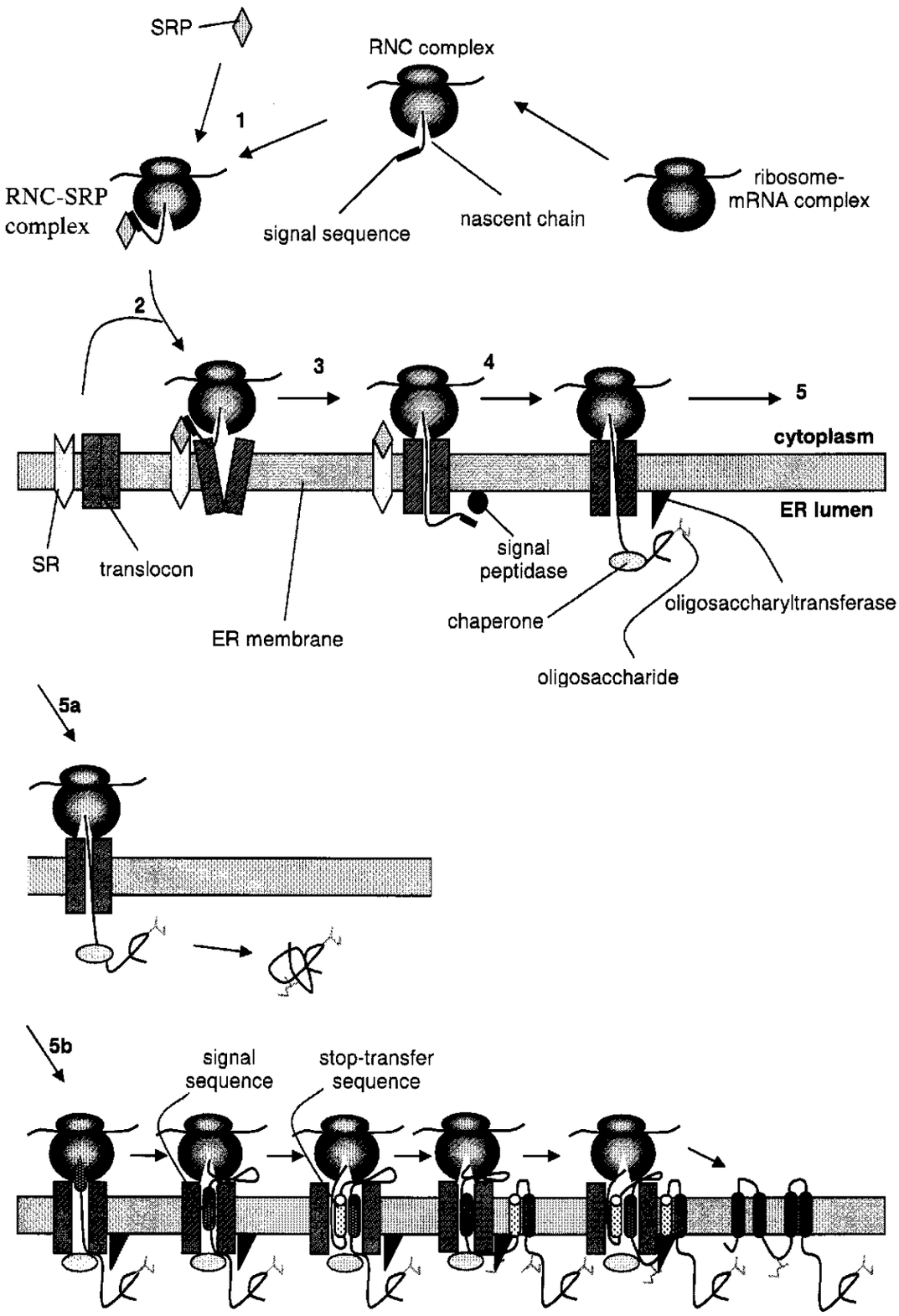
SRP
RNC complex
1
RNC-SRP
complex
signal sequence
nascent chain
ribosome-
mRNA complex
2
3
4
5
cytoplasm
ER lumen
SR
translocon
ER membrane
signal
peptidase
chaperone
oligosaccharyltransferase
oligosaccharide
5a
5b
signal
sequence
stop-transfer
sequence

nascent chain and is removed co-translationally via the activity of a lumenal signal peptidase (Blobel, 1980; Johnson and van Waes, 1999). The signal sequences of integral membrane proteins are usually built into their final sequence, often corresponding to the first membrane-spanning domain, and are therefore not cleaved off (Blobel, 1980; Johnson and van Waes, 1999). The signal sequences of secretory and integral membrane proteins interact with a signal recognition particle (SRP; Walter et al., 1981; for review see Nagai et al., 2003), causing a halt in elongation (Walter and Blobel, 1981a; 1981b; Halic et al., 2004). Mediated by GTPase activity (Mandon et al., 2003; Egea et al., 2004) the SRP interacts SRP receptor (SR), an integral glycoprotein of the ER (Meyer et al., 1982; Wiedmann et al., 1987), targeting the SRP-RNC complex to a translocation channel where nascent chain elongation continues. The translocation channel, also called the translocon, is an aqueous pore on the ER membrane (Blobel and Dobberstein, 1975a; 1975b; Walter and Lingappa, 1986; Johnson and van Waes, 1999) formed by a heterotrimer of integral membrane proteins called the Sec61 complex (Gorlich and Rapoport, 1993; Menetret et al., 2000; Beckmann et al., 2001). Together the RNC and the translocon form an ion-impermeable seal with the ER membrane, blocking cytosolic exposure of the nascent chain (Crowley et al., 1994; Hamman et al., 1998). Recent structural studies of the translocon have revealed a 15-20 Å gap at the RNC-translocon junction that is speculated to accommodate cytosolic loops of nascent integral membrane proteins (Menetret et al., 2000; Beckmann et al., 2001).

Translocation of secretory and integral membrane proteins can either occur co-translationally or post-translationally, but the event is more likely to occur co-translationally. Transient signal sequences are removed co-translationally in the lumen

by signal peptidase activity (Blobel, 1980; Johnson and van Waes, 1999). Glycosylation of secretory and integral membrane proteins also occurs co-translationally in the lumen of the ER (for review see Kalies and Hartmann, 1998; Johnson and van Waes, 1999). Molecular chaperones assist in folding of nascent polypeptides (Frydman, 2001; Trombetta and Helenius, 1998; Johnson and van Waes, 1999; Lambert and Prange, 2003).

Secretory proteins are released into the lumen and then translocated to their final destinations. The process of integral membrane protein integration into the ER membrane, where it will either remain or be translocated to the target membrane, is not well characterized. The process of polytopic protein integration is particularly unclear. The "linear insertion model" (Blobel, 1980), one of the early models of integration, suggested the first transmembrane segment determines the topological orientation (the topology) of the remaining transmembrane segments. Two topogenic sequences are necessary for linear insertion: the first hydrophobic domain behaves as an uncleaved signal sequence, targeting translation to the ER membrane, and the second hydrophobic domain behaves has a stop transfer sequence, which interrupts the translocation initiated by the signal sequence. Wessels and Spiess (1988) first demonstrated that the insertion of polytopic membrane proteins occurs sequentially by a series of signal and stop transfer sequences. Some studies have found that signal and stop transfer sequences are interchangeable (Audigier et al., 1987), and others have found that they are not (Rothman et al., 1988). One study suggested that the translation system used might influence stop transfer activity based on specific interactions between the ribosome and the ER membrane (Spiess et al., 1989).

It is likely that additional topogenic information is also involved in topological determination and thus may play an important role in the integration of transmembrane proteins. For example, there appears to be a selection for positively charged residues on the cytoplasmic face of a membrane, suggesting that the stretch of residues in between transmembrane domains also play a role in directing membrane insertion and thus affecting the topology (Beltzer et al., 1991; Sipos and von Heijne, 1993; Gafvelin et al., 1997; Sato et al., 1998). In addition, the membrane lipid composition (Bogdanov, 2002), glycosylation, signal peptidase and chaperone activities (Goder et al., 1999) have also been shown to affect the topology of polytopic proteins.

2.7 Topology of Membrane Proteins

Structural information about an enzyme can provide insight into the mechanism through which the enzyme functions. The three-dimensional structures of the various enzymes in FAS II has aided in the assignment of residues involved in substrate binding and catalytic activity (Athappilly and Hendrickson, 1995; Rafferty et al., 1995; Leesong et al., 1996; Davies et al., 2000; Fisher et al., 2000). With the exception of soluble GPAT (Turnbull et al., 2001), the acyltransferases involved in TAG synthesis are hydrophobic in nature and are associated with membrane lipid bilayers. Due to the complexities in the purification and solubilization of integral membrane proteins and maintaining enzymatic activity, purified enzyme preparations have not been easy to obtain, subsequently, their structures are more difficult to elucidate than those of soluble proteins. There are examples of crystallographic (Royant et al., 2001) and NMR (Thompson et al., 1992) studies revealing the structures of membrane bound proteins. Methods are being

developed in X-ray crystallography, including lipidic cubic phase crystallization where the membrane protein is incorporated into a highly ordered membrane system composed of a lipid bilayer of monoacylglycerols (Landau and Rosenbusch, 1996), and bicelle crystallization where membrane proteins are crystallized in a bicelle, which is a lipid bilayer formed from lipid-detergent mixture (Faham and Bowie, 2002). Methods in solid-state NMR involve labeling of amino acid residues (thus often limiting the study to recombinant or alternatively synthesized proteins) and incorporating the protein into a bilayer system (Watts et al, 2004). These methods are, however, still in their infancy, and are thus less advanced than the methods of soluble protein structural determination.

An increasingly popular approach in obtaining structural information of integral membrane proteins is to determine their membrane topology (Blobel and Dobberstein, 1975a; 1975b; Fraser et al., 1997; Pan et al., 1998; Tusnády and Simon, 1998; Balija et al., 2000; Gonzalez-Baró et al., 2001; Abell et al., 2002). The membrane topology of a protein is a two-dimensional picture of how the protein is associated with the membrane. In short, the membrane topology describes which amino acid residues are in the lipid bilayer, which residues are on the outside of the membrane, and which residues are on the inside of the membrane. Several methods in deducing the membrane topology of a protein are presented in the following sections.

2.7.1 Membrane Protein Topology Predictions. Topogenic information available from the primary structure can be used to predict the membrane topology of integral membrane protein. Stretches of hydrophobic residues are more likely to be 'transmembrane' regions interacting with the membrane bilayer, and stretches of

hydrophilic residues are more likely to form the 'loops' between the transmembrane regions (Kyte and Doolittle, 1982). Positively charged residues tend to form the cytoplasmic loops preferentially over exoplasmic loops—a phenomenon called the 'positive inside' rule (Sipos and von Heijne, 1993). Some studies have shown that creating a cluster of positive charges on exoplasmic loops of polytopic proteins results in the exclusion of a transmembrane domain from the lipid bilayer such that the positive charges remain on the cytoplasmic face (Gafvelin et al., 1997; Sato et al., 1998). In recent years, a variety of different membrane topology prediction programs have been developed and many are available through the Expasy Molecular Biology Server (http://ca.expasy.org). The most accurate topology prediction programs, TMHMM2 (Sonhammer et al., 1998) and HMMTOP2 (Tusnády and Simon, 2001), use a method called the hidden Markov model (HMM; Ikeda et al., 2002), which incorporates the probabilities based on sequence alignments with known topologies, such that the topologies are predicted based on amino acid distribution, rather then amino acid composition, contributing to the various structural components of proteins. These programs allow for greater accuracy in membrane topology predictions because they provide a more statistical approach in their predictions. While the accuracy of these predictions is relatively high (approximately 65-70% topologies are properly predicted; Nilsson et al., 2002), experimentally determined results are of course more reliable.

2.7.2 Experimental Approaches to Determining Membrane Topology. Topology predictions provide useful structural information, and can be used as a starting point for experimental determination. Experimental topology studies, however, provide more

concrete structural insight. Current methods in probing the topology of integral membrane proteins include immunofluorescence of selectively permeabilized cellular membranes, *N*-linked glycosylation-scanning mutagenesis and proteolytic mapping. All of these methods have their advantages and disadvantages. Investigators will often use more than one technique in their studies of assessing topology. These techniques involve the cloning and expression of the protein of interest, often with some kind of tag or marker gene fusion. cDNA constructs generated for topology studies can be strategically designed based on topology predictions. For example, clones can be generated to express truncations with one or more predicted transmembrane regions deleted. N- or C-terminal tag or marker fusions of full length or truncated clones can be generated, or modifications can be made to predicted loop or transmembrane regions. The choice of expression system will depend both on the method of probing the topology and on the protein of interest. Different expression systems have been shown to yield different topologies in some proteins (Spiess et al., 1989). In addition, different expression systems have different machinery for post-translational modifications. The following sections present different methods of expressing membrane proteins and different methods in probing topology.

2.7.2.1 Protein expression systems. Apart from transforming a species of interest with a particular clone, there are a variety of *in vivo* expression systems available. *E. coli* is a widely used protein expression system because it is the simplest and most efficient expression system available. The microorganism has a rapid growth phase, it is easy to manipulate and the biochemistry and molecular biology of the bacterium is well

documented (Sambrook and Russell, 2001; Ausubel et al., 2004). There are two major disadvantages, however, associated with *E. coli* expression systems: (*i*) eukaryotic-specific post-translational modifications are not observed in the prokaryotic expression systems (Ausubel et al., 2004), and (*ii*) expression of large amounts of protein, particularly membrane-associated proteins, will often aggregate in inclusion bodies (Kane and Hartley, 1988; Sambrook and Russell, 2001; Ausubel et al., 2004). Nonetheless, there are techniques available to isolate proteins from these inclusion bodies (Marston and Hartley, 1990).

Eukaryotic expression systems, including insect, mammalian and yeast cell expression, offer obvious advantages over *E. coli* in the expression of eukaryotic proteins. These advantages include the eukaryotic post-translational machinery and subcellular localization. Insect cell expression takes advantage of a baculovirus, known to infect arthropods. Baculovirus is an enveloped double-stranded circular DNA virus that expresses an infectious protein in very high levels (Oker-Blom et al., 2003). Recombinant baculovirus vectors can be prepared to express large quantities of a protein of interest in cultured insect cells (Miller, 1988) and are less prone to the solubility problems observed in bacteria (Ausubel et al., 2004). The recombinant baculovirus insect cell expression system also has advantages over mammalian systems due to its higher tolerance to by-product accumulation and higher levels of expression. On the other hand, while the invertebrate machinery for post-translational modifications is suitable for eukaryotic proteins, some of the post-translational modifications available in the mammalian system are absent in the insect cell system (Miller, 1988; Ausubel et al., 2004). Two approaches are available for protein expression in mammalian systems:

stable transfection, where the gene of interest is incorporated into the chromosomal DNA and yields moderate levels of the target protein (Sambrook and Russell, 2001); and transient transfection, which, as the name suggests, yields temporary infection, but target protein yields are high (Sambrook and Russell, 2001). The latter is used in the production of clonal cell lines (Sambrook and Russell, 2001), and the former is used for membrane topology studies (Crystal et al., 2003; Lin et al., 2003).

Offering the best of both worlds, the yeast expression systems have several advantages over prokaryotic and other eukaryotic systems. High levels of recombinant protein secretion can be obtained in a medium almost free of other proteins, and free of endotoxins and lytic viruses. The yeast expression system, like *E. coli*, has a rapid growth phase and is easy to manipulate. On the other hand, like mammalian and insect cell systems, yeast has eukaryotic post-translational machinery and subcellular localization (Li et al., 2001). The choice of the eukaryotic system used may depend on the specific post-translational modifications under investigation, and is often therefore dependent on the protein of interest.

Alternatively, cloned genes can be expressed *in vitro*. If the gene of interest is cloned in a bacterial vector with a T3, T7 or SP6 promoter, then mRNA can be transcribed from the isolated plasmid with a T3, T7 or SP6 RNA polymerase, respectively (Ausubel et al., 2004). The mRNA can then be used as a template for cell-free expression using a wheat germ extract (Erickson and Blobel, 1983) or a rabbit reticulocyte lysate preparation (Pelham and Jackson, 1975; Jackson and Hunt, 1983; Dasso and Jackson, 1989). *In vitro* translation of secretory and/or membrane proteins can be performed in the presence of microsomal membrane preparations, which have the

necessary machinery for *N*-linked glycosylation and proteolytic processing (Walter and Blobel, 1983). Microsomal membrane preparations, as described by Walter and Blobel (1983), have been successfully used in the study of secretory and integral membrane proteins for the past two decades (Dietrich et al., 1987; Haffar et al., 1988; Miao et al., 1992; Maldarelli et al., 1993; Abell et al., 1997; Bayle et al., 1997).

2.7.2.2 Probing membrane topology by cytoimmunofluorescence of selectively permeabilized cellular membranes. Various chemicals are capable of selective permeabilization of cellular membranes. Digitonin (Lin et al., 2003), activated streptolysin O (SLO; Zhang et al., 2004; Crystal et al., 2003) and staphylococcal α-toxin (Ahnert-Hilger et al., 1985) have been used for selective permeabilization of the plasma membrane. Saponin (Lin et al., 2003) and Triton X-100 (Crystal et al., 2003) have been used for permeabilization of membrane compartments within the cell in addition to permeabilization of the plasma membrane. Some investigators prefer to use mechanical methods of disrupting the membranes and have found chemical permeation to yield unreliable results (Murthy and Pande, 1987; van der Leij et al., 1999). In cytoimmunofluorescent studies, proteins or protein-tag fusions are expressed in an *in vivo* expression system, and protein specific antibodies or anti-tag antibodies, respectively, are given access either to the cytoplasm by selective permeabilization of the plasma membrane, or to all compartments by non-selective permeabilization of cellular membranes. Fluorescence-conjugated secondary antibodies and microscopic visualization of the cells are used in the detection of the primary antibodies. If the signal is observed in selectively permeabilized cells and in non-selectively permeabilized cells,

then the region detected by the antibody is found in the cytoplasm. If the signal is only observed in non-selectively permeabilized cells, then the region detected by the antibody is found in an exoplasmic compartment in the cell. In the case of proteins targeted to the ER, the exoplasmic region would be the ER lumen (Crystal et al., 2003; Lin et al., 2003; Zhang et al., 2004).

*2.7.2.3 **Probing membrane topology by N-linked glycosylation-scanning mutagenesis.*** *N*-linked glycosylation, involving the addition of high mannose polymers, occurs co-translationally in the ER lumen of membrane glycoproteins on asparagine (N) residues within the consensus sequence N*X*(S/T) (Kornfeld and Kornfeld, 1985). Since glycosylation occurs only in the ER lumen, only the exoplasmic loops of membrane glycoproteins will be glycosylated. A technique called glycosylation-scanning mutagenesis (Kornfeld and Kornfeld, 1985), which takes advantage of this knowledge, has been employed to aid in the determination of the membrane topologies of various integral membrane proteins (Bennet and Kanner, 1997; Bungert et al., 2001; Crystal et al., 2003; Zhang et al., 2004). *N*-linked glycosylation sites can be incorporated into predicted loops of integral membrane proteins via site-directed mutagenesis. Following protein expression (using either an *in vitro* or an *in vivo* expression system), glycosylation of the modified clone will be displayed by slower electrophoretic migration compared to the wild type. Digestion with protein *N*-glycosidase F (PNGase F), which removes *N*-linked oligosaccharides, can be used to confirm whether or not the shift in mobility corresponds to glycosylation (Crystal et al., 2003). One of the potential downfalls in this method is that the modifications generated to create glycosylation sites may affect the

native topology. Since glycosylation has been shown to potentially affect the topology of a protein (Goder et al., 1999), it would be wise to use additional methods to confirm *N*-linked glycosylation scanning mutagenesis results. Some investigators have been able to overcome these concerns by examining glycosylation sites already present in the protein of interest (Bungert et al., 2001).

2.7.2.4 Probing membrane topology by proteolytic mapping. Microsomal preparation containing proteins expressed *in vitro* or *in vivo* can be treated with one or more protease(s). Alternatively, intact cells containing expressed proteins can be selectively permeabilized with one or more protease(s). Only the loops exposed to the surface of the microsome are accessible to proteases. The transmembrane regions and the regions on the inside the microsome are therefore protease protected. Electrophoretic separation of the resulting polypeptides can be used to help determine which regions of the protein are on the outside of the membrane.

The conditions of proteolysis vary depending both on the protein preparation and on the investigator (Morimoto et al., 1983). Some of the commonly used enzymes for protease protection assays include trypsin (Walter and Blobel, 1983; Gonzalez-Baró et al., 2001; Lin et al., 2003), chymotrypsin (Walter and Blobel, 1983) and proteinase K (Morimoto et al., 1983; Gonzalez-Baró et al., 2001; Abell et al., 2002). Trypsin catalyzes the hydrolysis of amide bonds on the carboxyl side of arginine and lysine residues; chymotrypsin catalyzes the hydrolysis of amide bonds on the carboxyl side of aromatic or large hydrophobic residues; and proteinase K catalyzes complete hydrolysis. Although the optimum temperatures for these enzymes may be higher, protease protection assays

tend to be performed on ice to avoid the production of artifacts (Morimoto, 1983). Proteolysis is usually done in the presence of $CaCl_2$ to stabilize the microsomal vesicles and improve recovery of the protected fragments (Walter and Blobel, 1983). The reaction proceeds for 30-90 minutes and is terminated with the appropriate inhibitor and incubated on ice (Morimoto, 1983). Unprotected proteolysis control reactions are done in the presence of detergents such as Triton X-100 (Walter and Blobel, 1983; Renfrew and Hubbard, 1991; Gonzalez-Baró et al., 2001; Abell et al., 2002) and Nonidet P-40 (Gilstring and Ljungdahl, 2000).

One of the major disadvantages of proteolytic mapping, is the difficulty in confirming whether or not the protected fragment is inside the microsome or part of the lipid bilayer (Lin et al., 2003). Recently, a protease permeation method was developed to access the inside of the microsome, and the protease-protected fragments therefore correspond only to the membrane-spanning segments (Abell et al., 2002).

2.8 Topology Studies of Membrane Proteins Associated with Lipid Metabolism.

2.8.1 Membrane Topology of Oleosin. Oleosins are small hydrophobic proteins with hydrophilic N- and C-terminal portions that are targeted to oil bodies in the cytosol of developing seeds. Oil bodies are subcellular compartments of plants with a monolayer of phospholipids with a TAG enriched hydrophobic core (for review see Galili et al., 1998). While there has been speculation that the hydrophilic N- and/or C-termini of oleosin are found in the cytoplasm, Abell et al. (1997) provided evidence supporting this topology in a protease protection assay of various oleosin clones translated in a rabbit reticulocyte

lysate system in the presence of microsomes. They also found that there is no N-terminal signal sequence targeting the protein to the microsomes (Abell et al., 1997), and later demonstrated that the H-domain (the hydrophobic central domain of the primary structure) is sufficient for microsomal targeting (Abell et al., 2002).

2.8.2 Membrane Topology of Acyl-CoA:Cholesterol Acyltransferase. ACAT catalyzes the acyl-CoA dependent formation of cholesterol esters in mammalian tissues (Miyazaki et al., 2003). Two types of ACAT have been identified, ACAT1 is expressed in most tissues, whereas, ACAT2 expression is localized in the liver and intestine. Membrane topology predictions of African green monkey ACAT1 and ACAT2 revealed eight and seven transmembrane domains, respectively (Joyce et al., 2000). Using a combination of *N*-linked glycosylation, immunocytochemistry assays and protease mapping, Joyce et al., (2000) demonstrated that both ACAT1 and 2 have five transmembrane domains with the N-terminus in the cytoplasm and the C-terminus in the ER lumen. A serine residue essential for ACAT activity was found in the cytoplasm for ACAT1, and in the ER lumen for ACAT2. In contrast, human ACAT2 was shown to possess only two transmembrane domains through immunofluorescence studies (Lin et al., 2003).

2.8.3 Membrane Topology of Mitochondrial Glycerolphosphate Acyltransferase. Two membrane topology studies have been conducted on mtGPAT from rat liver (Balija et al., 2000; Gonzalez-Baró et al., 2001). Both topologies suggest the presence of two transmembrane regions, as predicted through hydropathy plot analysis. The two studies,

however, revealed opposite topologies that have not yet been reconciled. In the first study, antibodies were raised against a region in the N-terminal domain, the region between the two transmembrane domains, a region in the C-terminal domain. Immunoreactions with each of these antibodies resulted in loss of GPAT activity only with the antibody raised against the loop region. Activity remained intact for immunoreactions with antibodies raised against the N- and C-terminal domains. These data suggested that the N- and C-terminal domains were protected from the antibody (Balija et al., 2000). In protease protection assays of clones with N- and C-terminal GFP fusions, western blotting probed with anti-green fluorescent protein (GFP) antibodies revealed that both the N- and C-terminal GFP fusions were unaffected by trypsin digestion. These data supported the results from the immunoreactivity experiments that suggested that the N- and C-terminal domains are on the inner side of the outer mitochondrial membrane (Balija et al., 2000).

In the second study, the opposite topology was observed, where the N- and C-termini are located in the cytoplasm (Gonzalez-Baró et al., 2001). This second study supports previous data that the mtGPAT active site, which is located near the N-terminus, is in the cytoplasm (Hesler et al., 1985). Cytoimmunofluorescence of selectively permeabilized cells expressing several different epitope-tagged constructs were used in this study. All of the antibodies were detected in all of the clones following Triton X-100 permeation. Only the antibodies corresponding to the N- and C-terminal tags were detected following digitonin permeation, the tag between the two membrane-spanning regions was not detected.

2.8.4 Predicted Membrane Topology of Lysophosphatidyl Acyltransferase. Little structural information is available on LPAAT due to the difficulties in purifying the enzyme to homogeneity. With advances in cloning of LPAATs, more structural data is likely to become available. While no experimental structural data is available, the membrane topologies of several mitochondrial LPAATs have been predicted through hydrophobicity of the deduced amino acid sequences. Human, ovine and bovine LPAATS have four predicted transmembrane regions, with the N-terminus in the cytoplasm (Mistry and Medrano, 2002). *E. coli*, yeast and *B. napus* LPAATs have at least three predicted membrane-spanning regions (Bourgis et al., 1999), while coconut microsomal LPAAT has only two predicted transmembrane regions (Knutzon et al., 1995).

2.8.5 Predicted Membrane Topology of BnDGAT1 and BnDGAT2. Hydrophobicity analysis of BnDGAT1 and BnDGAT2 predicted by TMPRED (Hofmann and Stoffel, 1993) suggests that there are nine transmembrane regions for both enzymes (Nykiforuk et al., 2002), corresponding to BnDGAT1 residues 114-135, 159-178, 190-212, 217-239, 297-316, 394-368, 416-434, 443-459 and 468-492. A tenth putative membrane-spanning region has also been identified, BnDGAT1 residues 263-282, with a lower probability of spanning the membrane. The soluble N-terminus, absent in the BnDGAT2 sequence, is predicted to be located in the cytosol (Nykiforuk et al., 2002) where it possibly self-associates to form a tetramer (Weselake et al., 2004). Cheng et al. (2001) have demonstrated that human DGAT is a tetramer formed via self-association at the N-terminus. C-terminal truncations of human DGAT retain the ability to form tetramers,

but yield an inactive protein. Crystallographic studies are being conducted on the soluble N-terminus of BnDGAT1. Mini crystals have been generated, but they were too small for X-ray diffraction studies (Weselake et al., 2004). The conserved serine residue found in all DGATs and ACATs, S251, is found in the proposed cytosolic loop following the fourth hydrophobic domain, and is followed by the tyrosine/kinase phosphorylation signature in the same loop (Nykiforuk et al., 2002).

An invariant proline residue (P207) present in all DGATs, GPATs and LPAATs found in the third hydrophobic domain of BnDGAT1, is sandwiched between a phosphopantetheine attachment signature (residues 148-163) that spans part of the proposed lumenal loop and part of the second hydrophobic domain, and a thiolase acyl-enzyme intermediate signature (210-229) present in the third hydrophobic domain and part of the proposed lumenal loop that follows (Nykiforuk et al., 2002). Based on its proximity to these two signatures, P207 is believed to be involved in acyl-CoA substrate binding (Nykiforuk et al., 2002). Site-directed mutagenesis studies are being conducted to explore this possibility (Weselake et al., in progress). The current study investigates the membrane topology of BnDGAT1 and putative BnDGAT2 through protease mapping studies of (a) *in vitro* translated BnDGAT1 and truncations of BnDGAT1, and (b) microsomal preparations from *B. napus* cell suspension cultures followed by western blotting with two antibodies each recognizing sequences present in both BnDGAT1 and BnDGAT2.

3. MATERIALS AND METHODS

3.1 Definitions for *In Vitro* Translation Studies

cDNA encoding BnDGAT1 and BnDGAT1 truncations for *in vitro* translation reactions were named *cBDN*, where N is a number corresponding to a given clone. *cBDN* cloned into pBluescript KS+ were name pBS-BDN. The mRNA transcripts were named *mBDN*, and the translation products named BDN. BDN translation reactions run with rabbit reticulocyte lysate or wheat germ extract were name R-BDN or W-BDN. R-BDN translation reactions run in the presence of rat liver, *B. napus* or canine pancreatic microsomes were named RR-BDN, BR-BDN or CR-BDN, respectively. W-BDN translation reactions run in the presence of rat liver, *B. napus* or canine pancreatic microsomes were named RW-BDN, BW-BDN or CW-BDN, respectively.

3.2 Preparation of Microsomal Membranes for *In Vitro* Translation

Microsomal membranes were prepared from both *B. napus* cells suspension cultures and from rat liver microsomes for *in vitro* translation studies. The protocols for microsomal preparation, quantification and nuclease treatment are adapted from Walter and Blobel's (1983) preparation of canine pancreatic microsomes. Microsomes were quantified based on the absorbance at 280 nm of a 100 fold dilution of microsomal preparations in the resuspension buffers specified below and 1% SDS. Microsomal concentration units were adjusted to 50 A_{280} U mL^{-1}. If the absorbance at 280 nm of 1 μL of a microsomal preparation diluted 100 fold is 0.5, then the microsome concentration prior to dilution was 50 A_{280} U mL^{-1}. One microliter of microsome at 50 A_{280} U mL^{-1} is equal to 1 equivalent (Eq; Walter and Blobel, 1983). Fifty microliter aliquots of rat liver (1.8 Eq

μL^{-1}) and *B. napus* (0.88 Eq μL^{-1}) microsomes were frozen in liquid nitrogen and stored at –80°C. Prior to use with *in vitro* translation reactions, 50 µL rat liver or *B. napus* microsomes were treated with 40 U mL^{-1} S7 nuclease in the presence of 10 µM $CaCl_2$ for 10 min at 20°C. The addition of 25 µM ethylenebis(oxyethylenenitrilo)tetraacetic acid (EGTA), pH 8.0, was used to terminate nuclease treatment (Walter and Blobel, 1983). Unused nuclease-treated microsomes were frozen in liquid nitrogen and stored at –80°C and used in subsequent *in vitro* translation reactions. A maximum of two freeze-thaw reactions were allowed per aliquot of microsomal preparation.

3.2.1 Preparation of *Brassica napus* Microsomes. Microsomes were prepared from microspore-derived (MD) cell suspension cultures of *Brassica napus* L. cv Jet Neuf according to the method described by Abell et al. (1997) for soybean microsomal preparation. MD cell suspension culture was provided by Dr. J. Singh (Plant Research Centre, Agriculture Canada, Ottawa), and maintained since 1990 at the University of Lethbridge according to Orr et al. (1986), with a sucrose concentration of 2%. Cells were harvested and washed with water through a 60 µm nylon sieve, blotted dry and frozen in liquid nitrogen for storage at –80°C. Approximately 10 g of frozen cells were homogenized with a mortar and pestle in 50 mL homogenization buffer (250 mM sucrose, 50 mM triethanolamine (TEA), pH 7.5, 50 mM potassium acetate, pH 7.5, 5 mM magnesium acetate, 2 mM dithiothreitol (DTT)). The homogenate was centrifuged at 1000 g_{av} for 10 min, and the resulting supernatant was centrifuged at 10,000 g_{av} for 10 min and finally at 100,000 g_{av} for 60 min. All centrifugations steps were carried out at 4°C. The final pellet was slowly resuspended in 8 mL sucrose-TEA buffer (250 mM

sucrose, 25 mM TEA, pH 7.5, 4 mM DTT) using a Potter Elvehjem homogenizer. The resuspension was further diluted in 8 mL with 20 mM ethylenediaminetetraacetic acid (EDTA), 25 mM TEA (pH 7.5) and then immediately transferred to a sucrose cushion (500 mM sucrose, 25 mM TEA, pH 7.5, 25 mM potassium acetate, pH 7.5, 2 mM magnesium acetate, 4 mM DTT) at a microsome:sucrose cushion ratio of 3:1. Following a 10 min incubation on ice, the preparation was spun at 93,000 g_{av} for 90 min at 4°C. The pellet was resuspended in 1 mL resuspension buffer (250 mM sucrose, 25 mM TEA, pH 7.5, 1 mM DTT) and homogenized in two gentle strokes with a glass Potter Elvehjem homogenizer.

3.2.2 Preparation of Rat Liver Microsomes. Rat liver microsomes were prepared according to Rusinol et al. (1997). Decapitated rats were generously donated from Dr. G. Metz (Department of Neuroscience, University of Lethbridge). The livers were extracted immediately following decapitation and transferred to ice-cold buffer RA (250 mM sucrose, 50 mM TEA, pH 7.5, 50 mM potassium acetate, pH 7.5, 6 mM magnesium acetate, 1 mM EDTA, pH 7.5, 1 mM DTT, 0.5 mM phenylmethylsulfonyl fluoride (PMSF)). The livers were minced extensively with scissors and then homogenized in 4 mL of buffer RA per gram of fresh weight tissue with a mortar and pestle. The homogenate was centrifuged at 1000 g_{av} for 10 min, and the resulting supernatant was centrifuged at 10,000 g_{av} for 10 min, and the upper layer of fatty film was removed by aspiration. All centrifugations steps were carried out at 4°C. The final supernatant was transferred to a sucrose cushion (buffer RA in 1.3 M sucrose) at a supernatant:sucrose cushion ratio of 3:1, and spun at 100,000 g_{av} for 2.5 h. The supernatant, the interface and

the sucrose cushion were removed by aspiration, and the gelatinous pellet resuspended in 1 mL buffer RB (250 mM sucrose, 50 mM TEA, pH 7.5, 1 mM DTT) and homogenized with two gentle strokes with a glass Potter Elvehjem homogenizer. The microsomes were pelleted at 100,000 g_{av} for 60 min, and samples were homogenized in 0.5 mL buffer RB with two gentle strokes with a glass Potter Elvehjem homogenizer.

3.3 Membrane Topology Prediction

Four programs from the Expasy Molecular Biology Server (http://ca.expasy.org/) were used for topology predictions of the deduced BnDGAT1 and BnDGAT2 amino acid sequences: HMMTOP, (Tusnády and Simon, 1998; 2001), TMHMM (Sonnhammer, 1998; Krogh et al., 2001), TOPPRED (von Heijne, 1992; Claros and von Heijne, 1994) and TMPRED (Hofmann and Stoffel, 1993). The predicted topology of BnDGAT1 was in the rationale for the design of the genetic constructs for *in vitro* transcription/translation studies of the enzyme.

3.4 Cloning of cDNA Encoding Truncations of BnDGAT1

Primers were designed based on hydrophobicity topology prediction to generate various truncations of BnDGAT1. Forward and reverse primers incorporated an *Xba*I site to the 5' end of the cDNA and a *Swa*I to the 3' end of the cDNA, respectively (Figure 3.1). Fifty microliter polymerase chain reactions (PCR) were performed using 10 ng of full length *BnDGAT1* cloned into the pET26b vector (Novagen). Each reaction contained 1x cloned *Pfu* buffer, 0.2 mM deoxynucleoside triphosphates (dNTPs), 0.4 μM each of

Figure 3.1 Engineering restriction digest sites for cDNA ends. The gray rectangle represents the cDNA. Light gray rectangles on 5' and 3' ends of the cDNA represent the restriction sites. ATG and TGA represent the start and stop codons, respectively.

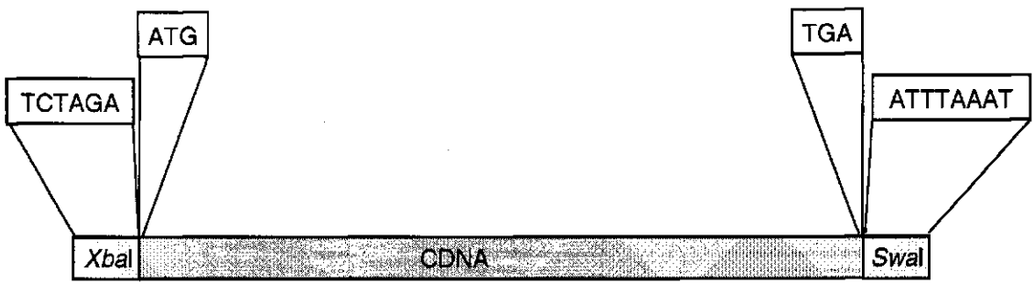
ATG
TGA
TCTAGA
ATTTAAAT
XbaI
CDNA
SwaI

forward and reverse primers, and 2.5 U cloned *Pfu* DNA polymerase (Stratagene). Following a 45 s start at 94°C, PCR reactions cycled 30 times at 94°C for 45 s, 55°C for 45 s, and 72°C for 1 min. A final extension step was run at 65°C for 10 min. PCR products were separated using agarose gel electrophoresis (1 % agarose in TAE buffer, 40 mM Tris base, 0.11 % (*v/v*) glacial acetic acid and 1 mM EDTA, pH 8.0), visualized under ultraviolet light. The DNA fragments were excised and purified with a Qiagen Gel Extraction Kit according to the manufactures protocol. The product was eluted from the column in water and ligated into the *Eco*RV site of pBluescript KS+ (Stratagene). In a 20 μL reaction, approximately 0.8 μg of pBluescript KS+ vector was linearized in the presence of 1x bovine serum albumin (BSA), 1x NE buffer 3 (New England Biolabs) and 20 U *Eco*RV (New England Biolabs). The reaction proceeded for 2 h at 37°C and terminated in a 20 min incubation at 65°C. Approximately 30 ng of PCR product was used in 20 μL ligation reactions containing 10 ng of pBluescript KS+ linearized at the *Eco*RV site, 1x T4 DNA ligase buffer, 0.5 mM adenosine 5'-triphosphate, 1 U T4 DNA ligase (Life Technology). Following a 16-h incubation at 15°C, 2 μL of the ligation reaction was incubated on ice with 50 μL of maximum efficiency DH5α competent cells for 30 min in preparation for transformation. Following a 45 s heat shock at 42°C, and the addition of 500 μL SOC (Invitrogen), the reaction was incubated at 37°C for 1 h under constant agitation. One hundred microliters of cells were plated on LB-agar containing 100 μg mL^{-1} ampicillin and incubated overnight at 37°C. Blue-white colony screening was used to select cells containing plasmids with inserts.

Colony PCR was used to confirm ligation and transformation of selected white colonies. Twenty-five microliter colony PCR reactions contained 1x PCR buffer minus

magnesium, 1.5 mM $MgCl_2$, 0.2 mM dNTPs, 0.5 μM each of forward and reverse primers, and 2.5 U *Taq* DNA polymerase (Life Technologies). The PCR reaction was inoculated with a sterile toothpick from one white colony. Following a 5-min incubation at 94°C to lyse the cells, the reaction cycled 35 times at 94°C for 1 min, 55°C for 1 min, and 72°C for 2 min. A final extension step was run at 65°C for 10 min. Products were separated via agarose gel electrophoresis (1% agarose in TAE buffer). Colonies with positive colony PCR results were used to inoculate 5 mL LB broth containing 100 μg mL^{-1} ampicillin. Following 16 h of growth at 37°C under constant agitation, 500 μL of liquid culture were mixed with 1 mL 50 % glycerol, frozen in liquid nitrogen, and stored at –80°C.

3.5 Plasmid Preparations

Streak plates on LB-agar with 100 μg mL^{-1} ampicillin were prepared from glycerol stocks. Plates were incubated overnight at 37°C. Single colonies were used to inoculate LB-broth. Cultures were grown for 16-20 h under constant agitation at 37°C. Plasmids were isolated with the SIGMA Genelute Plasmid Maxiprep kit following the manufacturer's protocol. Plasmids were resuspended in water and quantified against a Lamda/*Hind*III or Lambda/*Hind*III+*Eco*RI DNA marker on 1 % agarose electrophoresis gels in TAE buffer. Sequencing reactions were performed with ABI PRISM 377 DNA Sequencer with the ABI Prism Big Dye Terminator (Sequencing Analysis System V3.7, PE Applied Biosystems).

3.6 *In vitro* Transcription and Translation

Ten micrograms of plasmid DNA was linearized downstream of the stop codon by restriction digestion with 1 U *Swa*I per microgram of DNA. Reactions contained 1x bovine serum albumin (BSA) and 1x NE buffer 3 (New England Biolabs), and were carried out at 25°C for 16 h. The reaction was terminated with 1 μg of proteinase K per unit of *Swa*I. The DNA was purified with Qiagen's QIAquick PCR purification kit according to the manufacturer's protocol, and eluted in RNase-free water in a final volume of 50 μL. Success of restriction digest reactions were verified by agarose gel electrophoresis (1 % agarose in TAE buffer).

RNA was transcribed using Stratagene's mCAP RNA capping kit, according the manufacturers directions. T7 or T3 polymerase was used for transcription depending on the orientation of the insert in pBluescript KS+. Transcription reactions were terminated with the addition of 40 U RNase-free DNase I at 37°C for 5 min. RNA was cleaned either with (*i*) the phenol-chloroform separation followed by ethanol precipitation, as described in Stratagene's mCAP RNA capping kit manual, or (*ii*) Qiagen's RNeasy-cleanup kit according to the manufacturer's protocol. Transcribed RNA were quantified based on the absorbance at 260 nm as described by Ausubel et al. (2004) and was visualized by acrylamide-urea gel electrophoresis. Acrylamide-urea gels contained 6.84 M urea and acrylamide solution (4.3 % T, 0.2 % C) prepared in a TBE buffer (45.0 mM Tris, 1.23 mM EDTA and 44.5 mM boric acid, pH 8.3). The gels were polymerized by the addition of 0.04 % ammonium persulfate and 0.1 % N,N,N',N'-tetramethylethylenediamine. Samples were mixed with Stratagene's mCAP Stop Solution (1:1), heated for 5 min at 70°C, and separated by electrophoresis in a Biorad

electrophoresis apparatus in TBE buffer at 240 V for 30-60 min. Gels were stained with ethidium bromide and visualized under ultraviolet light. RNA transcripts (40 ng μL^{-1} final concentration) were used as a template for *in vitro* translation with either rabbit reticulocyte lysate (Promega) or wheat germ extract (Promega) systems, with [^{14}C]leucine, according to manufacturer's protocol. The translation system was supplemented with 2 μL canine pancreatic microsomes per 25 μL reactions (Promega), 2 Eq μL^{-1} rat liver microsomes or 1 Eq μL-1 *B. napus* microsomes. Translation reaction products (7 μL or 10 μL aliquots) were solubilized in sample buffer (Table 3.1) with a final volume of 14 μL or 20 μL, respectively, and incubated at room temperature for 30 min or heated in a boiling water bath for 2-3 min. Solubilized samples were separated by electrophoresis (Table 3.1) in Biorad's Mini-PROTEAN II with a 0.75 mm gel and either a 2.5 or 5.0 mm comb. Gels were fixed in 50% methanol and 10% acetic acid for 30 minutes, wrapped in Saran Wrap exposed to a multipurpose screen for 24 hrs and visualized with a Storage Phosphor Screen Phosphoimager (Canberra Packard Canada Ltd., Mississauga, Canada).

3.7 Protease Mapping of *In Vitro* Translation Reaction Products

Seven microliters of translation reaction were supplemented with 10 mM $CaCl_2$ and chilled on ice for 5 min. Proteinase K (100 μg mL^{-1}) introduced into the reaction mixture in the presence or absence of 1% Triton X-100. The reaction proceeded for 30 min on ice, and was terminated with the addition 5 mM PMSF and iced for another 5 min. Control reactions were run in the absence of Triton X-100 or proteinase K. The microsomes were pelleted by centrifugation at 220,000 g_{av} for 20 min at 4°C. Samples

Table 3.1 Conditions for protein electrophoresis. SDS-PAGE and native-PAGE from Ausubel et al. (2004) and Laemmli (1970); tricine-PAGE from Schägger and von Jagow (1987).

Gel Type	Acrylamide	Tris-HCl	pH	SDS	Glycerol	Glycine	Tricine	Urea
SDS-PAGE[a]								
Stacking Gel	4%T, 0.2%C	125 mM	6.8	0.25%	–	–	–	–
Resolving Gel	12%T, 0.6%C	375 mM	8.8	0.1%	–	–	–	–
Running Buffer	–	25 mM	–	0.1%	–	1.92 M	–	–
Sample Buffer[b]	–	25 mM	6.8	1%	5%	–	–	–
Urea Sample Buffer[b]	–	25 mM	6.8	1%	5%	–	–	4 M
Native-PAGE								
Stacking Gel	4%T, 0.2%C	125 mM	6.8	–	–	–	–	–
Resolving Gel	12%T, 0.6%C	375 mM	8.8	–	–	–	–	–
Running Buffer	–	25 mM	–	–	–	1.92 M	–	–
Sample Buffer[b]	–	25 mM	6.8	–	5%	–	–	–
Tricine-PAGE								
Stacking Gel	4%T, 3%C	744 mM	8.45	0.07%	–	–	–	–
Spacer Gel	10%T, 3%C	1 M	8.45	0.1%	–	–	–	–
Resolving Gel	16.5%T, 3%C	1 M	8.45	0.1%	–	–	–	–
Anode Buffer	–	233 mM	8.9	–	–	–	–	–
Cathode Buffer	–	100 mM	–	0.1%	–	–	100 mM	–
Sample Buffer[b]	–	50 mM	6.8	4%	12%	–	–	–

a. For continuous SDS-PAGE omit the stacking gel.
b. The sample buffer concentrations indicated are the final concentrations of sample diluted with sample buffer. Sample buffers were prepared at 2x the concentration indicated. SDS, urea and native sample buffers were supplemented with 0.05 % bromophenol blue, and the tricine sample buffer with 0.02 % Commasie-G250 as the tracking dye (final concentrations). All sample buffers were supplemented with 100 mM DTT (final concentration) immediately prior to use.

were resuspended in 10 µL tricine-sample buffer and resolved using a tricine-based SDS-PAGE system as presented in Table 3.1 (Schägger and von Jagow, 1987). Gels were transblotted in transfer buffer (25 mM Tris, 2.88 M glycine, 0.05% SDS, 20 % (*v/v*) methanol) to a 0.2 µm nitrocellulose membrane (pre-soaked in transfer buffer) at 100V for 60 min using a Biorad transfer apparatus (Towbin et al., 1979). Tricine-blots were wrapped in Saran Wrap, exposed to a multipurpose screen for 1 hr and visualized with a Storage Phosphor Screen Phosphoimager (Canberra Packard Canada Ltd., Mississauga, Canada)

3.8 Immunodetection Studies: Protease Mapping of BnDGAT1 and Putative BnDGAT2 from *B. napus* Microsomes.

An immunochemical approach was also used to probe the topology of BnDGAT1 and putative BnDGAT2. Microsomal preparations from *B. napus* cell suspension cultures were treated with proteinase K, transblotted to a nitrocellulose membrane and immunoreactions were performed with antibodies raised against two regions in BnDGAT1 defined in section 3.8.3. The residues corresponding to one of the two antigenic regions in BnDGAT1 is also present in putative BnDGAT2.

3.8.1 Preparation of *Brassica napus* Microsomes from Microspore-Derived Cell Suspension Cultures. Microsomes were prepared from MD cell suspension cultures of *Brassica napus* L. cv Jet Neuf maintained according to Orr et al. (1986), with a sucrose concentration of 6 %. Cells were harvested and washed with water through a 60 µm nylon sieve, blotted dry and frozen in liquid nitrogen for storage at –80°C.

Approximately 10 g of frozen cells were homogenized with a mortar and pestle in 40 mL grinding buffer (0.2 M HEPES-NaOH, pH 7.4, 0.5 M sucrose). The homogenate was centrifuged at 1,000 g_{av} for 30 min, and the resulting supernatant was centrifuged at 10,000 g_{av} for 30 min. All centrifugation steps were carried out at 4°C. The supernatant was filtered through 4 layers of cheesecloth and the filtrate centrifuged for 60 min at 100,000 g_{av} at 4°C. The pellet was resuspended in 2 mL resuspension buffer (100 mM HEPES-NaOH, pH 7.4) and homogenized with a Potter Elvehjem homogenizer, and then centrifuged for another 20 min 220,000 g_{av} at 4°C. The final pellet was resuspended in 1 mL resuspension buffer. Microsomes were quantified using Biorad's Bradford assay according to manufacturer's protocol. Previous electron microscopy studies in our lab have indicated that the inside of the microsome corresponds to the lumen of the ER (Weselake and Bray, unpublished data).

3.8.2 Protease Treatment. Microsomes (1 mg protein) were treated with 0.01 mg proteinase K (Invitrogen in manufacturer's buffer containing $CaCl_2$) per mg protein in a final reaction volume of 120 µL in 100 mM HEPES-NaOH, pH 7.4. The reaction proceeded for 30 min on ice, and was terminated with the addition of 0.1 mg PMSF per mg proteinase K in a final reaction volume of 150 µL, and incubated on ice for 5 min. Samples were diluted to 1 mL with resuspension buffer, and pelleted by centrifugation at 220,000 g_{av} at 4°C for 20 min. The pellets were resuspended with 150 µL sample buffer and 25 µL aliquots were prepared for electrophoresis.

3.8.3 Immunoblotting. Microsomes from protease treatment were resolved by

discontinuous sodium-dodecyl sulfate polyacrylamide gel electrophoresis (SDS-PAGE), with a 12 % resolving gel, according to Laemmli (1970). Samples were boiled in sample buffer for 2-3 min prior to electrophoresis. Following SDS-PAGE, the protein was blotted onto a nitrocellulose membrane as described in section 3.6 using a Biorad transfer apparatus at 100 V for 2 h (Towbin et al., 1979). Blots were immersed in blotto (10% skim milk powder in 100 mM Tris-HCl, pH 7.5, 0.9% NaCl, and 0.05% Tween-20) and incubated overnight at room temperature under agitation. Blots were transferred to fresh blotto containing 500 fold-dilution rabbit antiserum AbA (raised against amino acid stretch 21-LDRLHRRKSSSDSSN-35) or AbB (raised against amino acid stretch 278-CYQPSYPRSPCIRKG-292), and incubated at room temperature under agitation for 120 min. The blots were washed three times in fresh blotto; each wash consisted of a 10 min agitation at room temperature. Blots were transferred to fresh blotto containing 2857 fold-dilution goat anti-rabbit globulin (GAR), and incubated at room temperature for 90 min under agitation. The blots were washed three times in fresh blotto as described above. Biorad's Alkaline Phosphate (AP) color development was used according to manufacturer's protocol for protein detection.

4. RESULTS AND DISCUSSION

4.1 Probing the Membrane Topology of BnDGAT1 and Putative BnDGAT2

Proteolytic mapping was used as a tool to investigate BnDGAT membrane topology using both a molecular biology approach and an immunochemical approach. The molecular biology approach involves the generation of various clones used for *in vitro* transcription/translation studies in the presence of microsomal membrane preparations, followed by proteolytic mapping. The immunochemical chemical approach involves the preparation of microsomal membranes from *B. napus* cell suspension cultures followed by protease mapping and immunodetection of specific amino acid regions.

The next section presents the membrane topology scenarios of BnDGAT1 and BnDGAT2 based on computed topology predictions, and is followed by several sections pertinent to the *in vitro* translation studies of BnDGAT1. The last two sections in the Results and Discussion present the immunochemical approach to probing the membrane topology of BnDGAT1 and putative BnDGAT2.

4.2 Membrane Topology Predictions for BnDGAT1 and BnDGAT2

Prediction of membrane topology using four different programs (TMHMM, HMMTOP, TMpred, and TopPred) resulted in the identification of ten putative transmembrane helices in BnDGAT1 (Figure 4.1). These regions have been defined as TM1 through TM10, and while the specific residues corresponding to the putative membrane-spanning regions vary from program to program (Table 4.1). The consensus TM regions defined here are also presented in Table 4.1. TMHMM did not identify TM5 as a membrane-

Figure 4.1 Primary amino acid sequences for BnDGAT1 and BnDGAT2.

BnDGAT2 (341 residues long) appears to be a truncation of BnDGAT1 (503 residues long) sharing 96% sequence identity with BnDGAT1 residues 162-503. The BnDGAT1 sequence presented here is one of the variants of the consensus sequence published in the GenBank (accession number AAD445536). The variant presented was used as a template for the construction of BDN clones. The amino acid differences between the BnDGAT1 variant used in the current study and the sequence defined in the GenBank include F219L, W476G, L477S, S478A, T479S, and V488G. The BnDGAT2 sequence presented here is taken directly out of the GenBank (accession number AAD445536). Dark and light gray backgrounds indicate different amino acid sequences between the two sequences, caused by single and double nucleotide differences. BnDGAT1 and BnDGAT2 have calculated molecular masses of 56.9 and 39.4 kD, and isoelectric points of 8.4 and 8.9, respectively. A total of ten and nine putative membrane-spanning segments (boxed) have been identified in BnDGAT1and BnDGAT2, respectively, by hydrophobicity analysis (http://ca.expasy.org). One invariant proline residue and two invariant serine residues have been identified (BnDGAT1 residues P207, S237 and S25; BnDGAT2 residues P45, S75 and S89; marked with arrows). A putative acyl-CoA binding site has been identified in the N-terminus of BnDGAT1 (bold residues 96-116), and a putative tyrosine kinase phosphorylation site has been identified in BnDGAT1 (bold residues 298-320). Two antibodies, AbA and AbB, have been prepared raised against BnDGAT1 stretches A (21-LDRLHRRKSSSDSSN-35) and B (278-CYQPSYPRSPCIRKG-292), respectively (white text on black background).

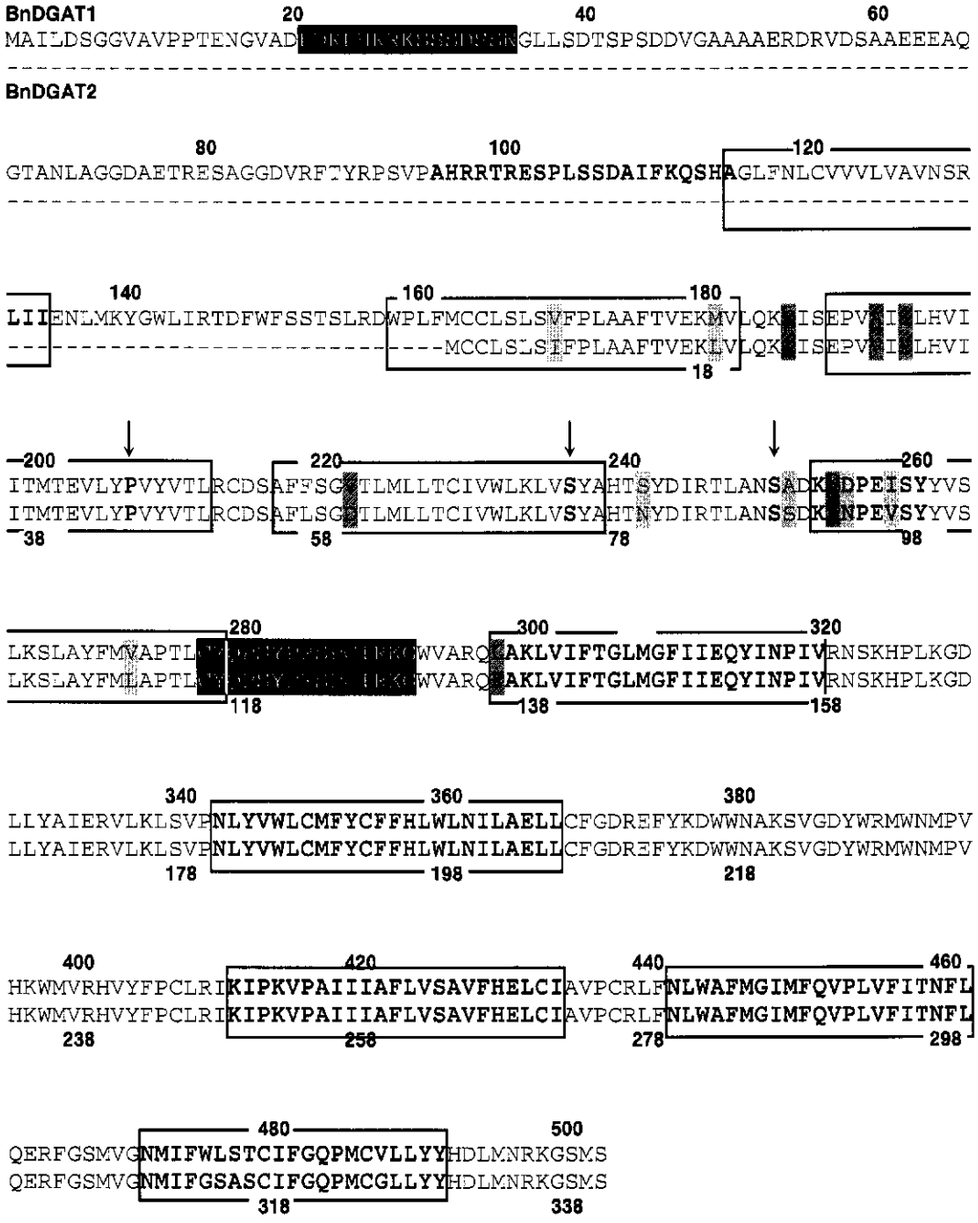
BnDGAT1
BnDGAT2

Table 4.1 Proposed membrane-spanning domains of BnDGAT1 and BnDGAT2.

The proposed membrane-spanning residues of BnDGAT1 and BnDGAT, corresponding to the regions TM1 to TM10, were predicted by TMHMM, HMMTOP, TMPRED and TOPPRED. The consensus TM regions defined here for BnDGAT1 were generated based on the combination of the TM regions defined by each program. The consensus TM regions for BnDGAT1 were used for primer design and cloning of BnDGAT1 and truncations of BnDGAT1.

	BnDGAT1					BnDGAT2			
	TMHMM	HMMTOP	TMPRED	TOPPRED	Consensus	TMHMM	HMMTOP	TMPRED	TOPPRED
TM1	116-135	116-135	114-135	113-133	116-135	—	—	—	—
TM2	159-178	159-178	159-178	159-179	159-178	—	—	1-17	1-21
TM3	190-212	191-210	190-212	190-210	190-212	28-50	28-48	29-50	28-48
TM4	217-239	216-235	217-239	216-236	216-239	55-77	57-76	55-77	54-74
TM5	—	259-278	263-282	259-279	258-279	—	97-116	101-120	97-117
TM6	298-320	301-320	297-316	297-317	298-320	136-158	131-150	135-154	135-155
TM7	346-368	341-365	349-368	345-365	345-368	184-206	184-203	187-206	183-203
TM8	408-430	418-437	416-434	416-436	415-434	246-268	256-274	254-272	254-274
TM9	440-462	443-462	443-459	442-462	442-462	278-300	281-300	281-297	280-300
TM10	474-496	468-492	468-492	466-486	472-492	312-334	311-330	306-330	304-324

spanning domain, and the remaining topology predictions indicated that TM5 has a lower probability of spanning the membrane. Two predicted topology scenarios for BnDGAT1 are presented here (Figure 4.2). In scenario 1a, all 10 predicted transmembrane helices (TM1-TM10) are membrane-spanning and the N- and C-termini are both in the cytosol. In scenario 1b, there are 9 membrane-spanning regions (corresponding to TM1-TM4, and TM6-TM10) and the N- and C-termini are in the cytosol and ER lumen, respectively. The serine residue (S251) is conserved among all type I DGATs and all ACATs identified to date (Nykiforuk et al., 2002). This residue, which has been shown to be essential for ACAT activity (Joyce et al., 2000), is localized in the cytosol in both topology scenarios 1a and 1b.

Three predicted topology scenarios for BnDGAT2 are presented here (Figure 4.2). In scenario 2a, there are 9 predicted transmembrane helices (corresponding to TM2-TM10 of BnDGAT1; TOPPRED and TMPRED) where the N-terminal residues (1-17) of BnDGAT2 are membrane-spanning (corresponding to TM2 of BnDGAT1) and the C-terminus is in the lumen of the ER. In scenario 2b, there are 8 predicted transmembrane regions (corresponding to TM3-TM10; HMMTOP) with both the N- and C-termini in the cytosol. In *scenario 2c*, there are 7 predicted transmembrane regions (corresponding to TM3-TM4, and TM6-TM10 of BnDGAT1; TMHMM) with the N- and C-termini in the cytosol and ER lumen, respectively. The conserved serine residue (S89) is found in the ER lumen in scenario 2a, and in the cytosol in scenarios 2b and 2c.

4.3 Design of Genetic Constructs

The genetic constructs for *in vitro* transcription/translation studies were designed based

Figure 4.2 Diagrams of membrane topology scenarios for BnDGAT1 and BnDGAT2. Ten putative membrane-spanning helices have been identified in BnDGAT1. The amino acid residues, and the corresponding residues of BnDGAT2, forming these putative helices have been named TM1-TM10 (numbered cylinders). Two scenarios are presented for BnDGAT1 (1a and 1b) and three for BnDGAT2 (2a, 2b and 2c). *Scenario 1a*. TM1-TM10 all span the membrane bilayer (gray rectangle). The N- and C-termini, and the invariant serine residue (black circle) are both located in the cytosol. *Scenario 1b*. TM1-TM4 and TM6-TM10 are membrane spanning. The N-terminus and the invariant serine residue are in the cytosol, and the C-terminus is in the lumen of the ER. *Scenario 2a*. TM2-TM10 are membrane spanning. TM2 is missing the homologous N-terminal residues of BnDGAT1 TM2, and there is no soluble N-terminus. The invariant serine residue and the C-terminus are in the lumen of the ER. *Scenario 2b*. TM3-TM10 are membrane spanning. The N- and C-termini and the invariant serine residue are all in the cytosol. *Scenario 2c*. TM3-TM4, TM6-TM10 are membrane-spanning. The N-terminus while the invariant serine residue are in the cytosol and the C-terminus is in the lumen of the ER.

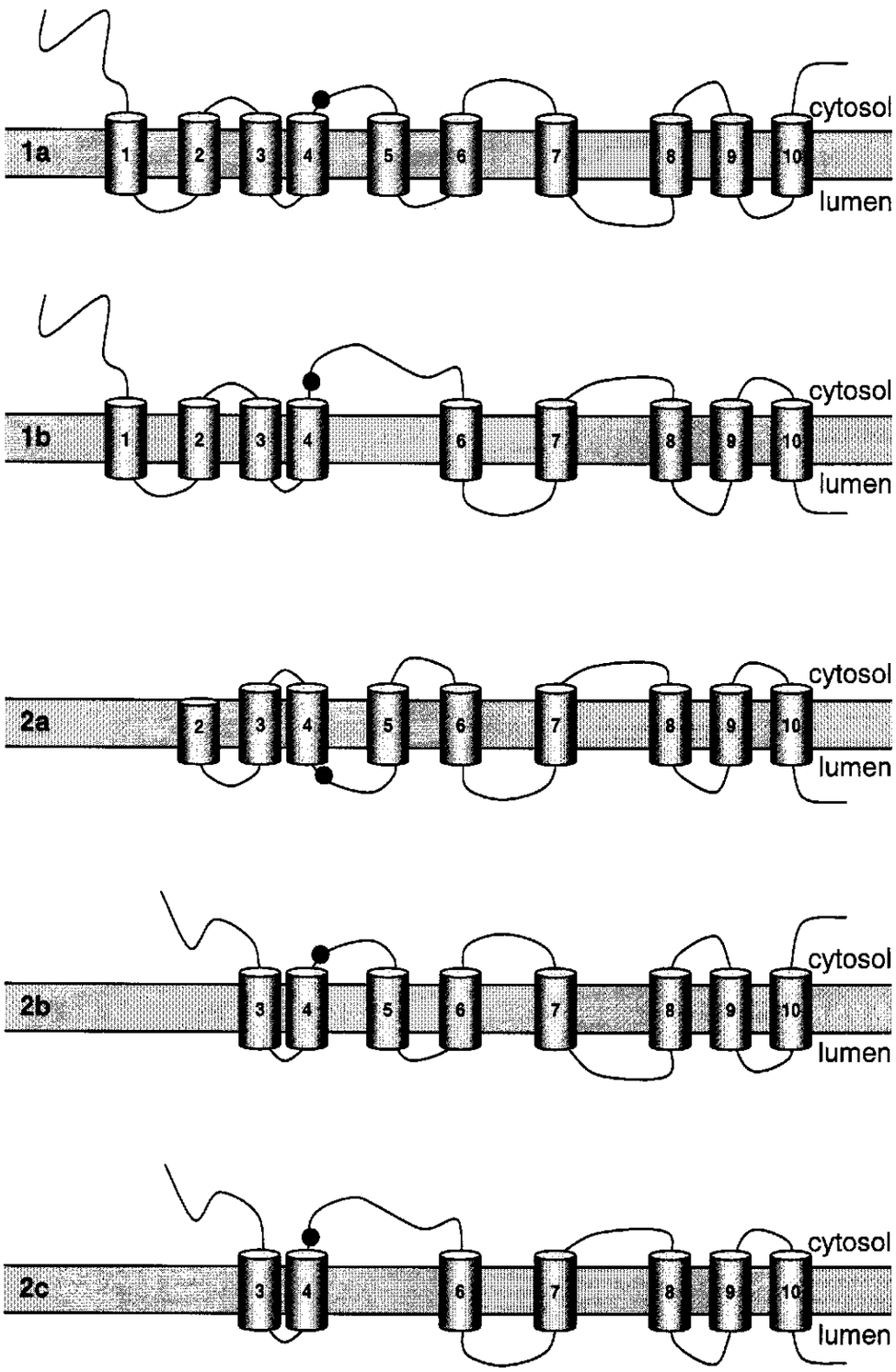
1a
1
2
3
4
5
6
7
8
9
10
cytosol
lumen
1b
1
2
3
4
6
7
8
9
10
cytosol
lumen
2a
2
3
4
5
6
7
8
9
10
cytosol
lumen
2b
3
4
5
6
7
8
9
10
cytosol
lumen
2c
3
4
6
7
8
9
10
cytosol
lumen

on the topology prediction. PCR primers were constructed to generate various truncations encoding polypeptides with one or more putative membrane-spanning regions including the downstream and upstream loops (Figure 4.3A and C). A total of 27 cDNAs can be generated with these primers, 19 of which are presented in Figure 4.4, and 11 of those were chosen as starting points for *in vitro* topology studies (Figure 4.3B). The 11 chosen cDNAs include: *cBDF* encoding full length BnDGAT1; *cBD1* encoding the single predicted membrane-spanning domain, TM1, including the upstream and downstream cytosolic and lumenal regions (or loops); *cBD12* through *cBD19* encoding C-terminal deletions of BnDGAT1 such that each clone from *cBD12* to *cBDF* sequentially excludes a predicted membrane-spanning domain from the C-terminus; and *cBD21* encoding an N-terminal deletion of BnDGAT1 designed to exclude TM1 (Figure 4.3B). The remaining 16 cDNAs include *cBD2* to *cBD10*, encoding single predicted transmembrane domains of BnDGAT1 (TM2 to TM10, respectively) including upstream and downstream cytosolic and lumenal regions, *cBD22* to *cBD28* encoding N-terminal deletions of BnDGAT1 such that each clone from *cBD22 to cBD28* sequentially excludes a predicted transmembrane domain from the N-terminus.

The 11 chosen cDNAs were successfully cloned into pBluescript KS+ DH5α, and restriction digest analysis was used to determine the orientation of each clone in the vector with respect to the T3 or T7 promoters. Clones in pBluescript KS+ were named pBS-BDN, where 'BDN' corresponds to the cDNA name. cDNAs in clones pBS-BDF, pBS-BD12, pBS-BD15, pBS-BD18, pBS-BD19, pBS-BD25, pBS-BD26 and pBS-BD29 were located upstream of the T3 promoter in pBluescript KS+. cDNAs in clones pBS-BD1, pBS-BD13, pBS-BD14, pBS-BD16, pBS-BD17 and pBS-BD21 were located

Figure 4.3 Genetic constructs of BnDGAT1 and truncations. ***A.*** The rectangle represents the amino acid sequence of BnDGAT1 (rectangle) with putative membrane-spanning coding domains (gray), numbered 1-10 for TM1-TM10. The arrows represent forward (1a-10a for BD1a-BD10a) and reverse primers (1b-10b for BD1b-BD10b). ***B.*** cDNAs encoding full length BnDGAT1 (*cBDF*) and the C-terminal truncation designed to sequentially exclude coding domains of putative membrane helices from the C-terminus (*cBD1, cBD12-cBD19*) and one N-terminal truncation (*cBD21*) designed to exclude the coding domain of the first putative membrane helix. ***C.*** Forward primers have an *Xba*I site engineered at the 5' end (italicized), followed by an ATG start codon (underlined). Reverse primers have a *Swa*I site engineered at the 5' end (italicized). A stop codon (TCA; underlined) was placed at the 5' end of the reverse primer. Bolded sequences correspond to the sequences that will prime to the template sequence.

A.

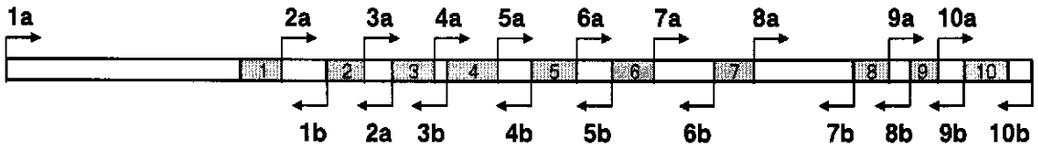

B.

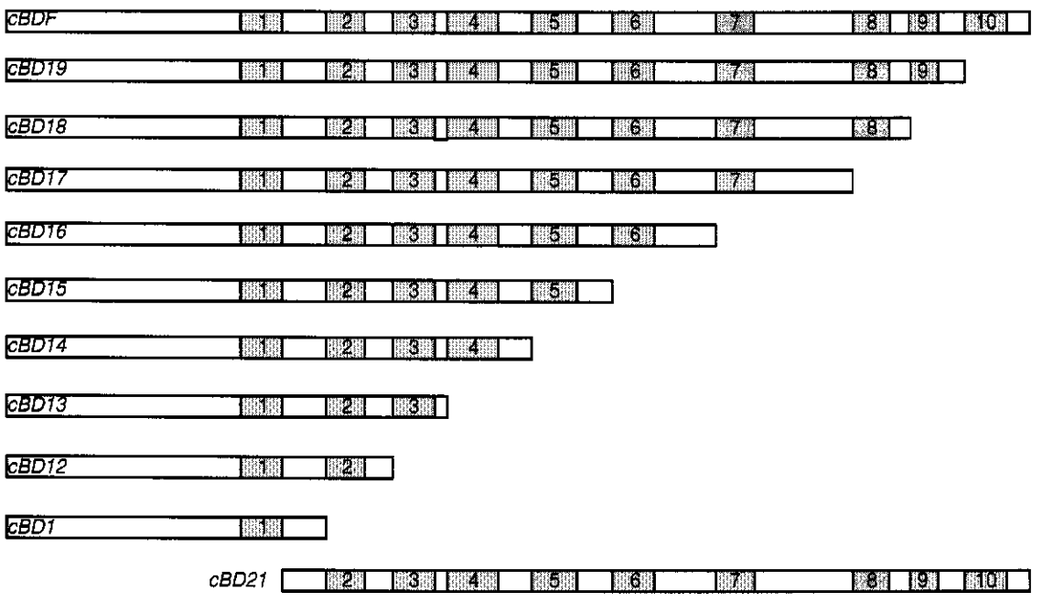

C.

BD1a 5′ *TCTAGA***ATG**GCGATTTTGGATTCTGGA 3′
BD2a 5′ *TCTAGAATG***GAAACCTCATGAAGTATGG** 3′
BD3a 5′ *TCTAGAATG***GAGAAAATGGTACTTCAGAA** 3′
BD4a 5′ *TCTAGAATG***AGGTGTGATTCTGCCTTCTT** 3′
BD5a 5′ *TCTAGAATG***CATACTAGCTACGACATAAG** 3′
BD6a 5′ *TCTAGAATG***CAGCCAAGCTATCCACGTTC** 3′
BD7a 5′ *TCTAGAATG***AGGAACTCAAAGCATCCTCT** 3′
BD8a 5′ *TCTAGAATG***TGCTTCGGGGACCGTGAATTC** 3′
BD9a 5′ *TCTAGAATG***GCAGTTCCTTGCCGTCTCTTCAA** 3′
BD10a 5′ *TCTAGAATG***CAAGAAAGGTTTGGCTCCAT** 3′
BD1b 5′ *ATTTAAATTCA***GTCTCGTAAGGATGTAGAAC** 3′
BD2b 5′ *ATTTAAATTCA***CTCAGATATGAATTTCTGAA** 3′
BD3b 5′ *ATTTAAATTCA***AGAATCACACCTCAGTGTGA** 3′
BD4b 5′ *ATTTAAATTCA***TTCAGGATCGACCTTATTATCAG** 3′
BD5b 5′ *ATTTAAATTCA***TTGACGAGCCACCCAACCCT** 3′
BD6b 5′ *ATTTAAATTCA***ATTTGGAACTGAAAGCTTCA** 3′
BD7b 5′ *ATTTAAATTCA***TTTTGGTATCTTGATGCGCA** 3′
BD8b 5′ *ATTTAAATTCA***ATTGAAGAGACGGCAAGGAA** 3′
BD9b 5′ *ATTTAAATTCA***GTTTCCCACCATGGAGCAA** 3′
BD10b 5′ *ATTTAAATTCA***GGACATGGATCCTTTGC** 3′

Figure 4.4 cDNAs encoding BnDGAT1 and truncations. One-hundred to two-hundred nanograms *cBD1* and *cBD12* to *cBD29* were loaded in lanes numbers 1 and 12 to 29, respectively. All cDNA products were of expected sizes. Samples were resolved by electrophoresis on 1 % agarose gels.

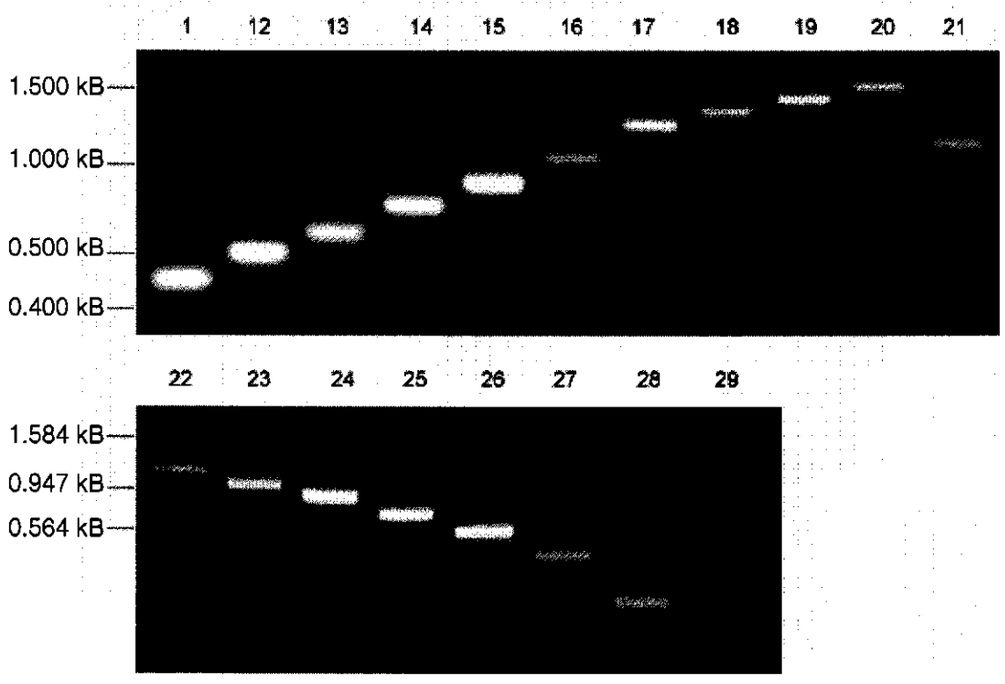
1
12
13
14
15
16
17
18
19
20
21
1.500 kB
1.000 kB
0.500 kB
0.400 kB
22
23
24
25
26
27
28
29
1.584 kB
0.947 kB
0.564 kB

upstream of the T7 in pBluescript KS+ (Figure 4.5). pBS-BD17, pBS-BD18 and pBS-BD21 lost the SwaI site and were not used for *in vitro* transcription/translation reactions. The remaining 8 clones were sequenced (Figure 4.6). A set of mutations was generated during cloning of pBS-BDF (D372A, R373G, and E374D) that was not present in any of the truncations. These mutations do not appear to affect the topology predictions (data not shown).

Messenger RNA transcription products of pBS-BDN were named *mBDN* and *in vitro* translation products of *mBDN* were named BDN. C-terminal deletion constructs were among the clones chosen for a starting point for *in vitro* translation studies for two reasons. A series of clones excluding predicted transmembrane regions would provide us with an efficient method of mapping the topology. A comparison of the protease mapping pattern of BDF with BD19 would help to confirm the presence or absence of TM10, and a comparison of the protease mapping pattern of BD19 with BD18 would help to confirm the presence or absence of TM9, and so on (Figure 4.7). No signal sequence has been identified in BnDGAT1 and while there are integral membrane proteins with signal sequences identified near the C-terminus (Carrere-Kremer et al., 2002), more often then not, signal sequences are found near the N-terminus (Fehrmann et al., 2003). For this reason, C-terminal deletions were chosen as a starting point for *in vitro* translation studies. N-terminal deletion construct pBS-BD21 was selected to verify the impact of this region in BnDGAT1. It is important to note the BD21 has all the sequences (and more) that are present in BnDGAT2. If BnDGAT1 and BnDGAT2 share the same topology, then the absence of the N-terminus and TM1 in BD21 would not likely have an impact on the topology. If the first transmembrane helix is a signal

Figure 4.5 cDNA orientation in pBluescript II KS +. ***A.*** cDNA were generated with an *Xba*I site upstream of the ATG start codon, and a *Swa*I at the 3' end, and cloned into the *EcoR*V site of pBluescript II KS + (Stratagene). ***B.*** Following digestion with *Xba*I, all clones in orientation for expression with the T3 promoter will release a product approximately equal to the size of the cDNA, while clones in orientation for expression with the T7 promoter will excise a product of approximately 40 base pairs (the distance between the *Xba*I site in the vector and the *Xba*I site from the cDNA). The 40 base pair product is too small to resolve on 1 % agarose gels, and would therefore not be visualized. Following digestion with *Spe*I and *Xho*I, all clones should generate products approximately equal in size to the cDNA, thus confirming successful cloning of the cDNA into pBluescript II KS +. Uncut pBS-BDN clones were run as a control to confirm successful digestion with *Xba*I or *Xho*I and *Spe*I.

A.

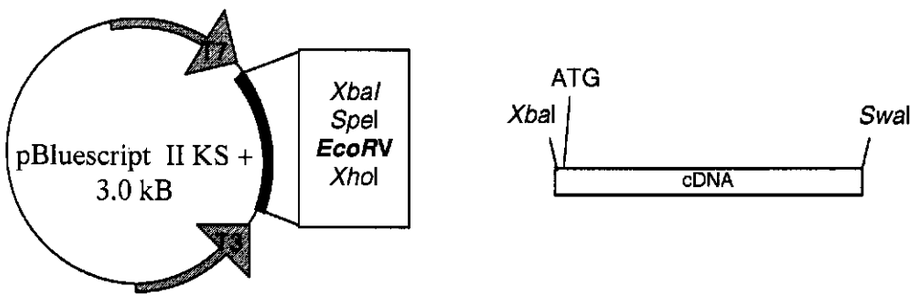
T7
pBluescript II KS +
3.0 kB
T3
XbaI
SpeI
EcoRV
XhoI
ATG
XbaI
SwaI
cDNA

B.

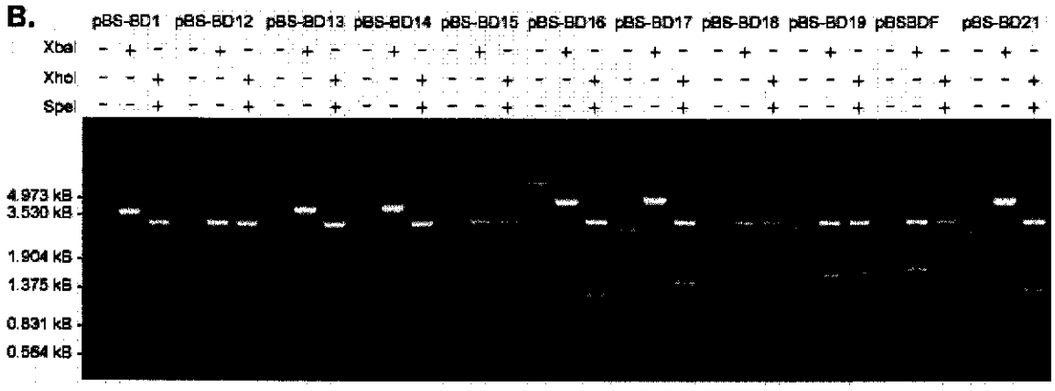
pBS-BD1
pBS-BD12
pBS-BD13
pBS-BD14
pBS-BD15
pBS-BD16
pBS-BD17
pBS-BD18
pBS-BD19
pBSBDF
pBS-BD21
XbaI
XhoI
SpeI
4.973 kB
3.530 kB
1.904 kB
1.375 kB
0.831 kB
0.564 kB

Figure 4.6 cDNA sequencing of BnDGAT1 clones. Nucleotide regions encoding TM1-TM10 are presented in bold. Three single nucleotide mutations were observed in the pBS-BDF clone (white font on black background), which translate into three mutations in the deduced polypeptide sequence of BDF (D372A, R373G, and E374D).

```
          1
BnDGAT1   atggcgattttggattctggaggcgtcgctgtaccgccgacggagaacggcgtcgcggatctcgacaggctccaccgtc
pBS-BD1   atggcgattttggattctggaggcgtcgctgtaccgccgacggagaacggcgtcgcggatctcgacaggctccaccgtc
pBS-BD12  atggcgattttggattctggaggcgtcgctgtaccgccgacggagaacggcgtcgcggatctcgacaggctccaccgtc
pBS-BD13  atggcgattttggattctggaggcgtcgctgtaccgccgacggagaacggcgtcgcggatctcgacaggctccaccgtc
pBS-BD14  atggcgattttggattctggaggcgtcgctgtaccgccgacggagaacggcgtcgcggatctcgacaggctccaccgtc
pBS-BD15  atggcgattttggattctggaggcgtcgctgtaccgccgacggagaacggcgtcgcggatctcgacaggctccaccgtc
pBS-BD16  atggcgattttggattctggaggcgtcgctgtaccgccgacggagaacggcgtcgcggatctcgacaggctccaccgtc
pBS-BD17  atggcgattttggattctggaggcgtcgctgtaccgccgacggagaacggcgtcgcggatctcgacaggctccaccgtc
pBS-BD18  atggcgattttggattctggaggcgtcgctgtaccgccgacggagaacggcgtcgcggatctcgacaggctccaccgtc
pBS-BD19  atggcgattttggattctggaggcgtcgctgtaccgccgacggagaacggcgtcgcggatctcgacaggctccaccgtc
pBS-BDF   atggcgattttggattctggaggcgtcgctgtaccgccgacggagaacggcgtcgcggatctcgacaggctccaccgtc

          80
BnDGAT1   gtaaatcgagttcggattcttccaacggactcctctccgatacttccccgtcggacgatgttggagctgcggcggccga
pBS-BD1   gtaaatcgagttcggattcttccaacggactcctctccgatacttccccgtcggacgatgttggagctgcggcggccga
pBS-BD12  gtaaatcgagttcggattcttccaacggactcctctccgatacttccccgtcggacgatgttggagctgcggcggccga
pBS-BD13  gtaaatcgagttcggattcttccaacggactcctctccgatacttccccgtcggacgatgttggagctgcggcggccga
pBS-BD14  gtaaatcgagttcggattcttccaacggactcctctccgatacttccccgtcggacgatgttggagctgcggcggccga
pBS-BD15  gtaaatcgagttcggattcttccaacggactcctctccgatacttccccgtcggacgatgttggagctgcggcggccga
pBS-BD16  gtaaatcgagttcggattcttccaacggactcctctccgatacttccccgtcggacgatgttggagctgcggcggccga
pBS-BD17  gtaaatcgagttcggattcttccaacggactcctctccgatacttccccgtcggacgatgttggagctgcggcggccga
pBS-BD18  gtaaatcgagttcggattcttccaacggactcctctccgatacttccccgtcggacgatgttggagctgcggcggccga
pBS-BD19  gtaaatcgagttcggattcttccaacggactcctctccgatacttccccgtcggacgatgttggagctgcggcggccga
pBS-BDF   gtaaatcgagttcggattcttccaacggactcctctccgatacttccccgtcggacgatgttggagctgcggcggccga

          159
BnDGAT1   aagggatcgggttgattccgctgccgaggaggaggctcagggaacagcgaatttagctggcggagatgccgaaactagg
pBS-BD1   aagggatcgggttgattccgctgccgaggaggaggctcagggaacagcgaatttagctggcggagatgccgaaactagg
pBS-BD12  aagggatcgggttgattccgctgccgaggaggaggctcagggaacagcgaatttagctggcggagatgccgaaactagg
pBS-BD13  aagggatcgggttgattccgctgccgaggaggaggctcagggaacagcgaatttagctggcggagatgccgaaactagg
pBS-BD14  aagggatcgggttgattccgctgccgaggaggaggctcagggaacagcgaatttagctggcggagatgccgaaactagg
pBS-BD15  aagggatcgggttgattccgctgccgaggaggaggctcagggaacagcgaatttagctggcggagatgccgaaactagg
pBS-BD16  aagggatcgggttgattccgctgccgaggaggaggctcagggaacagcgaatttagctggcggagatgccgaaactagg
pBS-BD17  aagggatcgggttgattccgctgccgaggaggaggctcagggaacagcgaatttagctggcggagatgccgaaactagg
pBS-BD18  aagggatcgggttgattccgctgccgaggaggaggctcagggaacagcgaatttagctggcggagatgccgaaactagg
pBS-BD19  aagggatcgggttgattccgctgccgaggaggaggctcagggaacagcgaatttagctggcggagatgccgaaactagg
pBS-BDF   aagggatcgggttgattccgctgccgaggaggaggctcagggaacagcgaatttagctggcggagatgccgaaactagg

          238
BnDGAT1   gaatccgccggaggcgatgtaaggtttacgtatcgaccgtcggttccagctcatcggaggacgagggagagtcctctca
pBS-BD1   gaatccgccggaggcgatgtaaggtttacgtatcgaccgtcggttccagctcatcggaggacgagggagagtcctctca
pBS-BD12  gaatccgccggaggcgatgtaaggtttacgtatcgaccgtcggttccagctcatcggaggacgagggagagtcctctca
pBS-BD13  gaatccgccggaggcgatgtaaggtttacgtatcgaccgtcggttccagctcatcggaggacgagggagagtcctctca
pBS-BD14  gaatccgccggaggcgatgtaaggtttacgtatcgaccgtcggttccagctcatcggaggacgagggagagtcctctca
pBS-BD15  gaatccgccggaggcgatgtaaggtttacgtatcgaccgtcggttccagctcatcggaggacgagggagagtcctctca
pBS-BD16  gaatccgccggaggcgatgtaaggtttacgtatcgaccgtcggttccagctcatcggaggacgagggagagtcctctca
pBS-BD17  gaatccgccggaggcgatgtaaggtttacgtatcgaccgtcggttccagctcatcggaggacgagggagagtcctctca
pBS-BD18  gaatccgccggaggcgatgtaaggtttacgtatcgaccgtcggttccagctcatcggaggacgagggagagtcctctca
pBS-BD19  gaatccgccggaggcgatgtaaggtttacgtatcgaccgtcggttccagctcatcggaggacgagggagagtcctctca
pBS-BDF   gaatccgccggaggcgatgtaaggtttacgtatcgaccgtcggttccagctcatcggaggacgagggagagtcctctca

          317
BnDGAT1   gctccgacgctatcttcaaacaaagccatgcaggattgttcaacctctgtgtagttgttcttgttgctgttaacagtag
pBS-BD1   gctccgacgctatcttcaaacaaagccatgcaggattgttcaacctctgtgtagttgttcttgttgctgttaacagtag
pBS-BD12  gctccgacgctatcttcaaacaaagccatgcaggattgttcaacctctgtgtagttgttcttgttgctgttaacagtag
pBS-BD13  gctccgacgctatcttcaaacaaagccatgcaggattgttcaacctctgtgtagttgttcttgttgctgttaacagtag
pBS-BD14  gctccgacgctatcttcaaacaaagccatgcaggattgttcaacctctgtgtagttgttcttgttgctgttaacagtag
pBS-BD15  gctccgacgctatcttcaaacaaagccatgcaggattgttcaacctctgtgtagttgttcttgttgctgttaacagtag
pBS-BD16  gctccgacgctatcttcaaacaaagccatgcaggattgttcaacctctgtgtagttgttcttgttgctgttaacagtag
pBS-BD17  gctccgacgctatcttcaaacaaagccatgcaggattgttcaacctctgtgtagttgttcttgttgctgttaacagtag
pBS-BD18  gctccgacgctatcttcaaacaaagccatgcaggattgttcaacctctgtgtagttgttcttgttgctgttaacagtag
pBS-BD19  gctccgacgctatcttcaaacaaagccatgcaggattgttcaacctctgtgtagttgttcttgttgctgttaacagtag
pBS-BDF   gctccgacgctatcttcaaacaaagccatgcaggattgttcaacctctgtgtagttgttcttgttgctgttaacagtag
```

```
          396
BnDGAT1   actcatcatcgaaaacctcatgaagtatggttggttgatcagaactgatttttggtttagttctacatccttacgagac
pBS-BD1   actcatcatcgaaaacctcatgaagtatggttggttgatcagaactgatttttggtttagttctacatccttacgagac
pBS-BD12  actcatcatcgaaaacctcatgaagtatggttggttgatcagaactgatttttggtttagttctacatccttacgagac
pBS-BD13  actcatcatcgaaaacctcatgaagtatggttggttgatcagaactgatttttggtttagttctacatccttacgagac
pBS-BD14  actcatcatcgaaaacctcatgaagtatggttggttgatcagaactgatttttggtttagttctacatccttacgagac
pBS-BD15  actcatcatcgaaaacctcatgaagtatggttggttgatcagaactgatttttggtttagttctacatccttacgagac
pBS-BD16  actcatcatcgaaaacctcatgaagtatggttggttgatcagaactgatttttggtttagttctacatccttacgagac
pBS-BD17  actcatcatcgaaaacctcatgaagtatggttggttgatcagaactgatttttggtttagttctacatccttacgagac
pBS-BD18  actcatcatcgaaaacctcatgaagtatggttggttgatcagaactgatttttggtttagttctacatccttacgagac
pBS-BD19  actcatcatcgaaaacctcatgaagtatggttggttgatcagaactgatttttggtttagttctacatccttacgagac
pBS-BDF   actcatcatcgaaaacctcatgaagtatggttggttgatcagaactgatttttggtttagttctacatccttacgagac

          475
BnDGAT1   tggccgcttttcatgtgttgtctttcactttcggtctttccttttggctgccttcacggtcgagaaaatggtacttcaga
pBS-BD12  tggccgcttttcatgtgttgtctttcactttcggtctttccttttggctgccttcacggtcgagaaaatggtacttcaga
pBS-BD13  tggccgcttttcatgtgttgtctttcactttcggtctttccttttggctgccttcacggtcgagaaaatggtacttcaga
pBS-BD14  tggccgcttttcatgtgttgtctttcactttcggtctttccttttggctgccttcacggtcgagaaaatggtacttcaga
pBS-BD15  tggccgcttttcatgtgttgtctttcactttcggtctttccttttggctgccttcacggtcgagaaaatggtacttcaga
pBS-BD16  tggccgcttttcatgtgttgtctttcactttcggtctttccttttggctgccttcacggtcgagaaaatggtacttcaga
pBS-BD17  tggccgcttttcatgtgttgtctttcactttcggtctttccttttggctgccttcacggtcgagaaaatggtacttcaga
pBS-BD18  tggccgcttttcatgtgttgtctttcactttcggtctttccttttggctgccttcacggtcgagaaaatggtacttcaga
pBS-BD19  tggccgcttttcatgtgttgtctttcactttcggtctttccttttggctgccttcacggtcgagaaaatggtacttcaga
pBS-BDF   tggccgcttttcatgtgttgtctttcactttcggtctttccttttggctgccttcacggtcgagaaaatggtacttcaga

          554
BnDGAT1   aattcatatctgagcctgttgccatcattcttcatgtcattataaccatgacagaggtcttgtatccagtctacgtcac
pBS-BD12  aattcatatctgag
pBS-BD13  aattcatatctgagcctgttgccatcattcttcatgtcattataaccatgacagaggtcttgtatccagtctacgtcac
pBS-BD14  aattcatatctgagcctgttgccatcattcttcatgtcattataaccatgacagaggtcttgtatccagtctacgtcac
pBS-BD15  aattcatatctgagcctgttgccatcattcttcatgtcattataaccatgacagaggtcttgtatccagtctacgtcac
pBS-BD16  aattcatatctgagcctgttgccatcattcttcatgtcattataaccatgacagaggtcttgtatccagtctacgtcac
pBS-BD17  aattcatatctgagcctgttgccatcattcttcatgtcattataaccatgacagaggtcttgtatccagtctacgtcac
pBS-BD18  aattcatatctgagcctgttgccatcattcttcatgtcattataaccatgacagaggtcttgtatccagtctacgtcac
pBS-BD19  aattcatatctgagcctgttgccatcattcttcatgtcattataaccatgacagaggtcttgtatccagtctacgtcac
pBS-BDF   aattcatatctgagcctgttgccatcattcttcatgtcattataaccatgacagaggtcttgtatccagtctacgtcac

          633
BnDGAT1   actgaggtgtgattctgccttcttgtcaggtgtcacgttgatgctgctcacttgcattgtgtggctgaagttggtttct
pBS-BD13  actgaggtgtgattct
pBS-BD14  actgaggtgtgattctgccttcttgtcaggtgtcacgttgatgctgctcacttgcattgtgtggctgaagttggtttct
pBS-BD15  actgaggtgtgattctgccttcttgtcaggtgtcacgttgatgctgctcacttgcattgtgtggctgaagttggtttct
pBS-BD16  actgaggtgtgattctgccttcttgtcaggtgtcacgttgatgctgctcacttgcattgtgtggctgaagttggtttct
pBS-BD17  actgaggtgtgattctgccttcttgtcaggtgtcacgttgatgctgctcacttgcattgtgtggctgaagttggtttct
pBS-BD18  actgaggtgtgattctgccttcttgtcaggtgtcacgttgatgctgctcacttgcattgtgtggctgaagttggtttct
pBS-BD19  actgaggtgtgattctgccttcttgtcaggtgtcacgttgatgctgctcacttgcattgtgtggctgaagttggtttct
pBS-BDF   actgaggtgtgattctgccttcttgtcaggtgtcacgttgatgctgctcacttgcattgtgtggctgaagttggtttct

          712
BnDGAT1   tacgctcatactagctacgacataagaaccctggccaattcagctgataaggtcgatcctgaaatctcctactatgtta
pBS-BD14  tacgctcatactagctacgacataagaaccctggccaattcagctgataaggtcgatcctgaaatctcc
pBS-BD15  tacgctcatactagctacgacataagaaccctggccaattcagctgataaggtcgatcctgaaatctcctactatgtta
pBS-BD16  tacgctcatactagctacgacataagaaccctggccaattcagctgataaggtcgatcctgaaatctcctactatgtta
pBS-BD17  tacgctcatactagctacgacataagaaccctggccaattcagctgataaggtcgatcctgaaatctcctactatgtta
pBS-BD18  tacgctcatactagctacgacataagaaccctggccaattcagctgataaggtcgatcctgaaatctcctactatgtta
pBS-BD19  tacgctcatactagctacgacataagaaccctggccaattcagctgataaggtcgatcctgaaatctcctactatgtta
pBS-BDF   tacgctcatactagctacgacataagaaccctggccaattcagctgataaggtcgatcctgaaatctcctactatgtta

          701
BnDGAT1   gcttgaagagcttggcgtatttcatggttgctcccacactgtgttatcagccaagctatccacgttctccatgtatccg
pBS-BD15  gcttgaagagcttggcgtatttcatggttgctcccacactgtgttatcagccaagctatccacgttctccatgtatccg
pBS-BD16  gcttgaagagcttggcgtatttcatggttgctcccacactgtgttatcagccaagctatccacgttctccatgtatccg
pBS-BD17  gcttgaagagcttggcgtatttcatggttgctcccacactgtgttatcagccaagctatccacgttctccatgtatccg
pBS-BD18  gcttgaagagcttggcgtatttcatggttgctcccacactgtgttatcagccaagctatccacgttctccatgtatccg
pBS-BD19  gcttgaagagcttggcgtatttcatggttgctcccacactgtgttatcagccaagctatccacgttctccatgtatccg
pBS-BDF   gcttgaagagcttggcgtatttcatggttgctcccacactgtgttatcagccaagctatccacgttctccatgtatccg
```

```
          870
BnDGAT1   gaagggttgggtggctcgtcaatttgcaaaactggtcatattcactggactcatgggatttataatagagcaatatata
pBS-BD15  gaagggttgggtggctcgtcaa
pBS-BD16  gaagggttgggtggctcgtcaatttgcaaaactggtcatattcactggactcatgggatttataatagagcaatatata
pBS-BD17  gaagggttgggtggctcgtcaatttgcaaaactggtcatattcactggactcatgggatttataatagagcaatatata
pBS-BD18  gaagggttgggtggctcgtcaatttgcaaaactggtcatattcactggactcatgggatttataatagagcaatatata
pBS-BD19  gaagggttgggtggctcgtcaatttgcaaaactggtcatattcactggactcatgggatttataatagagcaatatata
pBS-BDF   gaagggttgggtggctcgtcaatttgcaaaactggtcatattcactggactcatgggatttataatagagcaatatata

          949
BnDGAT1   aatcctattgttaggaactcaaagcatcctctgaaaggggaccttctatatgctattgaaagagtgttgaagctttcag
pBS-BD15  aatcctattgttaggaactcaaagcatcctctgaaaggggaccttctatatgctattgaaagagtgttgaagctttcag
pBS-BD16  aatcctattgttaggaactcaaagcatcctctgaaaggggaccttctatatgctattgaaagagtgttgaagctttcag
pBS-BD17  aatcctattgttaggaactcaaagcatcctctgaaaggggaccttctatatgctattgaaagagtgttgaagctttcag
pBS-BD18  aatcctattgttaggaactcaaagcatcctctgaaaggggaccttctatatgctattgaaagagtgttgaagctttcag
pBS-BD19  aatcctattgttaggaactcaaagcatcctctgaaaggggaccttctatatgctattgaaagagtgttgaagctttcag
pBS-BDF   aatcctattgttaggaactcaaagcatcctctgaaaggggaccttctatatgctattgaaagagtgttgaagctttcag

          1038
BnDGAT1   ttccaaatctatatgtgtggctctgcatgttctactgcttcttccacctttggttaaacatattggcagagctcctctg
pBS-BD16  ttccaaat
pBS-BD17  ttccaaatctatatgtgtggctctgcatgttctactgcttcttccacctttggttaaacatattggcagagctcctctg
pBS-BD18  ttccaaatctatatgtgtggctctgcatgttctactgcttcttccacctttggttaaacatattggcagagctcctctg
pBS-BD19  ttccaaatctatatgtgtggctctgcatgttctactgcttcttccacctttggttaaacatattggcagagctcctctg
pBS-BDF   ttccaaatctatatgtgtggctctgcatgttctactgcttcttccacctttggttaaacatattggcagagctcctctg

          1107
BnDGAT1   cttcggggaccgtgaattctacaaagattggtggaatgcaaaaagcgttggagattattggagaatgtggaatatgcct
pBS-BD17  cttcggggaccgtgaattctacaaagattggtggaatgcaaaaagcgttggagattattggagaatgtggaatatgcct
pBS-BD18  cttcggggaccgtgaattctacaaagattggtggaatgcaaaaagcgttggagattattggagaatgtggaatatgcct
pBS-BD19  cttcggggaccgtgaattctacaaagattggtggaatgcaaaaagcgttggagattattggagaatgtggaatatgcct
pBS-BDF   cttcgggg[ ][ ]gtga[ ]ttctacaaagattggtggaatgcaaaaagcgttggagattattggagaatgtggaatatgcct

          1186
BnDGAT1   gttcacaaatggatggttcgacatgtatactttccgtgcctgcgcatcaagataccaaaagtacccgccattatcattg
pBS-BD17  gttcacaaatggatggttcgacatgtatactttccgtgcctgcgcatcaagataccaaaa
pBS-BD18  gttcacaaatggatggttcgacatgtatactttccgtgcctgcgcatcaagataccaaaagtacccgccattatcattg
pBS-BD19  gttcacaaatggatggttcgacatgtatactttccgtgcctgcgcatcaagataccaaaagtacccgccattatcattg
pBS-BDF   gttcacaaatggatggttcgacatgtatactttccgtgcctgcgcatcaagataccaaaagtacccgccattatcattg

          1265
BnDGAT1   ctttcttagtctctgcagtctttcatgagttatgcatcgcagttccttgccgtctcttcaatctatgggctttcatggg
pBS-BD18  ctttcttagtctctgcagtctttcatgagttatgcatcgcagttccttgccgtctcttcaat
pBS-BD19  ctttcttagtctctgcagtctttcatgagttatgcatcgcagttccttgccgtctcttcaatctatgggctttcatggg
pBS-BDF   ctttcttagtctctgcagtctttcatgagttatgcatcgcagttccttgccgtctcttcaatctatgggctttcatggg

          1344
BnDGAT1   aattatgtttcaggtccctttggtctttatcacaaacttttttacaagaaaggtttggctccatggtgggaaacatgatc
pBS-BD19  aattatgtttcaggtccctttggtctttatcacaaacttttttacaagaaaggtttggctccatggtgggaaac
pBS-BDF   aattatgtttcaggtccctttggtctttatcacaaacttttttacaagaaaggtttggctccatggtgggaaacatgatc

          1423
BnDGAT1   tttggttcagcttcttgcattttcggacaaccgatgtgtgggcttctttattaccatgacctgatgaaccgcaaaggat
pBS-BDF   tttggttcagcttcttgcattttcggacaaccgatgtgtgggcttctttattaccatgacctgatgaaccgcaaaggat

          1502
BnDGAT1   ccatgtcctga
pBS-BDF   ccatgtcctga
```

Figure 4.7 Predicted protease mapping for the different truncations of BnDGAT1. ***A.*** Primary sequence of BnDGAT1 with numbered gray rectangles representing putative membrane helices. Figures *B-E* represents possible scenarios of BnDGAT and the expected protease mapping results. Rectangles represent primary sequence of the BDF, BD19, BD16 or BD15 with black rectangles representing protease-protected loops according to BnDGAT1 topology scenario 1a where TM1-TM10 are all membrane-spanning (Figures *B* and *D*) and scenario 1b where TM1-TM4, and TM6-TM10 are membrane-spanning (Figures *C* and *E*). BDF-PK, BD19-PK, BD16-PK or BD15-PK rectangles represent the protease-protected fragments of BDF, BD19, BD16 and BD15, respectively. ***B.*** If TM1-TM10 are all membrane-spanning regions and the N-terminus is in the cytosol (as predicted by topology scenario 1a) then 5 fragments would be protected in both BD19 and BDF, where one of the 5 fragments would be smaller in BD19 than in BDF. ***C.*** If TM1-TM9 are membrane-spanning domains (black font on gray background), and TM10 is not (white font on gray background) and the N-terminus is in the cytosol, then 5 fragments would be protected in both BD19 and BDF, where one of the 5 fragments would be smaller in BD19 than in BDF. ***D.*** The usefulness of sequential truncations is most evident when comparing BD16 to BD15. If TM1-TM10 are all membrane spanning domains and the N-terminus is in the cytosol, as predicted by topology scenario 1a, then three fragments would be protected in both BD15 and BD16. ***E.*** If TM1-TM4, and TM6-TM10 are membrane-spanning domains, and TM5 is not, as predicted by topology scenario 1b, then 3 fragments would be protected in both BD16 and only 2 fragments will be protected in BD15.

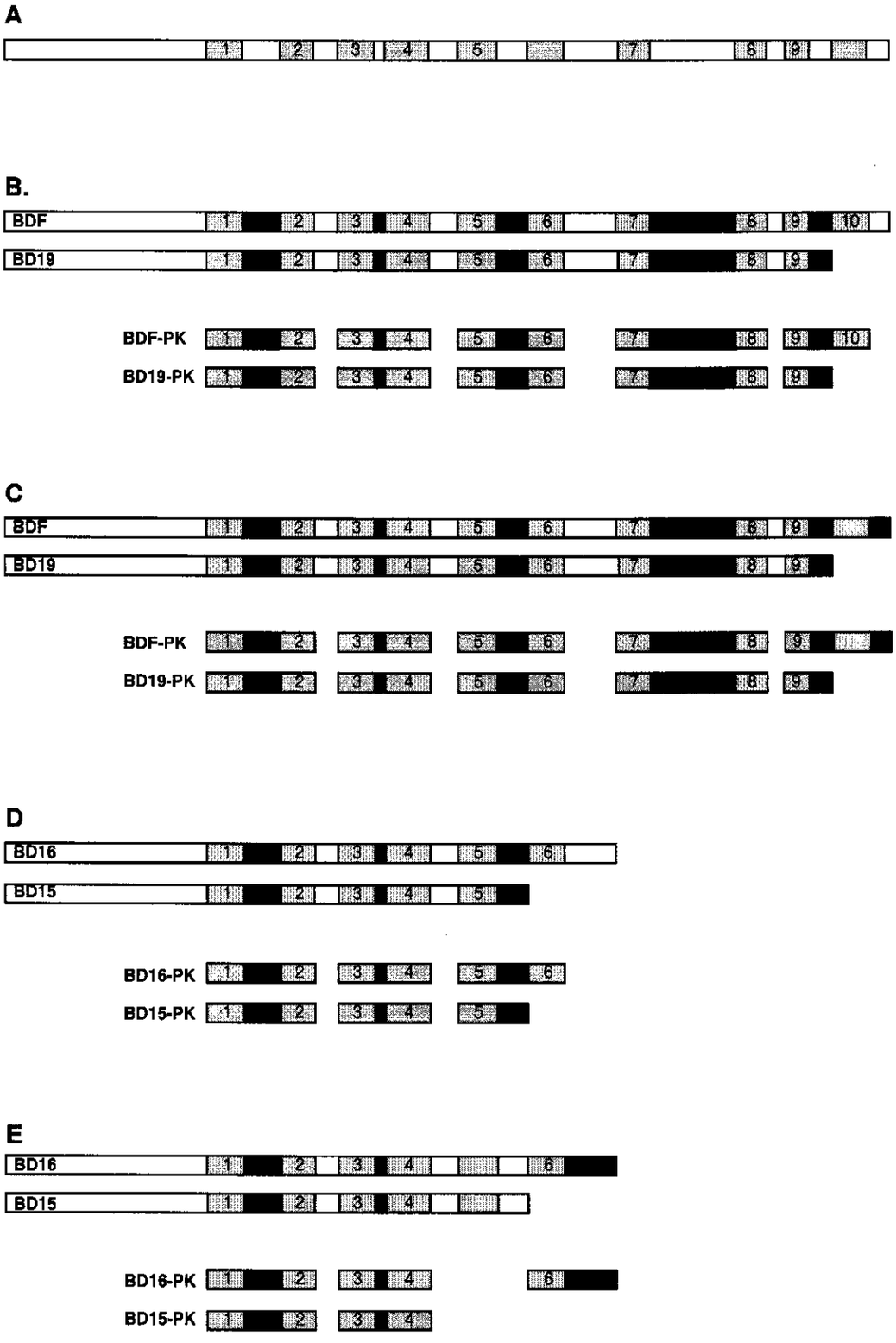
A
B.
BDF
BD19
BDF-PK
BD19-PK
C
BDF
BD19
BDF-PK
BD19-PK
D
BD16
BD15
BD16-PK
BD15-PK
E
BD16
BD15
BD16-PK
BD15-PK

sequence, then BD21 may not be incorporated into the microsome and fold properly, unless the BnDGAT1 signal and stop-sequences are interchangeable in the translation systems used here (Audigier et al., 1987; Spiess et al., 1989). If the domains are not interchangeable, and if the signal sequence is located at or upstream of TM1, then BD21 would not incorporate properly into the microsome (Figure 4.8A, B). If the domains are interchangeable, any truncation possessing membrane-spanning segments (including BD21) would successfully incorporate into the microsome. It is possible, in this case, that the opposite topology would be observed (Figure 4.8A, C). In other words, the cytosolic domains would be observed in the ER lumen and vice versa. If BD21 were to incorporate and fold into microsomes with the correct topology, then the ER targeting sequence may be located downstream of TM1. If an ER targeting sequence were in fact located downstream of TM1, then BD1 would not incorporate successfully into the microsome since TM1 is the only putative membrane-spanning segment present in BD1. If an ER targeting sequence is located closer to the C-terminus, then many of the C-terminal deletion clones would not fold properly into the microsomes. In this case, the N-terminal deletion clones could be used for *in vitro* transcription/translation.

4.4 Production of Recombinant BnDGAT in *Escherichia coli*

All of the bacterial cultures of clones under control of the T3 promoter grew less vigorously than the clones under control of the T7 promoter, and consequently plasmid yields were significantly lower (data not shown). In order to produce reasonable plasmid yields, cultures for clones under control of the T3 promoter were grown for 24 h, instead of 16 h more commonly used for *E. coli* cultures. It is possible that there is leaky

Figure 4.8 Interchanging signal and stop transfer sequences and the impact on the membrane topology of BD21. ***A.*** Topology scenario 1a is presented with a gray rectangle representing the membrane bilayer and numbered cylinders representing putative membrane-spanning helices TM1-TM10. The dark cylinders (1, 3, 5, 7 and 9) represent potential signal sequences and the light cylinders (2, 4, 6 and 8) represent potential stop-transfer sequences if BnDGAT1 incorporates into the microsome by sequential insertion mediated by alternating start and stop-transfer sequence. ***B.*** Topology of the BD21 truncation according to topology scenario 1a with non-interchangeable signal and stop transfer sequences. If the signal and stop transfer sequences are not interchangeable, then the topology (minus the N-terminus and TM1) would be preserved in BD21. The loop downstream of TM2 the ER lumen, and the invariant serine residue (black circle) and the C-terminus would be in the cytosol. ***C.*** Topology of BD21 truncation according to topology scenario 1a with interchangeable signal and stop transfer sequences. If the signal and stop-transfer sequences are interchangeable, then the opposite topology would be observed in BD21. TM2 would behave as signal sequence, instead of a stop-transfer sequence, and the loop downstream of TM2 would be in the cytosol, and both the invariant serine residue and the C-terminus would be in the lumen of the ER.

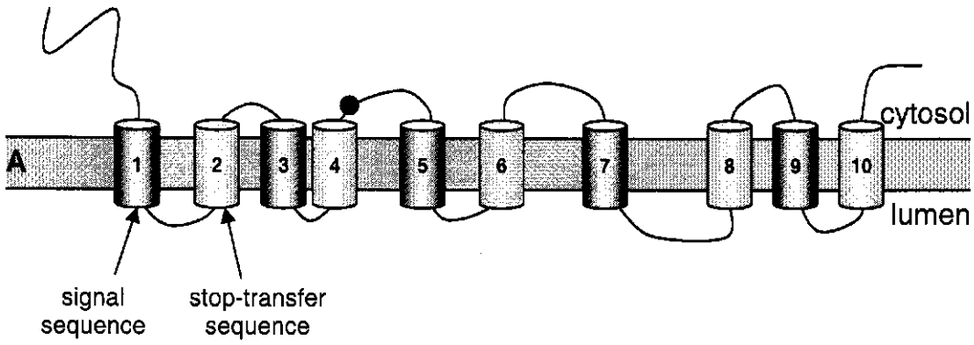
A
1
2
3
4
5
6
7
8
9
10
cytosol
lumen
signal sequence
stop-transfer sequence

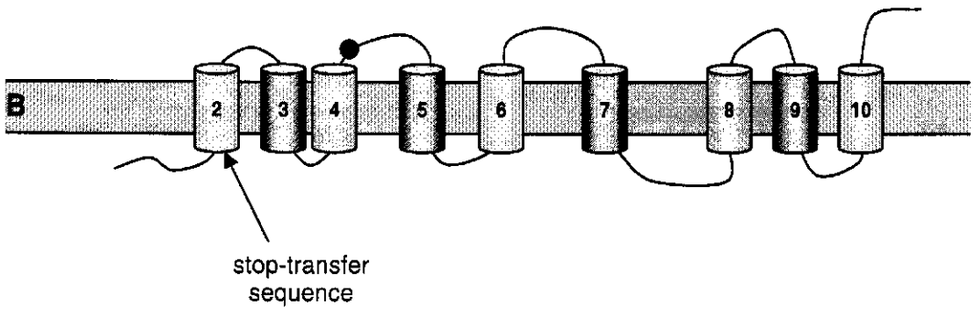
B
2
3
4
5
6
7
8
9
10
stop-transfer sequence

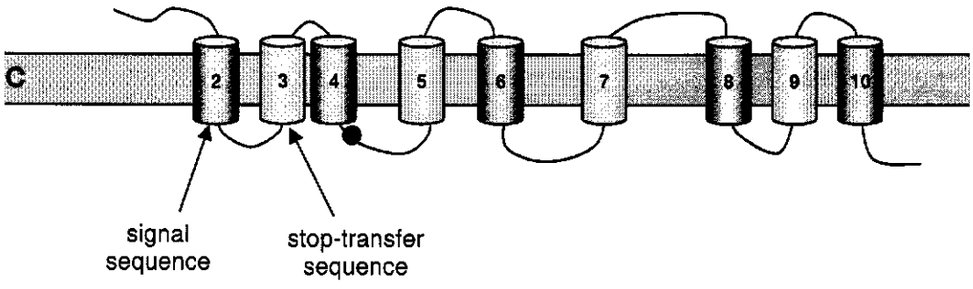
C
2
3
4
5
6
7
8
9
10
signal sequence
stop-transfer sequence

expression of clones under control of the T3 promoter during culture growth, and that BnDGAT1 inhibits *E. coli* cell growth. In previous work in our lab, we were unable to express full length BnDGAT1 using a pET-26b expression system with BL21(DE3) competent cells (Weselake et al., unpublished data). The soluble N-terminal fragment of BnDGAT1 was, however, expressed efficiently using a pET-26b expression system with BL21(DE3) competent cells (Weselake et al., 2004).

4.5 *In vitro* Transcription of Messenger RNAs

While clones under control of the T3 promoter were difficult to grow, only RNA transcripts of clones under control of the T3 promoter were obtained. The mRNAs *mBD12*, *mBD15*, *mBD19*, and *mBDF* were all observed at the expected sizes, slightly larger than (due to the presence of the 5' cap) 567, 891, 1416 and 1512 base pairs, respectively (Figure 4.9). RNA transcription of clones under control of the T7 promoter failed to produce any mRNA. These data suggest that the T7 promoter sequence has been mutated in the pBluescript vector used here. Sequencing reactions are being done on selected clones to determine whether or not there are mutations in both the T7 and T3 promoters. If the T7 promoter is not functional due to mutations, this may also explain why that there was no leaky expression inhibiting the bacterial growth of clones under control of the T7 promoter when we have evidence to suggest there may be leaky expression of clones under control of the T3 promoter (previous section).

Figure 4.9 Messenger RNA templates for *in vitro* translation reactions. RNeasy purified RNA transcription products quantified and the concentration adjusted to 1 mg mL^{-1}. One microgram of each of *mBD12*, *mBD15*, *mBD19* and *mBDF*, and 5 μg Invitrogen's 0.16–1.77 Kb RNA ladder (M) were resolved by electrophoresis as described in section 3.6.


M
rBD12
rBD15
rBD19
rBDF
M
1.770 kB
1.520 kB
1.285 kB
0.700 kB

4.6 *In Vitro* Translation of a β-lactamase Positive Control Using a Rabbit Reticulocyte Lysate System in the Presence of Rat Liver and *Brassica napus* Microsomal Preparations

A β-lactamase mRNA signal sequence positive control provided with Promega's canine pancreatic microsomes prepared for *in vitro* translation studies (Technical Manual No. 231) was translated in a rabbit reticulocyte lysate system in the presence of 1 and 2 Eq μL^{-1} of either rat liver microsomes (1RR-β and 2RR-β, respectively) or *B. napus* microsomes (1BR-β and 2BR-β, respectively). The unprocessed β-lactamase, or β-lactamase precursor, has an expected size of 31.5 kD, and the product processed by the microsome activity was 28.9 kD (Promega). Each of the four reactions here yielded two products of expected precursor and processed sizes (Figure 4.10). The results suggest that both the rat liver and *B. napus* microsomes can recognize the signal peptide and have the machinery to process the β-lactamase polypeptide. Increasing the concentration of microsomes in a translation reaction has been shown to increase the proportion of processed product (microsomal incorporation), but will also result in a yield reduction by reducing the efficiency of translation (Promega, Technical Manual No. 231). Similar product intensity, based on visual observations, was observed between processed and unprocessed products in both 1RR-β and 2RR-β reactions. The increase in concentration of rat liver microsomes from 1 to 2 Eq μL^{-1} did not appear to affect the yield or the level of processing. Two equivalents per microliter of rat liver microsomes has been successfully used in other studies with plant genes (B. Abell, University of Manchester, UK, personal communication), and was therefore chosen as a starting concentration for the translation reactions of BDN.

Figure 4.10 ***In vitro*** **translation of β-lactamase control using a rabbit reticulocyte lysate system in the presence of rat liver or** ***Brassica napus*** **microsomes.** Forty micrograms of β-lactamase mRNA per milliliter of reaction were translated using a rabbit reticulocyte lysate system. Reactions were run in the presence of either 1 or 2 Eq of rat liver microsomes (1RR-β or 2RR-β, respectively) or 1 or 2 Eq μL^{-1} of *B. napus* microsomes (1BR-β or 2BR-β, respectively). Unprocessed products were observed at 31.5 kD. Proteolytic processing by microsomal activity yielded the mature β-lactamase (processed products) at 28.9 kD. Samples (10 μL) were solubilized in SDS sample buffer at room temperature for 30 min and then resolved by SDS-PAGE on a discontinuous gel in 5 mm wide wells.

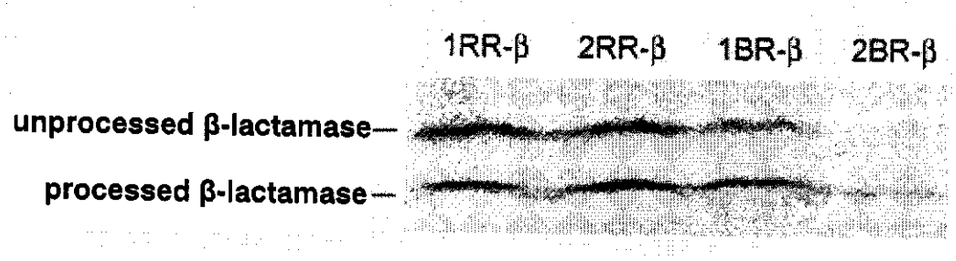
1RR-β
2RR-β
1BR-β
2BR-β
unprocessed β-lactamase—
processed β-lactamase—

In the 1BR-β reaction, the processed product was more intense than the unprocessed product in 1BR-β, indicating that more than half of the product was processed by 1 Eq μL^{-1} *B. napus* microsomes. The yield, however, appeared to be much less than that observed in 1RR-β, 2RR-β or 1BR-β, suggesting that 2 Eq μL^{-1} of *B. napus* microsomes inhibited the translation reaction (Figure 4.10). One equivalent per microliter of *B. napus* microsome was therefore chosen as a starting concentration for translation reactions of BDN.

4.7 *In Vitro* Translation of BnDGAT1 and Truncations

While *in vitro* translation was successful for the β-lactamase mRNA control in the presence of either rat liver or *B. napus* microsomes, *in vitro* translation with *BnDGAT mRNA* was not. Most of the troubleshooting reactions were run with *mBDF*, which encodes full length BnDGAT1. mRNA transcribed *in vitro* as described in section 3.6, and in early trials the template was cleaned using the phenol-chloroform RNA procedure, unless otherwise specified (section 4.7.1-4.7.3). mRNA quantifications following the phenol-chloroform RNA preparation were later found to be inaccurate (see section 4.7.4), and the concentrations indicated for these products are therefore apparent concentrations. The remaining reactions were run with mRNA purified using Qiagen's RNeasy cleanup kit. Unless otherwise indicated, translation reactions were run with the rabbit reticulocyte lysate system and 2 Eq μL^{-1} rat liver microsomes, and the translation products were boiled in SDS-sample buffer prior to SDS-PAGE as described in section 3.6.

4.7.1 Template and Microsomal Titrations. In the presence of either 1 or 2 Eq of rat liver microsomes, a series of apparent mRNA concentrations of 12-99 μg mL^{-1} were used in RR-BDF reactions. No products were detected (Figure 4.11). In the presence of 60-96 μg mL^{-1} canine pancreatic microsomes, a series of apparent mRNA concentrations of 5-70 μg mL^{-1} and 20-50 μg mL^{-1} were used in CR-BDF and CW-BDF reactions, respectively. No products were detected (Figure 4.11).

4.7.2 Magnesium and Potassium Ion Titrations. Salt concentrations have been known to affect the translation of certain mRNAs, and adjusting the magnesium and/or potassium ion concentration has been shown to improve translation of some mRNAs (Promega, Technical Manual No. 232). Using an apparent concentration of 17 μg mL^{-1} mRNA template, translation reactions were run with 20-100 mM KCl or 0.5-2.5 mM $MgCl_2$ in addition to salt concentrations present in the lysate system used. No products were detected (data not shown).

4.7.3 Phenol-Chloroform RNA Cleanup Versus Qiagen's RNeasy Cleanup and their Impact on *In Vitro* Translation Reactions. The recommended concentration of mRNA template when using mRNA transcribed *in vitro* is in the range of 5-80 μg mL^{-1}. Often components of the mRNAs transcription reaction will inhibit translation, and therefore, 5-20 μg mL^{-1} is often more successful (Promega, Technical Manual No. 232). A translation reaction containing both 17 μg mL^{-1} *rBDF* template (apparent concentration) and 40 μg mL^{-1} Promega's β-lactamase mRNA control was run in parallel with a reaction containing only 40 μg mL^{-1} Promega's β-lactamase mRNA control. Seventeen

Figure 4.11 Template and microsomal titrations for *in vitro* translation reaction. Template titrations were performed with *mBDF* transcription products cleaned by phenol-chloroform separation. Note that all *mBDF* concentrations used for translation reactions in the present figure may not be accurate (see section 4.7.4). The positive control reaction (+) is a β-lactamase signal sequence (Promega). Traces of products were sometimes observed at the bottom of the well of lanes with positive results, possibly due to aggregation of some products. ***A.*** RR-BDF translation reactions were performed with an apparent *mBDF* concentration of 12, 26 and 50 μg per mL of reaction (lanes 1, 2 and 3, respectively, in the presence of 1 Eq rat liver microsomes; lanes 4, 5 and 6, respectively, in the presence of 2 Eq rat liver microsomes); and 27, 41, 55, 69, 82, and 99 μg per mL of reaction (lanes 7, 8, 9, 10, 11 and 12, respectively, in the presence of 2 Eq rat liver microsomes). ***B.*** CR-BDF translation were performed with an apparent *mBDF* concentration of 5, 10 and 16 μg per mL of reaction (lanes 1, 3 and 5, respectively, in the presence of 60 μg mL^{-1} canine pancreatic microsomes); 5 and 11 μg per mL of reaction (lanes 2 and 4, respectively, in the presence of 96 μg mL^{-1} canine pancreatic microsomes); and 30, 50 and 70 μg per mL of reaction (lanes 7, 8 and 9, respectively, in the presence of 80 μg mL^{-1} canine pancreatic microsomes). ***C.*** CW-BDF translation reactions were performed with an apparent *mBDF* concentration of 20, 35 and 50 μg per mL of reaction (lanes 1, 2 and 3, respectively, in the presence of 80 μg mL^{-1}canine pancreatic microsomes). Samples (10 μL) were solubilized in SDS sample buffer in a boiling water bath for 2 min and then resolved by SDS-PAGE on a discontinuous gel with 5 mm wide wells.

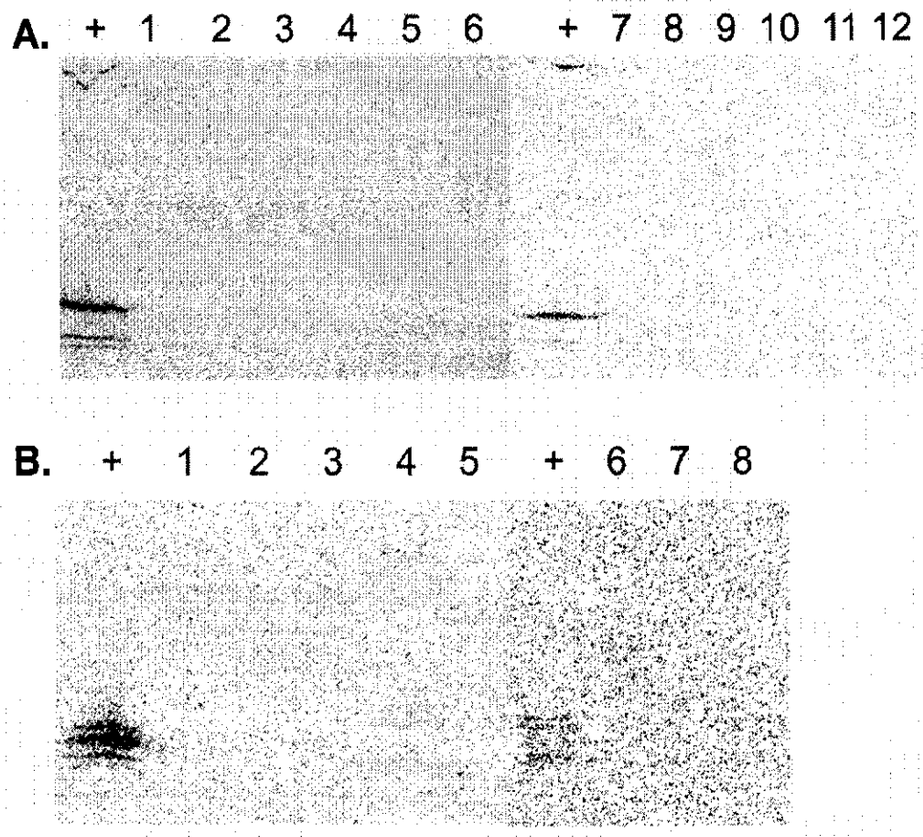
A.
+ 1 2 3 4 5 6 + 7 8 9 10 11 12
B.
+ 1 2 3 4 5 + 6 7 8
C.
+ 1 2 3

micrograms per milliliter of *mBDF* did not produce a BDF signal and did not appear to inhibit the production of β-lactamase, although the β-lactamase signal was reduced (Figure 4.12). Similar reactions containing 40 μg mL^{-1} Promega's β-lactamase mRNA control with either 27 μg mL^{-1} or 80 μg mL^{-1} *mBDF* (apparent concentrations) were run in parallel with a reaction containing only 40 μg mL^{-1} β-lactamase. These two concentrations of *mBDF* again did not produce any BDF polypeptide, but also resulted in loss of the β-lactamase product (Figure 4.12). The results suggest that higher concentrations of *mBDN* template prepared here inhibited translation reactions, possibly due to the quality of the RNA cleanup process. To determine whether or not the RNA cleanup was the cause of inhibition, new mRNA transcripts were prepared and Qiagen's RNeasy RNA cleanup was used in the place of the phenol-chloroform cleanup. A translation reaction containing both 104 μg mL^{-1} *mBDF* (actual concentration) and 40 μg mL^{-1} Promega's β-lactamase mRNA control was run in parallel with translation reactions containing either 40 or 80 μg mL^{-1} *mBDF* templates. The presence of 104 μg mL^{-1} *mBDF* not only did not inhibit the translation reaction of the β-lactamase control, but was successful in the translation of BDF (Figure 4.13). Successful translation of the *mBDF* was also observed in the 40 and 80 μg mL^{-1} *mBDF* template reactions. The *BDF* product, however, formed an aggregate that did not migrate far into the gel, a problem that will be discussed in section 4.7.5.

4.7.4 RNA Yields. Based on the absorbance at 260 nm, the yield of RNA preparations with phenol-chloroform appeared to be greater than that of RNA preparations with Qiagen's RNeasy cleanup kit. One microliter of RNeasy purified products with an

Figure 4.12 Effects of phenol-chloroform purified messenger RNA products on the *in vitro* translation of positive control reactions. 2RR-β control reactions were run using 40 μg mL^{-1} β-lactamase mRNA template (lanes 1, 3, and 5). 2RR-β control reactions were also run using 40 μg mL^{-1} β-lactamase mRNA template in the presence of *mBDF* with an apparent concentration of 17, 27 and 80 μg per mL (lanes 2, 4 and 6, respectively). *mBDF* template was cleaned by phenol-chloroform separation. Note that all *mBDF* transcript concentrations used for translation reactions in the present figure may not be accurate (see section 4.7.4). Traces of signal were sometimes observed at the bottom of the well in lanes with positive results, possibly due to aggregation of some products. Samples (10 μL) were solubilized in SDS sample buffer in a boiling water bath for 2 min and then resolved by SDS-PAGE on a discontinuous gel with 5 mm wide wells.

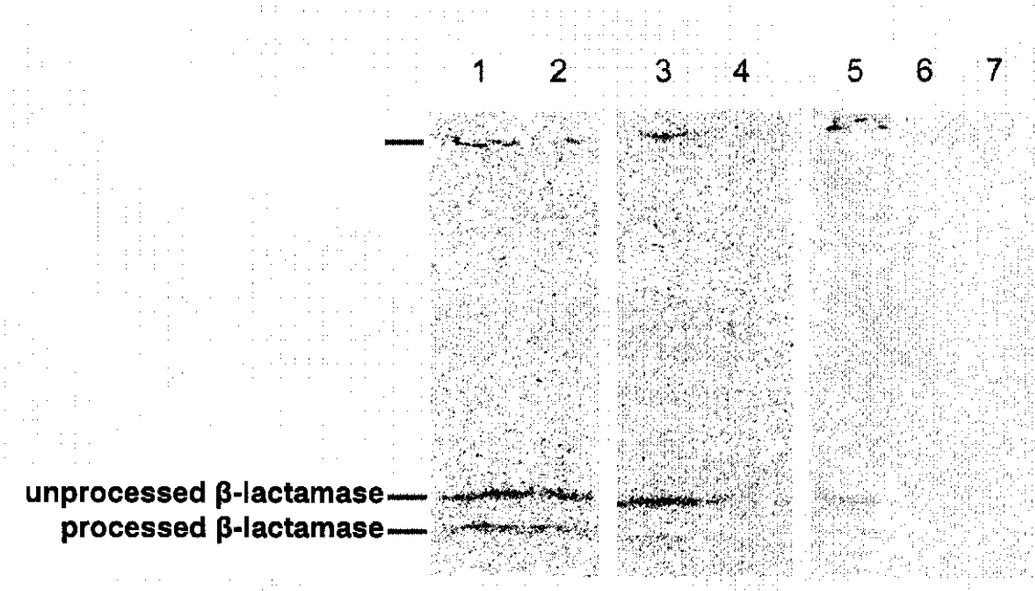
1
2
3
4
5
6
7
unprocessed β-lactamase
processed β-lactamase

Figure 4.13 Translation of RNeasy purified messenger RNA. All reactions above were performed with a rabbit reticulocyte lysate translation reactions in the presence of 2 Eq rat liver microsomes. Forty micrograms of β-lactamase mRNA per milliliter of reaction yielded unprocessed and processed β-lactamase products (lane 1). Forty micrograms of β-lactamase mRNA per milliliter of reaction together with 104 μg mL^{-1} *mBDF* yielded an intense signal at the top of the gel corresponding to and aggregation of BDF products, and some β-lactamase product at the bottom of the gel. The β-lactamase product appears to have a reduced signal possibly due to competition with the BDF transcript and/or aggregation with the BDF products (lane 2). Forty and 80 μg mL^{-1} *mBDF* both yielded intense signals at the top of the gel corresponding BDF aggregation products (lanes 3 and 4, respectively). Samples (10 μL) were solubilized in SDS sample buffer in a boiling water bath for 2 min and then resolved by SDS-PAGE on a discontinuous gel with 5 mm wide wells.

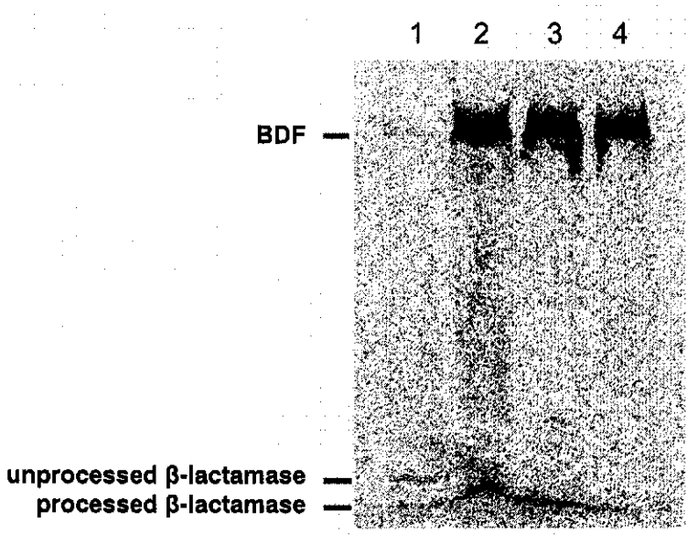
1
2
3
4
BDF
unprocessed β-lactamase
processed β-lactamase

apparent concentration of 1 mg mL^{-1} were, however, more readily visualized on an RNA gel than 10 μL of phenol-chloroform products with an apparent concentration of 0.775 mg mL^{-1} (Figure 4.14). It is likely that the phenol-chloroform purification and ethanol precipitation yielded contaminants that affected the absorbance readings and inhibited the translation reactions at higher concentrations. The concentration readings were inaccurately high in the samples cleaned by phenol-chloroform separation.

While the RNeasy cleanup RNA concentration readings were more accurate, the yields were particularly low. According to the Stratagene's mCAP RNA Capping Kit (www.stratagene.com, 'Frequently Asked Questions'), 3-8 μg of mRNA transcript can be expected for every microgram of plasmid template. Here, linearized plasmid templates were visually quantified against a Lambda/*Hind*III DNA ladder (Figure 4.15) and 8 μg of plasmid template were used in each transcription reaction. In an attempt to extract as much RNA as possible during the RNeasy cleanup, the products were eluted off of the RNeasy column in two 50 μL elutions, quantified, and subsequently dried down to a more useful concentration of 1 mg mL^{-1}. The total yield ranged from 7-15 μg. In other words, only 0.9-1.9 μg of mRNA transcript was synthesized per microgram of template.

In order to investigate the cause of these poor yields, positive control RNA transcription reactions should be run in parallel with the transcription of *cBDN* templates. Two forms of positive controls should be purchased from Stratagene for this purpose: a linearized template and a circular uncut template. In this way the plasmid preparation and template linearization methods used here could be compared to the already linearized template. If the plasmid preparation and template linearization method used here were to generate lower yields than those produced by the purchased linearized template, then an

Figure 4.14 RNA yields: a comparison of phenol-chloroform and RNeasy cleanup methods. The image on the left corresponds to 1 μg of each of *mBD12*, *mBD15*, *mBD19* and *mBDF*, of RNeasy purified products. The image on the right corresponds to phenol chloroform purified RNA transcript, *mBDF*, with an apparent yield of 7.75 μg. RNA was quantified by absorbance at 260 nm. Five micrograms of Invitrogen's 0.16–1.77 Kb RNA ladder (M) was used in both gels.

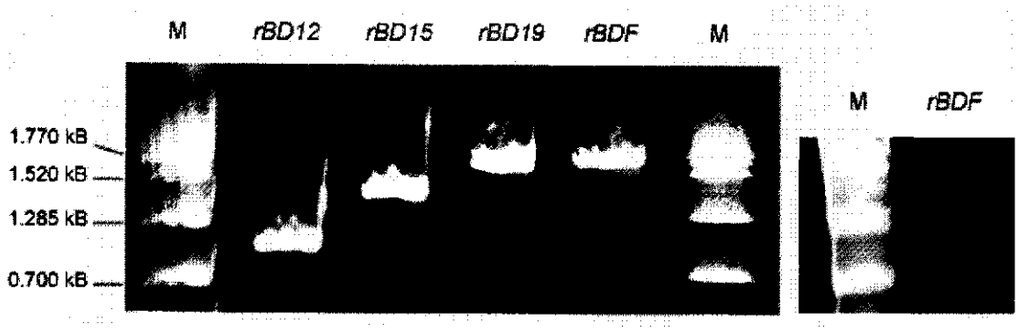
M
rBD12
rBD15
rBD19
rBDF
M
M
rBDF
1.770 kB
1.520 kB
1.285 kB
0.700 kB

Figure 4.15 Plasmid template preparation for *in vitro* translation reactions. Ten micrograms pBS- BD1, pBS-BD12-16, pBS-BD19 and pBS-BDF plasmids were linearized by restriction digest with *Swa*I and cleaned with Qiagen's PCR cleanup reaction with an elution volume of 50 μL. Half a microliter of linearized and cleaned products (lanes 1, 12-16, 19 and F, respectively) were separated by agarose gel electrophoresis and quantified against 500 ng Invitrogen's Lambda *Hind*III DNA (lanes M). The concentrations for linearized pBS-BD1, pBS-BD12-16, pBS-BD19 and pBS-BDF were calculate at 388, 388, 465, 388, 291, 194, 32 and 32 ng μL^{-1}, respectively, and their expected sizes are 3474, 3567, 3648, 3774, 3891, 4035, 4416 and 4512 base pairs, respectively.

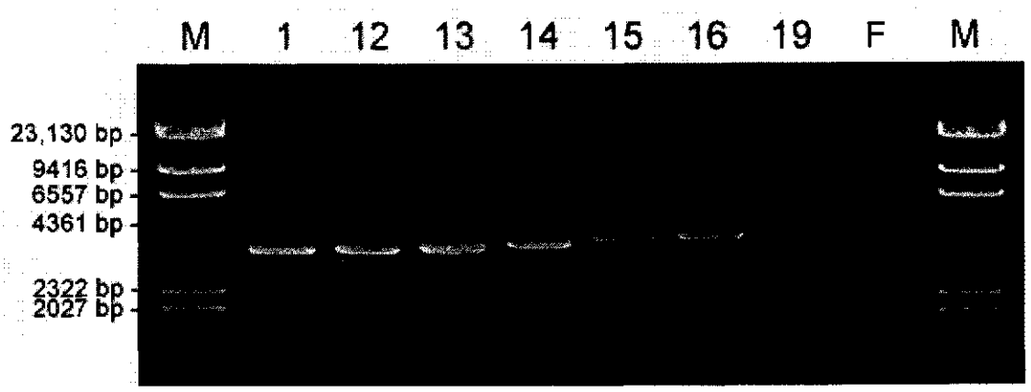
M
1
12
13
14
15
16
19
F
M
23,130 bp
9416 bp
6557 bp
4361 bp
2322 bp
2027 bp

alternative plasmid preparation and template cleanup system should be considered. It is unlikely, however, that template purity was the problem in the present study. The plasmid preparations and template cleanup yielded clean products, as visualized on agarose gel (Figure 4.15). In addition, the column purification methods used in the Sigma plasmid preparation and Qiagen DNA cleanup kits generally tend to provide good yields and clean products under our conditions.

If the plasmid preparation and template linearization used here were to generate yields similar to those generated from the purchased linearized template, then the cause of poor yields would be specific to the BDN clones. The most probable cause of poor RNA yields resides in the host vector pBluescript KS+, which was prepared from glycerol stocks, and may have been mutated by multiple culture preparations. The T7 promoter region may have mutation(s) that block transcription by way of not being recognized by the T7 RNA polymerase (see section 4.5). There may also be mutation(s) that are less detrimental and do not completely block transcription, but reduce the efficiency of T3 RNA polymerase activity. Sequencing of the promoter regions are currently being run.

4.7.5 Effects of Heating BnDGAT1 Translation Products Prior to Electrophoresis.

The expected size for full length BnDGAT1, BDF, is 56.9 kD. The BDF *in vitro* translation product ran near the top of the resolving gel, above the 215 kD marker. In contrast, microsomes from *B. napus* cell suspension cultures and boiled in SDS sample buffer for western blotting, yielded products of expected size when resolved by SDS-PAGE (see section 4.9). Since there is a suspicion that BnDGAT1 is a tetramer

Figure 4.16 Aggregation of *in vitro* translation products of BnDGAT1 clones. *In vitro* translation reactions were performed using the rabbit reticulocyte lysate system in the presence 2 Eq rat liver microsomes per μL of reaction. BD12, BD15, BD19 and BDF products all formed aggregations at the top of the gel. Samples (7 μL) were solubilized in SDS sample buffer, incubated in a boiling water bath for 2-3 min and then resolved by SDS-PAGE on a discontinuous gel in 2.5 mm wide wells. No signal was observed for the negative (-) control reaction, as expected. A 60 kD product was observed for the positive luciferase (+) control reaction, corresponding to the expected size of luciferase.

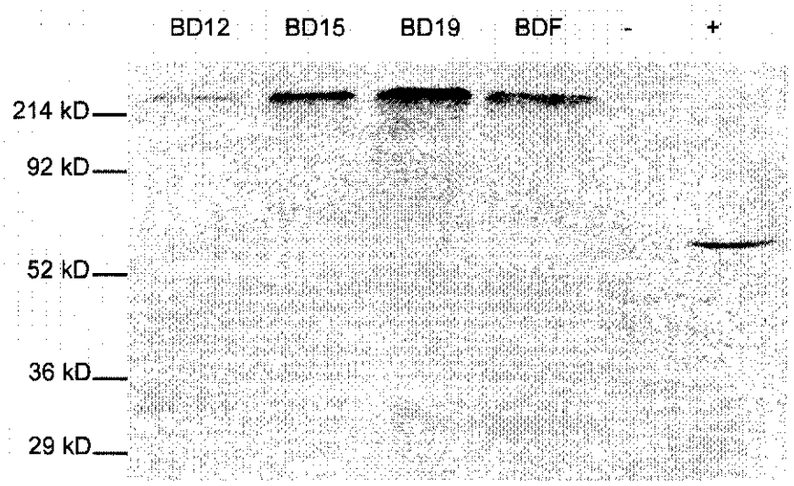
BD12
BD15
BD19
BDF
-
+
214 kD
92 kD
52 kD
36 kD
29 kD

(Weselake et al., 2004; see section 2.8.4), and since four times the predicted mass of BnDGAT1 is 227.6 kD, the possibility that RR-BDF runs as a tetramer under the denaturing SDS-PAGE conditions was considered. When *in vitro* translation products of the truncations RR-BD12, RR-BD15, and RR-BD19 also ran near the top of the resolving gel (Figure 4.16) this implicated that there was an aggregation problem and the previous speculation of tetramer formation was abandoned. Several trials were run in an effort to resolve the different products. Addition of 4 M urea to the sample buffer did not eliminate the aggregation problem (Figure 4.17A). In a discontinuous gel when the protein is stacked prior to entering the resolving gel, the increase in concentration and the transition to a higher pH will cause some proteins to aggregate (Ausubel et al., 2004). In those cases a continuous SDS-PAGE has been shown to prevent precipitation. A continuous 12% SDS-PAGE, however, did not resolve the *in vitro* translation products of BnDGAT1 (Figure 4.17B).

Chaperones are involved in mediating protein folding and thus prevent aggregation of products that are not properly folded (Becker and Craig, 1994). While both the rabbit reticulocyte lysate and the wheat germ extract are supplemented with a variety of common chaperones (Promega), there may be a chaperone specifically for BnDGAT folding that is absent from the system and thus leading to aggregation of RR-BDN translation products. Cytosol and cell lysate fractions were prepared from *B. napus* cell suspension cultures and added to the translation reactions, in hopes that the cell lysate or cytosol would provide the *in vitro* translation system with the necessary machinery for proper folding of BDN products. The homogenate and the supernatant following the 100,000 g_{av} centrifugation step of the protocol for preparation of microsomal membranes

Figure 4.17 Analysis of RR-BDN products under various electrophoresis conditions. All *in vitro* translation reactions (right) were run with 40 μg *mBDN* per mL of reaction using a rabbit reticulocyte lysate system in the presence of 2 Eq rat liver microsomes. ***A.*** Samples were boiled in SDS-sample buffer in the presence of 4 M urea prior to discontinuous SDS-PAGE with a 12 % resolving gel. Lanes 1, 2, 3 and 4 correspond to BD12, BD15, BD19 and BDF. ***B.*** Samples were boiled in SDS-sample buffer prior to continuous SDS-PAGE on a 12 % gel. Lanes 1 and 2 correspond to BD19 and BDF. ***C.*** Samples were separated by discontinuous native PAGE on a 12 % gel. A negative control, a luciferase positive control, BD15 and BDF were incubated for ten minutes in the presence of native sample buffer at room temperature (lanes 1 through 4, respectively) or SDS-sample buffer at 50°C for 10 min (lanes 5 through 8, respectively). Samples in all gels were loaded in 7 μL aliquots (excluding the buffer volume) in 2.5 mm wide wells.

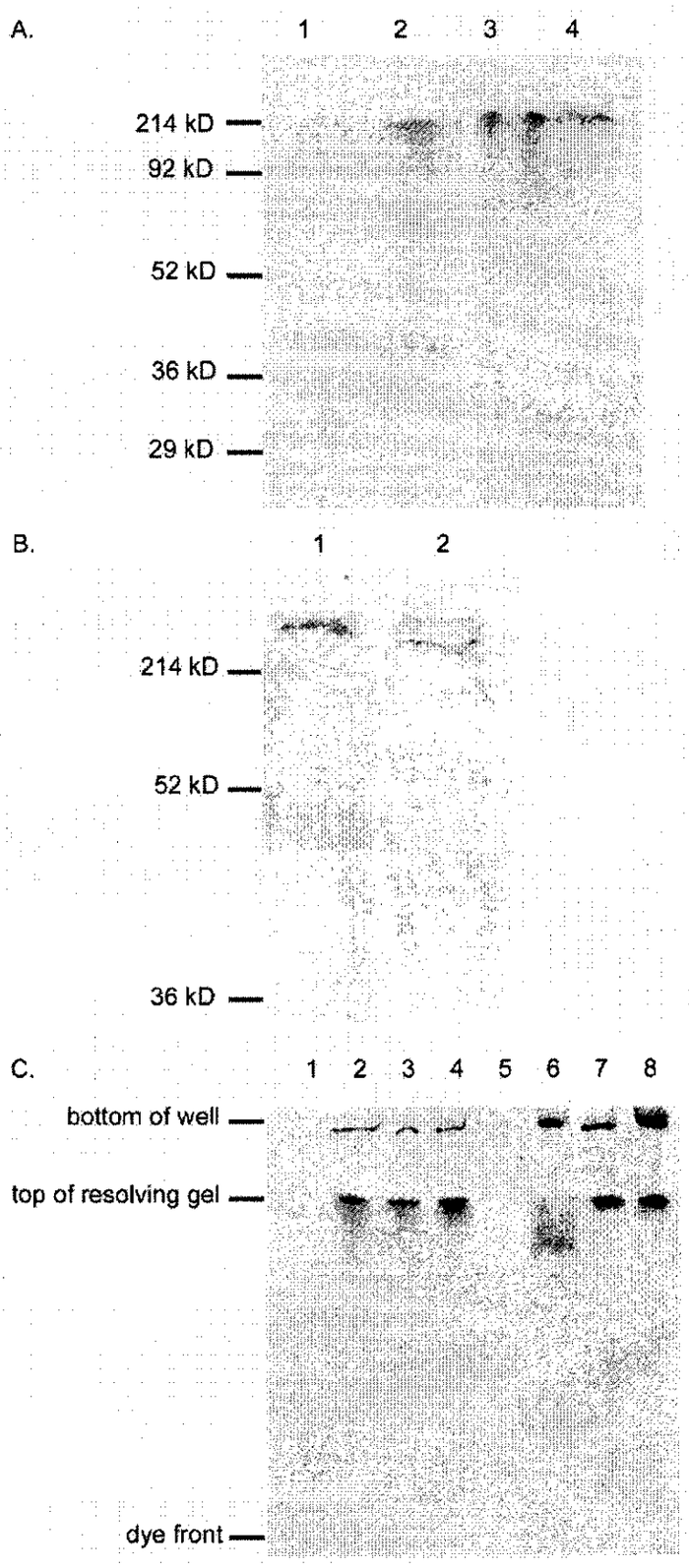
A.
1
2
3
4
214 kD
92 kD
52 kD
36 kD
29 kD
B.
1
2
214 kD
52 kD
36 kD
C.
1
2
3
4
5
6
7
8
bottom of well
top of resolving gel
dye front

(section 3.8.1) were used as the cell lysate and cytosol preparations, respectively. Cytosol and cell lysate preparations were nuclease treated prior to translation reactions, following the same method of nuclease treatment described in Materials and Methods for microsome preparations (section 3.1). RR-BDF and BR-BDF reactions were run in the presence or absence of cytosol, and R-BDF reactions were run in the presence of cell lysate (which theoretically contains *B. napus* microsomes). The presence of *B. napus* cytosol and cell lysate did not solve the aggregation problem (data not shown).

DGAT is a highly hydrophobic protein with many predicted transmembrane regions. Some hydrophobic proteins will precipitate in the presence of SDS (Ausubel et al., 2004). Translation reactions run in the absence of microsomes were separated on native PAGE either with native sample buffer and no heat treatment prior to run, or with SDS sample buffer and heated at 50°C for 10 min prior to run (Figure 4.17C). The aggregation at the top of the gel was still observed with either of the sample buffers on the native gel. These results suggested that SDS was not the cause of aggregation.

Heating has also been shown to cause precipitation in some proteins (Ausubel et al., 2004). This can usually be resolved by lowering the temperature of denaturation prior to electrophoresis to 70°C or 80°C. Heating at 50°C, however, in the presence of SDS followed by separation on a native gel did not eliminate aggregation. In their studies with DGAT from castor bean (*Ricinus communis*) McKeon et al. observed similar behavior (2004, United States Department of Agriculture, Albany, CA, personal communication). RcDGAT (which shares 71 % sequence identity with BnDGAT1) isolated from castor bean resolved at expected size, but expression in yeast yielded an aggregated product. Heating at 37°C for 30 min, however, circumvented the denaturation

problem (T. McKeon, 2004, personal communications). In the current study, RR-BD15 and RR-BDF translation products were incubated for 30 min at room temperature, 30°C, 37°C and 50°C with SDS sample buffer, and separated on SDS-PAGE. At 50°C the aggregation problem was observed, but as the denaturing temperature decreased, there was less aggregation. At room temperature, no aggregation was observed (Figure 4.18). The expected sizes for BD15 and BDF are 32.7 kD and 56.9 kD, respectively, but the products observed resolved at 40 kD and 32.0 kD, respectively. There unexpected apparent sizes are discussed in the next section.

4.7.6 *In Vitro* Translation of BnDGAT1 and Truncations Using a Rabbit Reticulocyte Lysate System in the Presence of Rat Liver Microsomes.

The expected sizes for BD12, BD15, BD19 and BDF are 20.5, 32.7, 53.5, and 56.9 kD, respectively. As discussed in section 4.7.5, translation products did not exhibit aggregation when separated by SDS-PAGE if samples were not subjected to heat treatment prior to electrophoresis. In the RR-BDN reactions, however, none of translation the products ran at their expected sizes (Figure 4.19). The products for RR-BD12 and RR-BD15 are larger than expected, at approximately 32.0 and 40 kD, respectively. Two translation products were observed for each of RR-BD19 and RR-BDF at approximately 32 and 40 kD. Both of these products are smaller than the expected sizes of either BD19 or BDF.

In the absence of any microsomes, translations of BD12, BD15, BD19 and BDF using either the rabbit reticulocyte lysate system or the wheat germ extract system yielded products at approximately 32, 40, 55 and 56 kD, respectively, when solubilized

Figure 4.18 Temperature effects on SDS-PAGE resolution of RR-BDN. BD15 and BDF translation products were denatured at various temperatures in SDS sample buffer for 30 min prior to electrophoresis. Lanes 1, 3, 5 and 7 correspond to BD15 incubated at room temperature, 30, 37 and 50°C, respectively. Lanes 2, 4, 6 and 8 correspond to BDF incubated at room temperature, 30, 37 and 50°C, respectively. Solubilized samples (7 μL) were resolved by SDS-PAGE on a discontinuous gel in 2.5 mm wide wells.

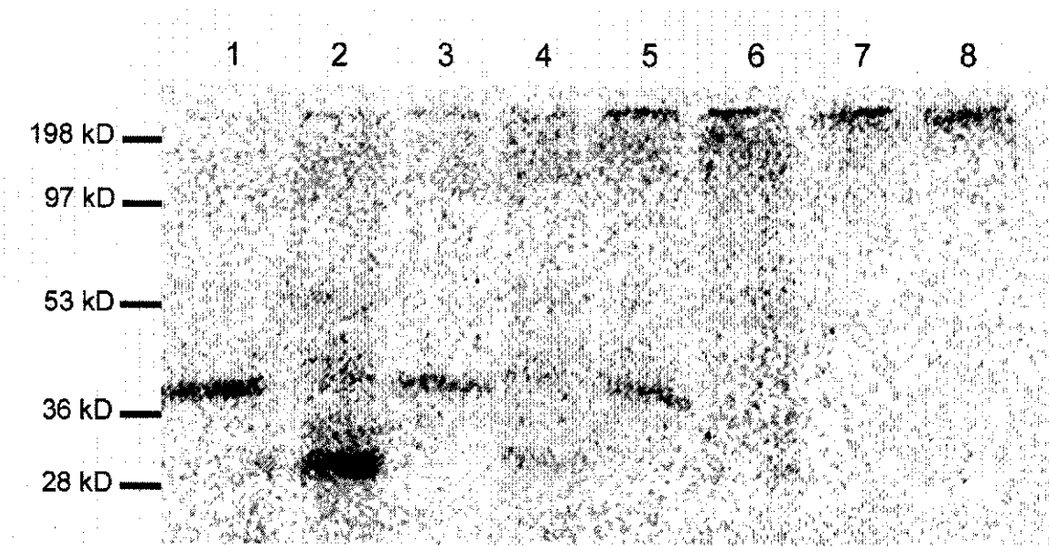
1
2
3
4
5
6
7
8
198 kD
97 kD
53 kD
36 kD
28 kD

Figure 4.19 ***In vitro*** **translation of BDN using a rabbit reticulocyte lysate system in the presence of 2 Eq rat liver microsomes.** Forty micrograms per milliliter of reaction of *mBD12*, *mBD15*, *mBD19* and *mBDF* templates were translated. Samples (7 μL) were solubilized in SDS sample buffer at room temperature for 30 min and then resolved by SDS-PAGE on a discontinuous gel in 2.5 mm wide wells.

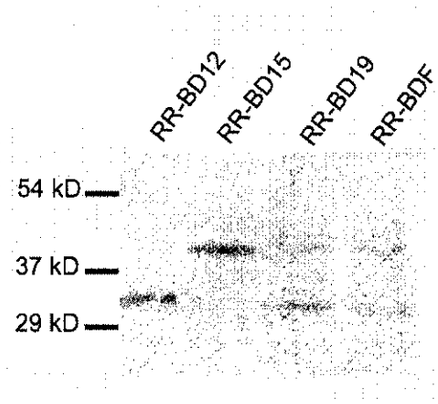
RR-BD12
RR-BD15
RR-BD19
RR-BDF
54 kD
37 kD
29 kD

in SDS sample buffer at room temperature (Figure 4.20). Translation with wheat germ extract gave stronger product signals than the rabbit reticulocyte lysate kit, suggesting that the wheat germ extract system may produce higher BDN yields than the rabbit reticulocyte lysate system. Although some products of reactions ran in the absence of microsomes were larger than expected, it should be noted that protein migration in SDS-PAGE does not always reflect the actual size of a given protein (Ausubel et al., 2004). The differences between the observed product sizes of each sample reflected their expected size differences, suggesting that in the absence of any microsomes, the polypeptides were synthesized in full length with respect to the cDNA construct.

In the presence of rat liver microsomes, the rabbit reticulocyte lysate system yielded what appeared to be full length products for BD12 and BD15 since these products migrated the same distance in the presence or absence of rat liver microsomes. In the presence of rat liver microsomes, the rabbit reticulocyte lysate system, however, yielded truncated products for both BD19 and BDF. Since BD12 and BD15 are both truncations of either BD19 or BDF, then both BD19 and BDF have sequences that are absent in both BD12 and BD15. It is possible that there are proteolytic processing site(s) located at TM6 or downstream of TM6 (these site(s) would therefore be absent in BD12 and BD15) recognized by rat liver microsome activity (Figure 4.21A). There are two possible size patterns that would support this explanation, described here as pattern 1 and 2. In pattern 1, if the proposed processing site of BD19 and BDF is at TM6 (or downstream of TM6), then the processed products of BD19 and BDF would be equal to (or larger than) the BD15 product. A schematic representation of this explanation is presented Figure 4.21B. In pattern 2, if the proposed processing site downstream of TM6 (or at TM6) created a

Figure 4.20 ***In vitro*** **translation of BDN using a rabbit reticulocyte lysate or wheat germ extract system in the absence of any microsomes.** Forty micrograms of *mBD12*, *mBD15*, *mBD19* and *mBDF* templates were translated per milliliter of reaction using a rabbit reticulocyte lysate system (lanes 1, 2, 3 and 4, respectively), and a wheat germ extract system (lanes 5, 6, 7 and 8, respectively). Seven microliters of translation products were solubilized in SDS sample buffer at room temperature for 30 min and then resolved by SDS-PAGE on a discontinuous gel in 2.5 mm wide wells.

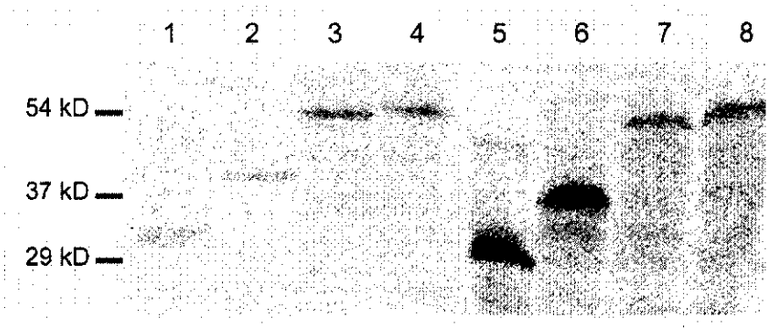
1
2
3
4
5
6
7
8
54 kD
37 kD
29 kD

Figure 4.21 Schematic representation of potential proteolytic processing site. ***A.*** The diagrams represent the primary amino acid sequence of BDF, BD19, BD15 and BD12 (rectangle) with putative membrane-spanning coding domains (gray), numbered 1-10 for TM1-TM10. The arrows indicate a potential proteolytic processing site immediately upstream of TM6, potential processing sites may also be present downstream of TM6. These potential processing sites are only found in BDF and BD19, since BD15 and BD12 do not contain the proposed residues. ***B.*** The expected products for sizes BDF, BD19, BD15 and BD12, if a proteolytic processing site is present immediately upstream of TM6, as presented in *A*. ***C.*** The expected products for sizes BDF, BD19, BD15 and BD12, if a proteolytic site is present immediately upstream of TM6, as presented in *A*, creating a nick in the polypeptide. In this case BDF and BD19 would have two products.

A.

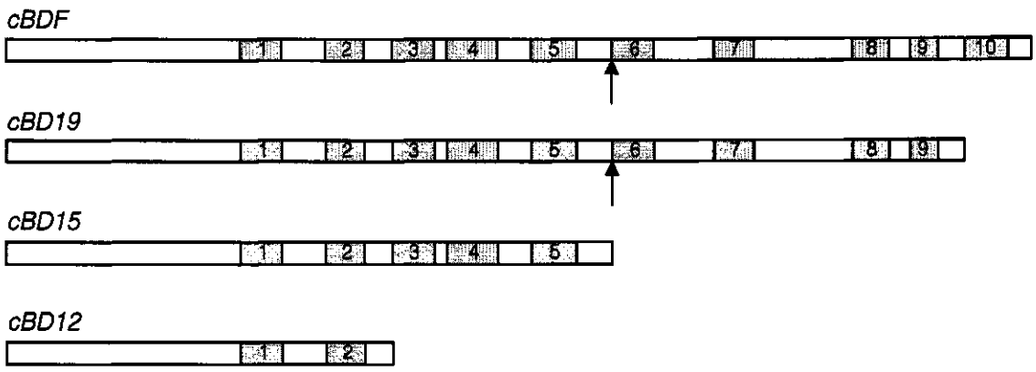
cBDF
1
2
3
4
5
6
7
8
9
10
cBD19
1
2
3
4
5
6
7
8
9
cBD15
1
2
3
4
5
cBD12
1
2

B.

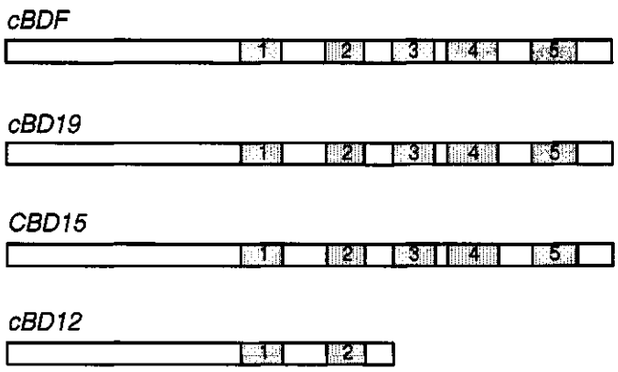
cBDF
1
2
3
4
5
cBD19
1
2
3
4
5
CBD15
1
2
3
4
5
cBD12
1
2

C.

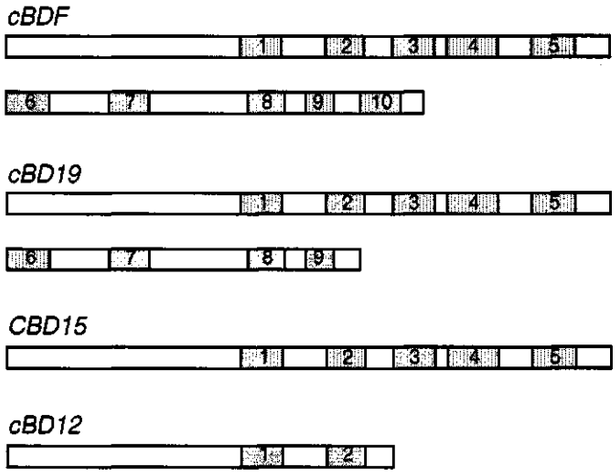
cBDF
1
2
3
4
5
6
7
8
9
10
cBD19
1
2
3
4
5
6
7
8
9
CBD15
1
2
3
4
5
cBD12
1
2

nick in the product, then two products would be visualized on the gel. According to this explanation, the sum of the two products would be equal to the expected size of the unprocessed product (Figure 4.21C).

Here, we observed a band for each of BD19 and BDF that was equal in size to the BD15 product (Figure 4.19), which would appear to support pattern 1 (Figure 4.21B), except that a second product was observed for each of BD19 and BDF. The observed full length product sizes for BD19 and BDF (55 and 56 kD, respectively), appear to be very close in size, suggesting that a similar band pattern could be observed in each both reactions upon processing according to pattern 2. A difference in size would, however, still be observed in the smaller fragment upon processing according to pattern 2 (Figure 4.21C). Based on the expected sizes, the smaller fragment of processed BDF should be larger than full length BD12, and the smaller fragment of processed BD19 should be smaller than full length BD12. While it is likely that the proposed processed products in pattern 2 may run anomalously, since the unprocessed products run anomalously, it is unlikely that upon processing according to the second explanation, the smaller fragment of both BD19 and BDF would both appear to be exactly the same size as BD12. In addition, it is suspicious that a nick would be present immediately downstream of BD15, yielding one product exactly the same size as BD15, and a second product exactly the same size as BD12. The explanation according to pattern 2 (Figure 4.21C) therefore does not correspond to the observed results (Figure 4.19). To further investigate these results, all four samples were translated with each of the rabbit reticulocyte lysate and the wheat germ extract translation systems in the presence of either rat liver microsomes or *B. napus* microsomes.

4.7.7 *In Vitro* Translation of BnDGAT1 and Truncations Using Rabbit Reticulocyte Lysate or Wheat Germ Extract Systems in the Presence of Either *Brassica napus* or Rat Liver Microsomes. Microsome fractions of RR-, RW-, BR- and BW-BDN reactions (Figure 22A, B, C, and D, respectively) were pelleted by ultracentrifugation from a 7 µL aliquots of *in vitro* translation product, and resuspended in 7 µL of 10 mM HEPES-NaOH, pH 7.4. Seven microliters of each of the translation products, the resuspended microsome pellets and their supernatants were resolved by SDS-PAGE (Figure 4.22 lanes TL, P and S, respectively).

BR-BD12 and BW-BD12 reactions both generated products at 32 kD (Figure 4.22C and D). BR-BD15 and BW-BD15 both generated products at 40 kD (Figure 4.22C and D). In each of these reactions, the respective products were also observed in the microsome fractions. BR-BD12 and BR-BD15 products were also observed in the supernatant at 32 and 40 kD. BR- and BW-BD19 reactions both generated products at 55 kD, and BR- and BW-BDF reactions both generated products at 56 kD. A faint signal was also observed between 40 and 55 kD in all four reactions. Faint signals were observed in the BR- and BW-BD19 microsome fractions. No obvious signals were observed for the BR- and BW-BDF microsome fractions.

In vitro translation with *B. napus* microsomes exhibited lower yields than reactions with rat liver microsomes. Poor yields in these reactions may be attributed to the *B. napus* microsomes, since the microsome source is the only difference between the BR- and BW-BDN reactions and the RR- and RW-BDN reactions. A couple of potential explanations for the poor yields with *B. napus* microsomes are presented here. First, the *B. napus* microsomes may not be as compatible with the rabbit reticulocyte lysate and

Figure 4.22 BDN incorporation into rat liver and *Brassica napus* microsomes. Forty micrograms of *mBD12*, *mBD15*, *mBD19* and *mBDF* templates were translated per milliliter of reaction (translation, or TL, lanes 1, 2, 3 and 4, respectively). Translation reactions were performed using a rabbit reticulocyte lysate system in the presence of 2 Eq of rat liver microsomes (***A***) or 1 Eq *B. napus* microsomes (***C***) per microliter of reaction, or a wheat germ extract system in the presence of 2 Eq of rat liver microsomes (***B***) or 1 Eq *B. napus* microsomes (***D***) per microliter of reaction. Microsomes were pelleted from translation reaction products and the BD12, BD15, BD19 and BDF microsomal fraction (pellet, or P, lanes 1, 2, 3 and 4, respectively) and supernatant (S lanes 1, 2, 3 and 4, respectively). Samples were solubilized in SDS sample buffer at room temperature for 30 min and then resolved by SDS-PAGE on a discontinuous gel in 2.5 mm wide wells.

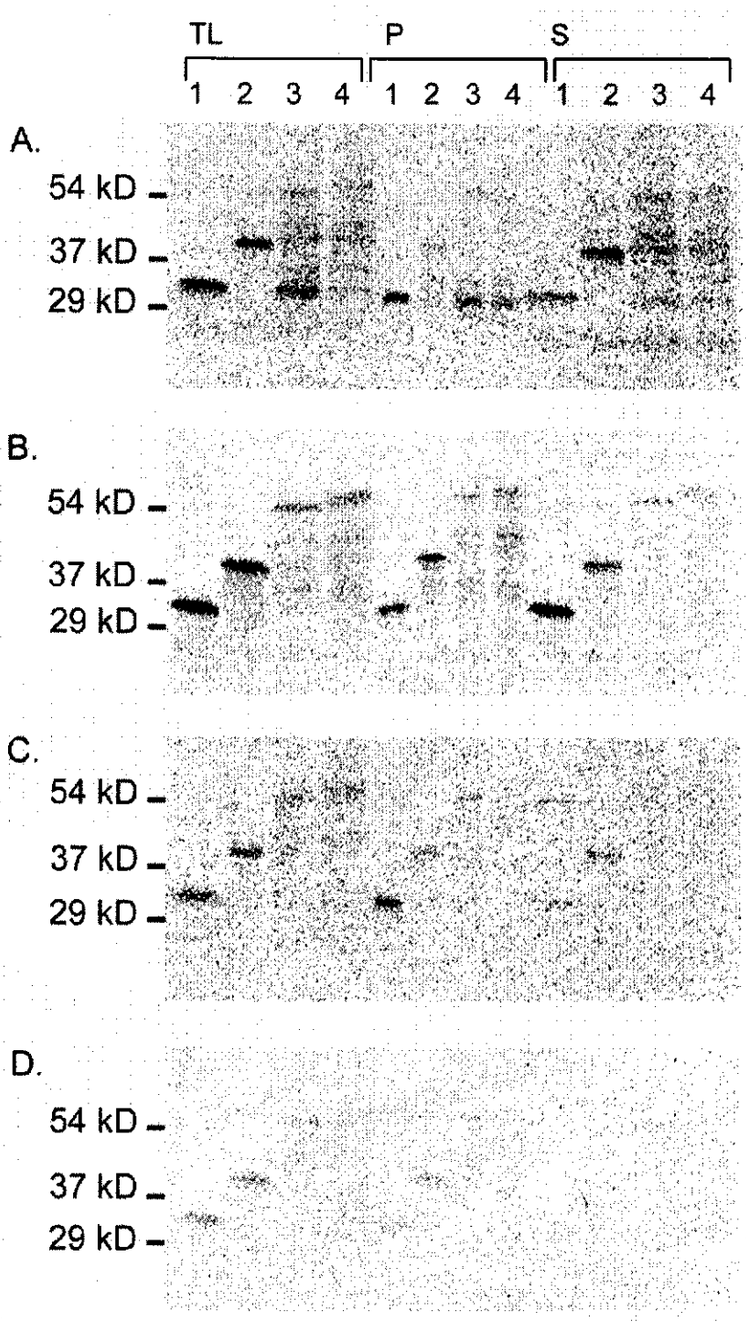
TL
P
S
1 2 3 4 1 2 3 4 1 2 3 4
A.
54 kD
37 kD
29 kD
B.
54 kD
37 kD
29 kD
C.
54 kD
37 kD
29 kD
D.
54 kD
37 kD
29 kD

wheat germ extract systems. It is known that in the presence of canine pancreatic microsomes, *in vitro* translation of ER targeted mRNA is more successful with the rabbit reticulocyte system than with the wheat germ extract system. This is because the canine pancreatic microsomes do not recognize the SRP of the wheat germ extract, and therefore must be supplemented with the appropriate SRP for optimal translation conditions (Promega, *In Vitro* Expression Guide). A similar explanation may be appropriate for the observed yield reduction in the presence of *B. napus* microsomes. The *B. napus* microsomes may not recognize the SRP, or some other component of the translation machinery, of the rabbit reticulocyte lysate or wheat germ extract systems. *B. napus* microsomes are capable of processing β-lactamase products of *in vitro* translation using the rabbit reticulocyte lysate system (section 4.6). These data suggests that these *B. napus* microsomes have the appropriate signal peptidase for processing of this protein. Since signal peptidase activity generally occurs co-translationally at the ER membrane (or at the microsomes in an *in vitro* expression system), these data also imply that this protein can be translated at the *B. napus* microsomes in a rabbit reticulocyte lysate translation system. The yields β-lactamase yields, however, appeared to be lower when translated in the presence of *B. napus* microsomes than when translated in the presence of rat liver microsomes (section 4.6; Figure 4.10). In addition, an increase in the *B. napus* microsome concentration in the reaction further reduced the β-lactamase yields. This, however, is not unusual. Increasing microsome concentrations in the *in vitro* translation reactions is known to reduce the yield while increasing the amount of microsomal processing events.

Another possible explanation for the *B. napus* microsome induced yield reduction is the quality of the microsomal preparations. Both the *B. napus* and rat liver microsomes were prepared according to protocols (Abell et al., 1997; Rusinol et al., 1997, respectively) adapted from the canine pancreatic microsomal preparation method for *in vitro* translation first described by Walter and Blobel (1983). In one of the final centrifugation steps of the protocol for canine pancreatic microsomal preparation, microsomes are pelleted through a 1.3 M sucrose cushion. The sucrose cushion used for the rat liver microsomal preparation was also 1.3 M, but the sucrose cushion used in plant microsomal preparation was only 0.5 M. An increase in the concentration of the sucrose cushion may lead to further purification of the microsomes and eliminate potential contaminants that could affect the *in vitro* translation reaction (possibly resulting in a yield reduction).

Several things can be tried to improve the yield of *in vitro* translation in the presence of *B. napus* microsomes. Among these, further purification of the *B. napus* microsomes, by running the microsomes through a 1.3 M sucrose cushion, as described above, may reduce reaction inhibition due to the presence of these microsomes. Reducing the concentration of *B. napus* microsomes may improve the yields by reducing the concentration of the potential reaction contaminants in the *B. napus* preparation. This may, however, also reduce the amount of product incorporated into the microsomes. Only one trial and one set of reaction conditions was attempted for each of BR- and BW-BDN reactions (the only combination of template and microsome concentrations used in either BR-BDN or BW-BDN reactions was 40 $\mu g\ mL^{-1}$ and 1 Eq μL^{-1}). Increasing or

decreasing the template concentration may also affect the yields, possibly providing enough products for use in post-translational analysis.

When yields were greater for translation reactions in the presence of rat liver microsomes than in the presence *B. napus* microsomes, translation reactions in the presence of rat liver microsomes were associated with other difficulties, namely background and/or secondary product formation and microsome incorporation. The background signal and the secondary products observed in the reactions with the rat liver microsomes suggest that either premature chain termination or proteolytic processing was generating various truncated products of the longer chain clones (namely BD19 and BDF). The fact that this level of background and secondary products was not observed in the reactions with *B. napus* microsomes suggests that the premature chain termination or proteolytic processing may be an event caused by the presence of the rat liver microsomes.

RR-BD12 and RR-BD15 products resolved at 32 and 40 kD, respectively, with a product observed at the respective sizes in both the supernatant and in the microsomes (Figure 4.22A). The majority of the RR-BD12 signal appeared in the microsome, and the majority of the RR-BD15 appeared in the supernatant. A high level of background was observed in RR-BD19 and RR-BDF translation product, with distinct bands at 32, 40, and 55 kD, and at 32, 40 and 56 kD respectively. BD19 had a particularly distinct signal at 32 kD. This level of background was not observed in previous RR-BD19 and RR-BDF reactions. During the temperature gradient trials (section 4.7.5), RR-BDF solubilized in SDS sample buffers at room temperature for 30 min produced an intense signal at 32 kD, with some backgrounds signal including distinct bands at 40 and 53 kD (Figure 4.16). In

the RR-BDN reactions described in section 4.7.6, no obvious background was observed for RR-BD19 ad RR-BDF, and two distinct bands were observed in each at 32 and 40 kD (Figure 4.19). In Figure 4.22A, the 32 kD product of RR-BD19 and RR-BDF appeared in the microsome fraction. The supernatant fractions of RR-BD19 and RR-BDF, both with high levels of background, contained faint products at 32, 40 and 55 kD, and 32, 40 and 56 kD, respectively.

The RW-BDN reactions produced more promising results than the RR-BDN reactions. As in the RR-BDN reactions, RW-BD12 and RW-BD15 products resolved at 32 and 40 kD, respectively, with products observed at the respective sizes in both the supernatant and in the microsomes (Figure 4.22B). The RW-BD15 microsome fraction appeared to have a stronger signal than the RR-BD15 microsome fraction. The most distinct products of RW-BD19 and RW-BDF reactions appeared at 55 and 56 kD, respectively. Secondary products were also observed between 32 and 40 kD, and between 40 and 55 kD, in both RW-BD19 and RW-BDF reactions. The 55 and 56 kD signals appeared in both the microsome and supernatant fractions of RW-BD19 and RW-BDF, respectively. The secondary products of both reactions appeared in the microsome fractions.

These results suggest that the RR- and RW- BD12, and RR- and RW-BD15 products were incorporated in the microsomes, since these products were all observed in the microsome fractions. All of these products were also prevalent in the supernatant, suggesting that not all of the products are incorporated in the microsomes. RR-BD15 product is the least prominent in the microsome fraction showing only a faint signal, and a more distinct signal in the supernatant, suggesting that BD15 displayed more difficulty

incorporating into the rat liver microsomes when translated with the rabbit reticulocyte lysate translation system than with the wheat germ extract system.

In the presence of rat liver microsomes, the longer chain length products (BD19 and BDF) displayed more difficulty in translating full length products that are incorporated into the microsomes. This phenomenon was more prevalent in the rabbit reticulocyte lysate translation system than in the wheat germ extract translation system. As mentioned above, the generation of various products including the 55 and 56 kD products of both RR- and RW-BD19, and RR- and RW-BDF, respectively, may be a consequence of either proteolytic processing or premature chain termination during *in vitro* translation. While it is speculated that the proteolytic processing and/or premature chain termination is specific to the rat liver microsomes, since these results appear to be specific to the translation reactions in the presence of rat liver microsomes, there does appear to be some background/secondary product formation to a lesser degree in the reactions with *B. napus* microsomes. It is also important to consider the impact that the lower yields observed in reaction run in the presence of *B. napus* microsomes might have on the interpretation of these results. If there were fewer products being synthesized in BR and BW reactions than in RR and RW reactions, then the concentration of processed products or prematurely terminated reactions would be lower. In this case, by increasing the yields, more processed/prematurely terminated products would be visually observed than at present in the BR and BW reactions. In addition, if the cause of secondary product formation was in fact related to proteolytic processing, then in the case of lower yields the processing events may have lead to more complete protease digestion, leaving fewer secondary products to be observed.

The RR-BDN results support premature chain termination over proteolytic processing. RR-BD12 and RR-BD15 were synthesized to full length (Figure 4.22A). The smaller product (RR-BD12) was incorporated into the microsomes, with some product in the supernatant. The larger product (RR-BD15) was also incorporated into the microsomes, but the majority of the product was found in the supernatant. Although only two samples are compared here, these results suggest that as the chain length increased microsomal incorporation was less successful. This explanation is supported by the results of RR-BD19 and RR-BDF. Three major products were formed in both RR-BD19 and RR-BDF reactions: one equal in size to BD12, one equal in size to BD15, and one equal in size to full length BD19 and BDF, respectively. All three products are observed in the supernatant, but the only products observed in the microsomes are those that are equivalent in size to BD12. This provides evidence supporting the explanation that increasing the chain length of BDN products reduces the success of microsomal incorporation.

If BnDGAT1 is incorporated into the microsome co-translationally, then these data suggest that synthesis downstream of TM2 in rat liver microsomes is inhibited by the rat liver microsomes. Consider the following explanation. The products found in the supernatant may correspond to products that were synthesized in the 'cytosol' and not in the microsomes, or they may correspond to products whose syntheses were initiated at the rat liver microsomes, but were then released from the microsomes following synthesis of residues downstream of TM2. The latter explanation is more plausible in this study, since the rabbit reticulocyte lysate (and wheat germ extract) *in vitro* translations of both *mBD19* and *mBDF* in the absence of any microsomes synthesized only full length

products. In the absence of any microsomes, only one product for each of BD19 and BDF were observed at 55 and 56 kD, respectively (Figure 4.20). If the products found in the supernatant of RR-BD19 and RR-BDF reactions were synthesized in the 'cytosol', then one would expect to see only the 55 and 56 kD products, respectively, because one would expect to see the same products observed in the reactions run in the absence of any microsomes.

BD15 has three more predicted membrane-spanning domains than BD12. It is possible that upon synthesis of one of these additional membrane-spanning domains in BD15, membrane integration becomes too complicated for the given system and the product is no longer associated with the rat liver microsomes, and that this dissociation leads to premature chain termination. Consider the following while supposing three statements are true of the system here: (*i*) BnDGAT1 is co-translationally integrated into the microsomes, (*ii*) the secondary products observed in RR-BD19 and RR-BDF are in fact prematurely terminated products, and (*iii*) synthesis downstream of TM2 is blocked and products larger than BD12 are released from the microsomes. RR-BD12 is synthesized to full length, and is primarily associated with the microsome fraction. RR-BD15 is also synthesized to full length, but is primarily associated with the supernatant. Under the three conditions described above, all of the membrane-spanning domains of BD12 are capable of maintaining associating with the microsomes, likely due to successful membrane integration. BD15 is not capable of maintaining association with the microsomes, possibly due to unsuccessful incorporation of additional membrane-spanning domain(s), specifically domains that are not found in the BD12 sequence.

RR-BD19 and RR-BDF reactions had three distinct products. The smallest product is equivalent in size to BD12, and remained associated with the microsome fractions. This product likely corresponds to the N-terminus up to the residues immediately upstream of TM3, and is therefore equivalent in sequence to BD12. The smallest product of both RR-BD19 and RR-BDF would therefore behave the same way as RR-BD12, with successful membrane integration. The second smallest product of RR-BD19 and RR-BDF reactions are equivalent in size to BD15, and did not remain associated with the microsome fractions. This product likely corresponds to the N-terminus up to the residues immediately upstream of TM6, and therefore is equivalent in sequence to BD15. The second smallest product of both RR-BD19 and RR-BDF would therefore behave the same way as RR-BD15 and would be unsuccessful in remaining associated with the microsome fraction. The largest product of RR-BD19 and RR-BDF reactions are equivalent in size to their respective full length products, and were not associated with the microsome fraction. The fact that the second smallest product of RR-BD19 and RR-BDF reactions are 'equivalent' to BD15 and not smaller than BD15, then the proposed membrane-spanning segment incapable of successful microsome incorporation is likely TM5, and not TM4 or TM3. If the proposed membrane-spanning segment causing the difficulties were TM4 or TM3, then the product would be 'released' from the microsomes and translation would be halted after or during the synthesis of TM4 or TM3, respectively, resulting in a product smaller than BD15. Full length RR-BD19 and RR-BDF products were, however, also observed in the supernatant, which suggests that either not all of the reactions released from the microsomes are halted, or that not all of the reactions are released from the microsomes following synthesis

downstream of TM5. This is supported by the presence of RR-BD15 product in the microsome fractions. One the other hand BD15 'equivalent' products are not observed in the microsome fractions of either RR-BD19 or RR-BDF.

A similar analysis of RR-BD1, -BD13, -BD14, -BD16, -BD17 and -BD18 reactions may provide a complement to the data presented here, possibly providing relevant insight into the topology of BnDGAT1 independent of a protease mapping study. In the absence of these analyses and/or complementary studies, it is difficult to come to any conclusions with the current results. Furthermore, RW-BDN data does not corroborate nor dismiss the above explanation. No BD-12 or BD-15 'equivalent' products were observed in either RW-BD19 or RW-BDF reactions, although there were multiple products in the translation reaction products and in the microsome fractions. The supernatant contained only the full length products of RW-BD19 and RW-BDF reactions. It is possible that with the wheat germ extract system a different predicted membrane-spanning domain is responsible for unsuccessful integration into the rat liver microsomes. The fact the truncated products are observed in the microsome fraction and not in the supernatant suggest that the translation may be halted after synthesis of specific membrane-spanning domains, but that these products are not released from the microsomes. Translation studies with additional BnDGAT1 truncations may provide further insight to support or disregard this explanation supporting premature chain termination.

Additional studies can also be done to test whether or not proteolytic processing is a valid explanation of secondary product formation. *In vitro* translation reactions can be run in the presence or absence of protease inhibitors. If in the presence of protease

inhibitors only full length products are observed, then it is likely that proteolytic processing is in fact the cause of secondary product formation. The addition of microsomes to a reaction following translation may also provide further insight into the events leading to secondary product formation. Translation in the absence of any microsomes is known to produce full length products (Figure 4.20). If following the addition of rat liver microsomes to translation reaction products additional products are observed, then post-translational proteolytic activity of the rat liver microsomes are likely the cause of the secondary product formation observed in Figure 4.22A and B. If additional products are not observed, then (a) BnDGAT1 and truncations are co-translationally inserted into the microsomes and proteolytic processing occurs co-translationally, or (b) the microsomes do not exhibit proteolytic activity towards BnDGAT1 and truncations.

4.8 Protease Mapping of BnDGAT1 and Truncations

Microsomes were pelleted from the *in vitro* translation products and then treated with proteinase K in the presence or absence of Triton X-100. Electrophoresis of proteinase K treated RR-BDF products on a 12% discontinuous SDS-PAGE gel revealed a thick band at the dye front, suggesting that the fragments produced by protease treatment are 7 kD and smaller (Figure 4.23). The expected sizes of truncations, based on BnDGAT1 topology scenario 1a and 1b are presented in Figure 4.24. Tricine-based gels can be used for the resolution of proteins or polypeptides as small as 1 kD (Schägger and von Jagow, 1987). Tricine-based gels of proteinase K treated RR-BDF products resulted in a smear of indistinct bands between 1 and 26 kD, the smear was most intense between

Figure 4.23 Protease treatment of RR-BDF resolved by SDS-PAGE. Forty micrograms per milliliter of reaction of *mBDF* was translated in a rabbit reticulocyte lysate system in the presence of 2 Eq rat liver microsomes. The pelleted microsomes from the translation reaction was resuspended in 10 μL of 10 mM HEPES-NaOH, pH 7.4 and treated with proteinase K, solubilized in SDS sample buffer at room temperature for 30 min and then resolved by discontinuous SDS-PAGE in 5 mm wide wells. A single band was observed at the dye front.

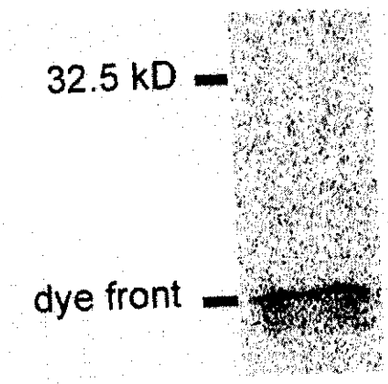
32.5 kD
dye front

Figure 4.24 Predicted protease protected fragments of BDF. ***A.*** The primary sequence of BnDGAT1 (rectangle) with putative membrane-spanning coding domains (gray), numbered 1-10 for TM1-TM10. ***B.*** Topology scenario 1a: TM1-TM10 are all membrane spanning domains, the black regions indicate predicted lumenal loop regions. The corresponding protease protected fragments are presented below, with their expected molecular mass. *C.* Topology scenario 1b: TM1-M4 and TM6-TM10 are membrane-spanning domains. Proposed region TM5 (white font on gray background) is predicted to be in the cytosol. The black regions indicate predicted lumenal loop regions. The predicted protease protected fragments are presented below, with their expected molecular mass.

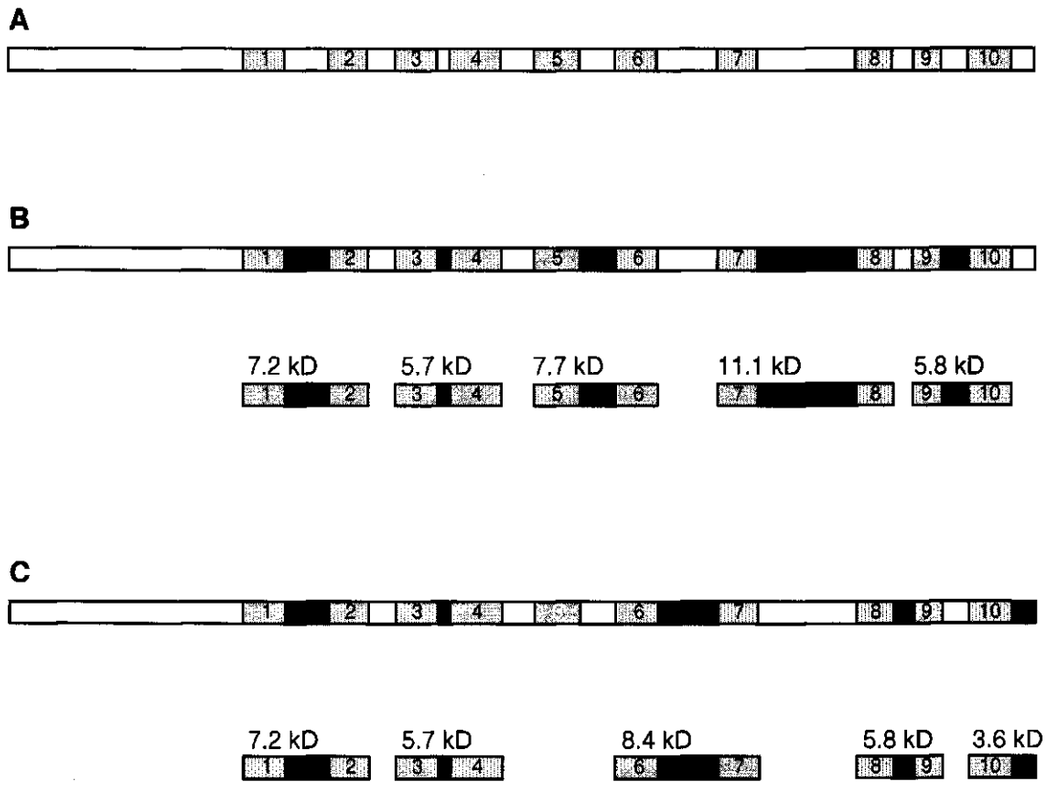
A
1
2
3
4
5
6
7
8
9
10
B
1
2
3
4
5
6
7
8
9
10
7.2 kD
5.7 kD
7.7 kD
11.1 kD
5.8 kD
C
1
2
3
4
5
6
7
8
9
10
7.2 kD
5.7 kD
8.4 kD
5.8 kD
3.6 kD

1 and 6 kD. Protease treatment in the presence of Triton X-100 also gave a smeared product, although the signal was less intense (Figure 4.25). Since multiple bands of incomplete polypeptide synthesis or proteolytic processing and membrane integration problems were observed in RR-BDF reactions (section 4.7.7), it is not surprising that the proteinase K treatment was not successful.

Protease treatment of RW-BDN reactions showed the same type of smearing in either the presence or absence of Triton X-100 (Figure 4.25). Background signal was also observed in RW-BDN translation products, particularly in RW-BD19 and RW-BDF, suggesting that premature termination or proteolytic processing was also taking place in these reactions (section 4.7.7). The background signal in RW-BD19 and RW-BDF, with several distinct bands, was prominent in the microsome fractions. If all of the polypeptides synthesized in one reaction (both full length and secondary polypeptide products) were folded properly in the microsomes, then the protease treatment should theoretically still produce distinct fragments. All of the protease protected fragments of the prematurely terminated reaction products, should theoretically be present in similar (if not the same) sizes in the protease protected fragments of the full length reaction product. Furthermore, proteinase K treatment of RW-B12 should theoretically provide distinct bands following protease treatment, since the background signal was virtually absent in the RW-BD12 microsome fraction suggesting that there was predominantly one product present in the microsome. The fact that protease treated RW-BD12 did not yield distinct bands, suggests that the polypeptide was not folding properly into the microsomes.

Since RR-BDN and RW-BDN translation products appeared to exhibit folding difficulties (section 4.7.7), and since BR-BDN and BW-BDN translation yields

Figure 4.25 Proteolytic analysis of *in vitro* translated BDN products. RR-BDN (left image), RW-BDN (center image) and CR-BDN (right image) were treated with proteinase K in the presence or absence of Triton X-100 (TX100). Protease treated products were resolved by Tricine-based gel electrophoresis in 2.5 mm wide wells and transblotted onto a 0.2 μm nitrocellulose membrane.

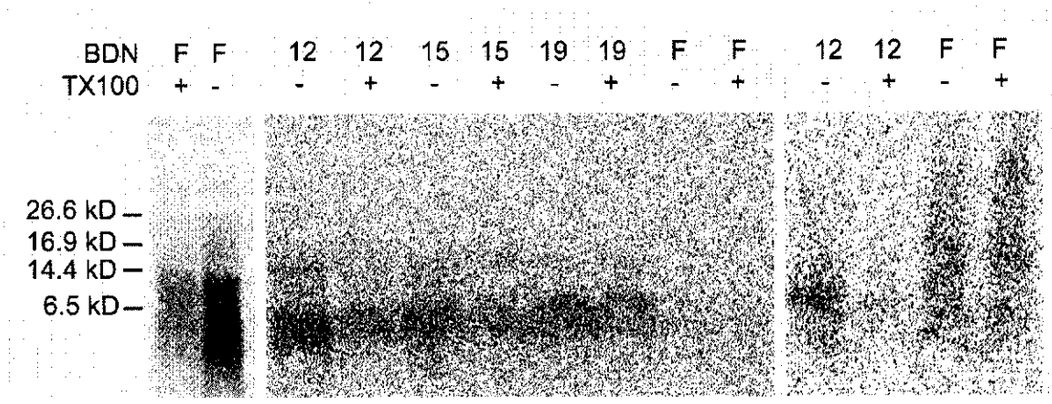
BDN F F 12 12 15 15 19 19 F F 12 12 F F
TX100 + - - + - + - + - + - + - +
26.6 kD
16.9 kD
14.4 kD
6.5 kD

were so low, translation in the presence of canine pancreatic microsome (Promega) was attempted. CR-BDN reactions gave products of expected sizes (Figure 4.26A). CW-BDN reactions were inhibited by the presence of canine pancreatic microsome (Figure 4.26B). Proteinase K treated CR-BD12 and CR-BDF, resulted in the same smear observed in previous proteinase K treatments described above (Figure 4.25). The smearing observed in protease treated translation products may be a consequence of improperly folded polypeptides. If some products were not folded properly into the microsomes, or if some products were folded differently than others, than we would expect to see too much background, or a smear, following protease treatment. The protease analyses here suggest that the products were not folding properly into the microsomes. In support of this, prior to protease treatment, the translation reactions appeared to exhibit folding problems as discussed in the previous section. CR-BDN reactions also appeared to exhibit folding problems, while considerably less background or secondary product formation was observed, the majority of the product was found in the supernatant fraction and only faint products were observed in the microsome fraction (Figure 4.26A).

Something may be absent from the translation systems used here, possibly a chaperone, that was required for proper folding. If a required chaperone was missing from the translation system, then supplementing the system with cytosol (or various fractions of cell lysate) from the *B. napus* cell suspension cultures may solve the folding problem. Studies with cytosol additions have been carried out using RR-BDN reactions. These were, however, attempted prior to solving the aggregation problem (see section 4.7.6), and we therefore do not have a cytosol addition study to address the

Figure 4.26 BDN incorporation into canine pancreatic microsomes. Forty micrograms per milliliter of reaction of *mBD12*, *mBD15*, *mBD19* and *mBDF* templates were translated (translation, or TL, lanes 1, 2, 3 and 4, respectively). Translation reactions were performed using a rabbit reticulocyte lysate system (***A***) or a wheat germ extract system (***B***) in the presence of 96 μg mL^{-1} canine pancreatic microsomes. Samples were solubilized in SDS sample buffer at room temperature for 30 min and then resolved by SDS-PAGE on a discontinuous gel in 2.5 mm wide wells.

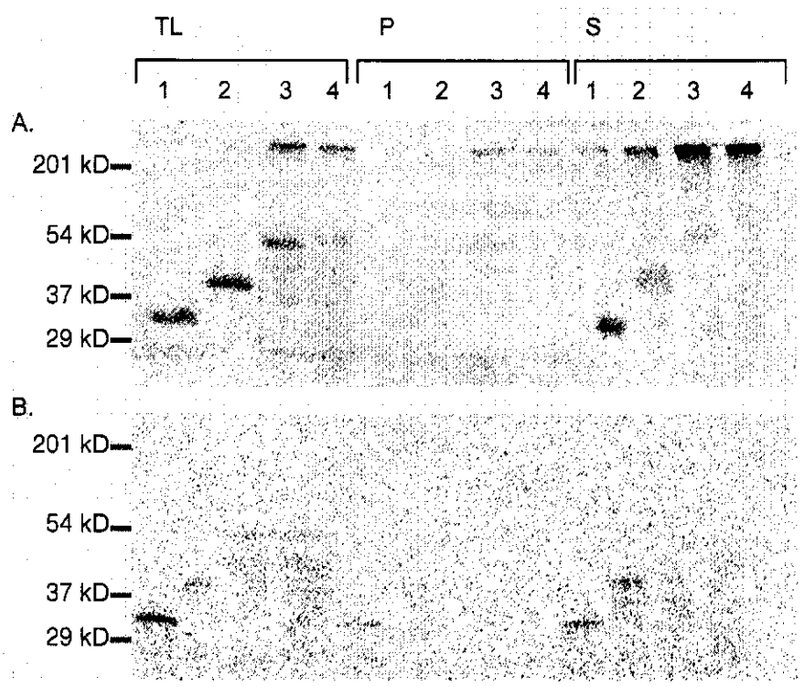
TL
P
S
1 2 3 4 1 2 3 4 1 2 3 4
A.
201 kD
54 kD
37 kD
29 kD
B.
201 kD
54 kD
37 kD
29 kD

putative folding problem discussed here.

4.9 Identification of a Putative BnDGAT2 from *Brassica napus* Cell Suspension Cultures

BnDGAT2 was originally identified in microspore-derived cell suspension culture of *B. napus* L. cv Jet Neuf at the RNA level during BnDGAT cloning (Nykiforuk et al., 1999b). No studies have been done, however, to confirm that BnDGAT2 is translated into a functional protein in the cell suspension cultures. Western blotting of microsomal preparations from cell suspension cultures revealed one product (approximately 56 kD) when detected with Antibody A (AbA), and two products (approximately 30 and 56 kD) when detected with Antibody B (AbB; Figure 4.27). The 56 kD band detected by both AbA and AbB is believed to correspond to BnDGAT1, which has a predicted molecular weight of 56 kD. The 30 kD band detected by AbB may correspond to BnDGAT2, which has a predicted molecular weight of 39.5 kD. Although there is quite a gap in molecular mass between 30 and 39.5 kD, it is not unusual for proteins (particularly hydrophobic ones) to run anomalously. Alternatively, the 30 kD polypeptide may represent a degradation product of BnDGAT1. AbA interacts with amino acid stretch A (21-LDRLHRRKSSSDSSN-35; Figure 4.1), which is located at the N-terminus of BnDGAT1. BnDGAT2 lacks the soluble N-terminal portion present in BnDGAT1, which contains amino acid stretch A, and therefore cannot be recognized by AbA. AbB interacts with amino acid stretch B (278-CYQPSYPRSPCIRKG-292; Figure 4.1), which is located between TM5 and TM6 of BnDGAT1. Stretch B is located in the equivalent region in BnDGAT2 (residues 116-CYQPSYPRSPCIRKG-130), with 100% sequence

Figure 4.27 Detection of BnDGAT protein in *Brassica napus* microspore-derived cell suspension cultures. Microsomal preparations were resolved by discontinuous SDS-PAGE in 5 mm wide wells and transferred to a nitrocellulose membrane. Immunoreactions with AbA led to the detection of a single band at approximately 56 kD, corresponding to detection of BnDGAT1. Immunoreactions with AbB led to detection of two bands at approximately 56 kD, corresponding to BnDGAT1, and 30 kD, possibly corresponding to putative BnDGAT2.

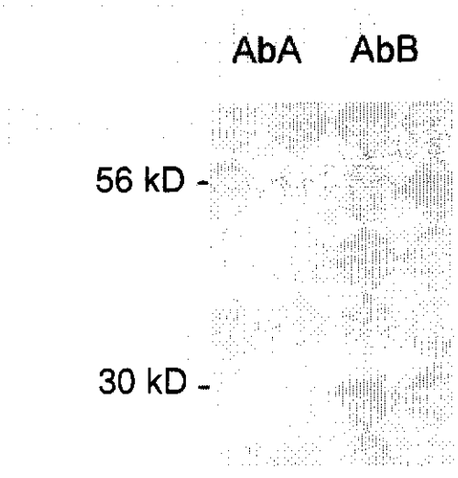
AbA
AbB
56 kD -
30 kD -

identity to BnDGAT1 (Figure 4.1). If the 30 kD signal observed does in fact correspond to BnDGAT2, this is the first experimental evidence of BnDGAT2 expression at the protein level in the cell suspension cultures.

N-terminal sequencing can be used to confirm whether or not this signal corresponds to BnDGAT2. In order to send the product for N-terminal sequencing, however, putative BnDGAT2 would have to be separated from other microsomal proteins. Immunodetection studies, using AbB, of purified microsomes from *B. napus* cell suspension cultures and resolved by 2D-PAGE is the most obvious and efficient course of action in obtaining a band free of contaminating proteins for N-terminal sequencing. The calculated isoelectric points of BnDGAT1 and BnDGAT2 (8.4 and 8.9, respectively) are quite high in comparison to many well characterized proteins, and separation in the first dimension should be resolved at 7-10 pH range. Our lab is currently working on optimizing solubilization conditions to resolve proteins from *B. napus* cell suspension culture microsomes in this pH range.

4.10 Probing the Membrane Topology of BnDGAT1 by Protease Mapping and Immunodetection Studies.

Immunochemical reactions with both antibody preparations AbA and AbB of proteinase treated *B. napus* microsomal vesicles were not detected (Figure 4.28). These results suggest that amino acid stretches A (21-LDRLHRRKSSSDSSN-35) and B (278-CYQPSYPRSPCIRKG-292), respectively recognized by AbA and AbB, are not protease protected and are therefore likely located in the cytosol. Amino acid stretch A is found in the N-terminal portion of BnDGAT1, and membrane topology predictions (Figure 2.2;

Figure 4.28 Protease mapping of microsomal preparations from *Brassica napus* microspore-derived cell suspension cultures. Microsomal preparations were treated with proteinase K (PK) and resolved by discontinuous SDS-PAGE in 5 mm wide wells and transferred to a nitrocellulose membrane. The signal detected at 56 kD with AbA and AbB corresponds to BnDGAT1 and the 30 kD signal is believed to correspond to BnDGAT2 detected with AbB were lost upon proteinase K treatment. No additional signals were observed with AbA and AbB detection following proteinase K treatment.

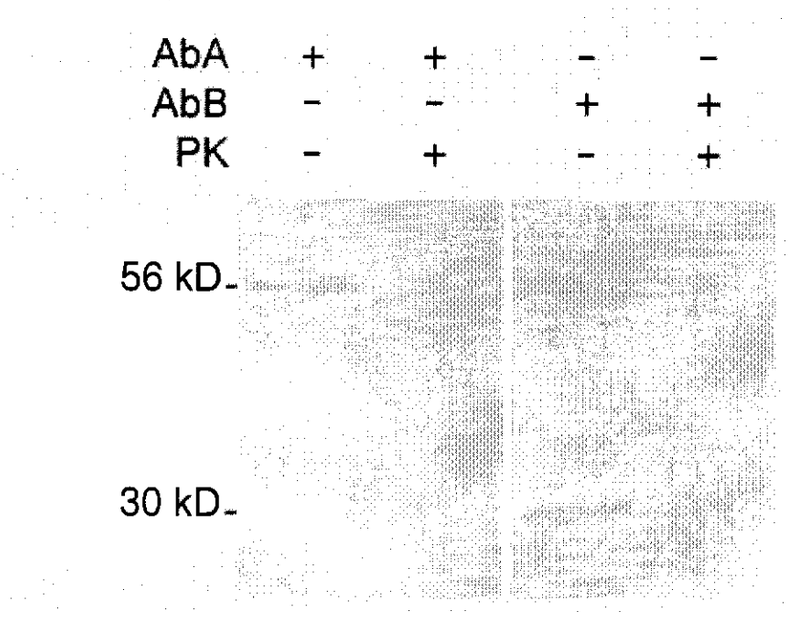
AbA + + - -
AbB - - + +
PK - + - +
56 kD
30 kD

scenario 1a and 1b) support the results here that place the N-terminus in the cytosol. The N-terminal region of BnDGAT1, as aforementioned, may be involved in the regulation of substrate selectivity or may serve as a capture site for acyl-CoAs. It is not surprising that this region is located in the cytosol, where the enzyme can interact with the acyl-CoA pool in the cytosol.

Amino acid stretch B includes one or two residues of the C-terminal portion of TM5 and the downstream loop region. The loss of the AbB signal upon protease treatment indicates that stretch B is also located in the cytosol, supporting the 9-transmembrane topology scenario for BnDGAT1 (scenario 1a) where the TM5 is not membrane-spanning, but rather part of a cytosolic loop. Although the implication that TM5 is not a membrane-spanning domain is contradicted in the discussion in section 4.7.7, where the incorporation into the microsome appears to be interrupted by the synthesis of TM5, the results here are more reliable. The BnDGAT1 analysis here is of the enzyme expressed in the cell suspension cultures from which it was cloned, and subsequently extracted from the cells in the microsomal fraction. The *in vitro* translation study, however, is expressing BnDGAT1 into a foreign environment, and the enzyme may not behave as it would in its native environment. In addition, it has been shown that the expression system used may affect the topology of a given protein (Spiess et al., 1989).

In the 9-transmembrane topology scenario, the loop downstream of TM4 and upstream of TM6 is located in the cytosol. Although TM5 is a more hydrophobic stretch of residues, as indicated by topology prediction, in the cytosol the TM5 region may form a hydrophobic pocket, possibly forming an active site based on its proximity to the two

invariant serine residues. Depending on the topology prediction program used, TM4 is believed to end either at residue 235, 236 or 239 (Table 4.1). The invariant serine residue, shown to be essential for ACAT activity, and identified in all sequenced DGATs and ACATs, corresponds to amino acid residue 237 of BnDGAT1 (Nykiforuk et al., 2002). If this residue is involved in activity, it is likely part of a loop rather than part of a membrane-spanning region, thus implicating residue 235 or 236 as the end of TM4. A second invariant serine residue, S251, also located in the loop downstream of TM4, has also been identified in BnDGAT1 (Nykiforuk et al., 2002). These invariant serine residues are adjacent to a putative tyrosine kinase phosphorylation site (100% sequence identity at residues 254-261), overlapping with TM5. There is conflicting data available regarding whether or not DGAT is deactivated by phosphorylation (Haagsman et al., 1981; Rodriquez et al., 1992; Lau and Rodriguez, 1996; Byers et al., 1999; Yu et al., 2002). Previous studies by Byers et al., (1999) suggested that microsomal DGAT activity from *B. napus* cell suspension cultures may not be regulated by phosphorylation. If, however, DGAT is deactivated by phosphorylation, then the putative tyrosine kinase phosphorylation site, which overlaps with TM5, would not be membrane-spanning. The results here, implicating that the two invariant serine residues (one of which has been shown to be essential for activity in related ACAT enzymes) and the adjacent putative tyrosine kinase phosphorylation site are located in the cytosol (likely as part of the same loop), warrants further investigation into the potential role of phosphorylation in regulating BnDGAT activity.

The corresponding residues to BnDGAT1 stretch B are also present in BnDGAT2 with 100% sequence identity located downstream of TM5. If the 30 kD signal

recognized by AbB in the untreated microsomal fraction does correspond to BnDGAT2, as we suspect (see section 4.9), then the loss of AbB signal in protease treated microsomes suggest that stretch B of both BnDGAT1 and of putative BnDGAT2 are located in the cytosol. If the region downstream of TM5 in BnDGAT2 is a cytosolic loop, this places the invariant serine residues (S75 and S89) in the cytosol, supporting both the 7 and 8 transmembrane scenarios for BnDGAT2 (Figure 2.2; scenario 2b and 2c, respectively). If BnDGAT2 is in fact derived from a truncation and amino acid mutations of BnDGAT1, as the high degree of sequence identity suggests (see section 4.9; Figure 4.1), then it is likely that the critical residues (including active site residues) of BnDGAT1 and BnDGAT2 are located on the same face of the membrane. Since in both BnDGAT1 topology scenarios 1a and 1b, the invariant serine residues are located in the cytosol, it is more likely that the corresponding residues of BnDGAT2 are also located in the cytosol, further supporting BnDGAT2 topology scenarios 2b and 2c (Figure 4.2). Furthermore, if BnDGAT2 is derived from a truncation and mutations of BnDGAT1, it is likely that the BnDGAT2 membrane topology is identical to that of its corresponding residues in BnDGAT1. If TM5 is not membrane-spanning in BnDGAT1, it is likely also not membrane-spanning in BnDGAT2, thus supporting BnDGAT topology scenario 2b (Figure 4.2).

5. CONCLUSION

Nine cDNAs were successfully cloned in pBluescript for *in vitro* translation studies, to encode various lengths of BnDGAT1. The clones under control of the T7 RNA polymerase were not successfully transcribed *in vitro*, possibly due to mutations in the T7 promoter region of the host vector. The four clones under control of the T3 RNA polymerase were capable of synthesizing messages of expected size. Some problems associated with the T3 clones were, however, encountered. These include (*i*) an apparent reduction in the rate of bacterial growth, possibly due to leaky expression of BDN products that may be lethal to *E. coli* cells, and (*ii*) extremely poor transcribed RNA yields were observed, suggesting that their may also be a mutation at the T3 promoter region of the host vector that did not inhibit but reduced RNA polymerase activity. The sequences of T7 and T3 promoter regions of the pBS-BDN clones are currently being investigated to determine whether or not there are in fact mutations in the T7 and/or T3 promoters.

Conditions for effective *in vitro* translation and incorporation of BDN into microsomes were not achieved. Microsomes purified from both rat liver and *B. napus* cell suspension cultures, and purchased microsomes from canine pancreas (Promega) were, however, compatible with both the rabbit reticulocyte lysate and wheat germ extract systems, since all preparations were successful in the processing of a β-lactamase signal sequence. Translation efficiency in both the rabbit reticulocyte lysate and wheat germ extract systems appeared to be reduced by *B. napus* microsomes. The RR-BDN reactions generated BDN products, and the smaller polypeptides, BD-12 and BD-15,

were of expected size. Multiple products were observed in RR-BDN reactions of the larger polypeptides, BD19 and BD-F. These products appear to be a result of either premature chain termination or proteolytic processing events. Both the CR-BDN and RW-BDN reactions synthesized full-length polypeptides of BDN, although some secondary products were observed in RW-BD19 and RW-BDF reactions. The secondary products in RW-BDN reactions were less abundant or distinct than those observed in RR-BDN reactions. BDN *in vitro* translation products formed aggregations upon heating that prevented their resolution by gel electrophoresis. The products were best resolved when samples were incubated in sample buffer at room temperature for 30 min, instead of boiling for 2-3 min, prior to run. Subsequent protease mapping of *in vitro* translation products resulted in smears indicative of a potential folding problem observed in these reactions.

Immunochemical studies have putatively identified protein expression of BnDGAT2 in the cell suspension cultures. This is the first report of possible BnDGAT2 expression at the level of the protein, since the enzyme has only been observed as the encoding mRNA. Protease mapping, followed by immunochemical reactions, of *B. napus* microsomal membranes has putatively placed two regions in BnDGAT1, stretch A (21-LDRLHRRKSSSDSSN-35) and stretch B (278-CYQPSYPRSPCIRKG-292), on the cytosolic face of the ER membrane.

6. FUTURE DIRECTIONS

Immunodetection studies have provided us with some insight into the membrane topology of BnDGAT1 and putative BnDGAT2. It has been speculated that the N-terminal regions of DGATs are localized in the cytosol (Hobbs et al., 1999), and we have provided evidence that supports this hypothesis for BnDGAT1. The current study has provided evidence supporting topology scenarios for each of BnDGAT1 and putative BnDGAT2. Immunodetection of TM5 of BnDGAT1, and possibly putative BnDGAT2, was lost in a protease protection assay, suggesting that TM5 is in the cytosol and therefore accessible to proteases. While some insight was gained into the topology of BnDGAT1 and putative BnDGAT2, providing data to support topology scenario 1a for BnDGAT1, and scenarios 2b for BnDGAT2, the whole topology still remains unresolved. Support for these two topology scenarios was based on experimental evidence suggesting that two stretches of amino acid residues of BnDGAT1 and one stretch of amino acid residues of putative BnDGAT2 are localized in the cytosol. Nonetheless, there remain many stretches of amino acid residues who's localization has not been demonstrated experimentally. The importance of experimentally determined topology can be emphasized in the topology study of African green monkey ACAT1 and ACAT2, where 8 and 7 putative membrane spanning regions were identified through hydrophobicity analysis, respectively. Experimental studies, however, revealed that there were only 5 membrane-spanning regions in each (Joyce et al., 2000). ACATs and DGATs share a high degree of sequence identity, and it would not be surprising if they also shared similar topologies.

A few lines of action should be taken to help solve the challenges encountered in the *in vitro* translation studies towards the resolution of DGAT topology. Optimizing the reaction conditions by changing salt, template or microsomal concentrations, or by the addition of *B. napus* cell lysate or different chaperones can be attempted in an effort to improve folding. As discussed in section 4.6, increasing microsome concentration tends to increase the amount of processed products at the risk of reducing the yield (Promega, Technical Manual No. 231), which may also improve the prospects of better folding. As mentioned in section 4.8, a chaperone involved in BnDGAT folding may be absent from the translation system, and by adding *B. napus* cell suspension culture lysate preparations we may be present the system with what is lacking. While these efforts may be worth investigating, an alternative method may provide us with a more efficient solution. Several methods available include N-linked glycosylation scanning mutagenesis (Kornfeld and Kornfeld, 1985; Bungert et al., 2001; Crystal et al., 2003; Zhang et al., 2004), cytoimmunofluorescence of selectively permeabilized membranes (Zhang et al., 2004; Crystal et al., 2003; Lin et al., 2003), and of course protease mapping (Lin et al., 2003; Abell et al., 2002; Gonzalez-Baró et al., 2001; Walter and Blobel, 1983; Morimoto et al., 1983).

Cytoimmunofluorescent studies of selectively permeabilized membranes should be the next effort in probing the membrane topology of BnDGAT1 expressed in yeast. A cytoimmunofluorescent method to determine the topology of BnDGAT1 has several advantages over protease protection studies and N-linked glycosylation scanning mutagenesis. First, it has been shown that BnDGAT1 and BnDGAT2 can be successfully expressed, yielding functional enzymes, in a yeast expression system (*Pichia pastoris*;

Nykiforuk et al., 2002), suggesting that the enzyme is properly folded when expressed in yeast. N-linked scanning mutagenesis would involve the use of an expression system that has not been tried for BnDGAT, and may therefore involve unnecessary and time consuming troubleshooting steps. A yeast expression would not be available for N-linked glycosylation studies. O-linked glycosylation is more typically observed in yeast expression systems (Invitrogen), and no N-linked scanning mutagenesis studies in yeast have been reported to our knowledge. An insect cell expression system would therefore be more suitable for N-linked glycosylation studies.

A protease protection study of microsomes extracted from the cell suspension culture using protein specific antibodies, would involve a system that expresses BnDGAT1 and putative BnDGAT2 in their native form. There are, however, other problems associated with immunodetection studies of microsomes purified from cell suspension cultures that outweigh the advantage of probing the topology in the native form. These problems will be addressed shortly.

Another advantage of cytoimmunofluorescent studies of selectively permeabilized membranes is that the clones already generated for BnDGAT1 *in vitro* translation studies can be used in the proposed study. The clones from the current study are in pBluescript and encode C-terminal truncations, and full length BnDGAT1. The truncations are designed to encode a given number of putative membrane-spanning domains starting from the soluble N-terminus, and include the putative loop region upstream from the last putative membrane-spanning domain. All of these clones can be cut out of pBluescript and pasted into a yeast expression vector with a C-terminal epitope tag fusion, and the full length cDNA, *cBDF*, can also be cloned with an N-terminal tag fusion. These clones

can then be expressed in yeast. The antibodies recognizing the tags can access either the cytosol or the lumen through selective permeabilization with of the plasma membrane with digitonin or streptolysin O (SLO), or nonselective permeabilization with saponin or Triton X-100, respectively, and then detected by fluorescence microscopy.

Clones from the current study would also be useful for *N*-linked glycosylation studies, although site-directed mutagenesis (not an uninvolved step) would still be necessary for each clone since *N*-linked glycosylation sites are not found in the native BnDGAT1 sequence. The full length BnDGAT1 could be used as a template for site-directed mutagenesis, generating clones to introduce *N*-linked glycosylation sites in different predicted loop areas. Ideally, one clone would be required for each predicted loop and for each of the N- and C-termini. One of the major disadvantages of the N-linked glycosylation studies is that some investigators have provided evidence suggesting that glycosylation contain topogenic information and may therefore affect the topology of some proteins (Göder et al., 1999).

No cloning would be involved in immunodetection studies of *B. napus* cell suspension culture microsomes. Immunodetection studies of BnDGAT1 and putative BnDGAT2 presented here (see section 4.10). This protease mapping/immunodetection study can be further explored by creating additional protein specific antibodies for each predicted loop region and for the C-terminus, providing coverage of a larger portion of the protein. Preparation of antibodies may, however, be time consuming and leave the door open for other troubleshooting steps. Once the antibodies have been prepared, conditions for immunodetection would need to be optimized. The two antibodies used in the current study, AbA and AbB, did not generated particularly strong signals—and these

two amino acid stretches used, stretch A and B, respectively, were regions with high antigenic indexes as determined by Mac Vector (International Biotechnologies, New Haven, CT). Antibodies would need to be generated to detect each of the predicted loop regions in order to resolve the full topology, and the preparation of antibodies against other stretches of amino acids may not be as successful as the preparation of AbA and AbB. While these steps may be worthwhile, one underlying disadvantage remains involving the separation of the protease protected fragments of BnDGAT1 from the protease-protected fragments of putative BnDGAT2. If the detectable region is not protected in either BnDGAT1 or putative BnDGAT2, then it is fairly safe to assume that the region of interest is located in the cytosol. If, however, the detectable region were protected in one of BnDGAT1 or putative BnDGAT2, how would one determine which enzyme the protected fragment is from? Likewise, if the detectable region is protected in both BnDGAT1 and putative BnDGAT2, and the protected fragments are the same size (which would likely be the case for most protein specific antibodies that would be used, since the sequence identity between the two enzymes 96 %), then how can we determine that the protected fragment comes from one or two enzymes? These are not trivial concerns associated with an immunodetection protease mapping study of *B. napus* cell suspension cultures.

Given the advantages and disadvantages of all three possible routes, the cytoimmunofluorescent study appears to be the most effective and reliable means of probing the membrane topology of BnDGAT1.

7. REFERENCES

Abell, B. M., High, S. and Moloney, M. M. 2002. Membrane protein topology of oleosin is constrained by its long hydrophobic domain. *J. Biol. Chem.* 277:8602-8610.

Abell, B. M., Holbrook, L. A., Abenes, M., Murphy, D. J., Hills, M. J. and Moloney, M. M. 1997. Role of the proline knot motif in oleosin endoplasmic reticulum topology and oil body targeting. *Plant Cell* 9:1481-1493.

Águila, M. B., Loureiro, C. C., da Rocha Pinheiro, A. and Mandarim-de-Lacerda, C. A. 2002. Lipid metabolism in rats fed diets containing different types of lipids. *Arq. Bras. Cardiol.* 78:32-38.

Ahnert-Hilger, G. Bhakdi, S. and Gratzl, M. 1985. Minimal requirements for exocytosis. A study using PC 12 cells permeabilized with staphylococcal alpha-toxin *J. Biol. Chem.* 260:12730-12734.

Alberts, A. W. and Vagelos, P. R. 1968. Acetyl-CoA carboxylase, I. Requirement for two protein fractions. *Proc. Natl. Acad. Sci. USA* 59:561-568.

Alberts, A. W., Nervi, A. M. and Vagelos, P. R. 1969. Acetyl-CoA carboxylase, II. Demonstration of biotin-protein and biotin carboxylase subunits. *Proc. Natl. Acad. Sci. USA* 63:1319-1326.

Andersson, M., Wettesten, M., Borén, J., Magnusson, A., Sjöberg, A., Rustacus, S., Olofsson, S.-O. 1994. Purification of diacylglycerol:acyltransferase from rat liver to near homogeneity. *J. Lipid Res.* 35:535-545.

Athappilly, F. K. and Hendrickson, W. A. 1995. Structure of biotinyl domain of acetyl-coenzyme A carboxylase determined by MAD phasing. *Structure* 3:1407-1419.

Audigier, Y., Friedlander, M. and Blobel, G. 1987. Multiple topogenic sequences in bovine opsin. *Proc. Natl. Acad. Sci. USA* 84:5783-5787.

Ausubel, F. M., Brent, R., Kingston, R. E., Moore, D. D., Seidman, J. G., Smith, J. A. and Struhl, K. 2004. Current Protocols in Molecular Biology. John Wiley and Sons, New York, NY.

Bagnato, C. and Igal, R. A. 2003. Overexpression of diacylglycerol acyltransferase-1 reduces phospholipid synthesis, proliferation, and invasiveness in simian virus 40-transformed human lung fibroblasts.
J. Biol. Chem. 278:52203-52211.

Balija, V. S., Chakraborty, T. R., Nikonov, T. R., Morimotoi, T., and Haldar, D. 2000. Identification of two transmembrane regions and a cytosolic domain of rat mitochondrial glycerophosphate acyltransferase. *J. Biol. Chem.* 275:31668–31673.

Bao, X. and Ohlrogge, J. 1999. Supply of fatty acid is one limiting factor in the accumulation of triacylglycerol in developing embryos. *Plant Physiol.* 120:1057-1062.

Bayle, D., Weeks, D., Hallen, S., Melchers, K., Bamberg, K. and Sachs, G. 1997. *In vitro* translation analysis of integral membrane proteins. *J. Recept. Signal Transduct. Res.* 17:29-56.

Becker, J. and Craig, E. A. 1994. Heat-shock proteins as molecular chaperones. *Eur. J. Biochem.* 1994. 219:11-23.

Beckmann, R., Spahn, C. M., Eswar, N., Helmers, J., Penczek, P. A., Sali, A., Frank, J. and Blobel, G. 2001. Architecture of the protein-conducting channel associated with the translating 80S ribosome. *Cell* 107:361-372.

Beltzer, J. P., Fiedler, K., Fuhrer, C., Geffen, I., Handschin, C., Wessels, H. P. and Spiess, M. 1991. Charged residues are major determinants of the transmembrane orientation of a signal-anchor sequence. *J. Biol. Chem.* 266:973-978.

Bemelmans, W. J. E., Muskiet, F. A. J., Feskens E. J. M., de Vries, J. H. M., Broer, J., May, J. F. and Meyboom-de Jong, B. 2000. Associations of alpha-linolenic acid and linoleic acid with risk factors for coronary heart disease. *Eur. J. Clin. Nutr.* 54:865-871.

Bennett, E. R. and Kanner, B. L. 1997. The membrane topology of GAT-1, a (Na^+ + Cl^-)-coupled γ-aminobutyric acid transporter from rat brain. *J. Biol. Chem.* 272:1203-1210.

Bertrams, M. and Heinz, E. 1981. Positional specificity and fatty-acid selectivity of purified sn-glycerol 3-phosphate acyltransferases from chloroplasts. *Plant Physiol.* 68:653-657.

Blanchard, C. Z., Lee, Y. M., Frantom, P. A. and Waldrop, G. L. 1999. Mutations at four active site residues of biotin carboxylase abolish substrate-induced synergism by biotin. *Biochemistry* 38:3393-3400.

Blobel, G. 1980. Intracellular membrane topogenesis. *Proc. Natl. Acad. Sci. USA* 77:1496.

Blobel, G. and Dobberstein, B. 1975a. Transfer of proteins across membranes. I. Presence of proteolytically processed and unprocessed nascent immunoglobulin light chains on membrane-bound ribosomes of murine myeloma. *J. Cell Biol.* 67:835-851.

Blobel, G. and Dobberstein, B. 1975b. Transfer of proteins across membranes. II. Reconstitution of functional rough microsomes from heterologous components. *J. Cell Biol.* 67:852-862.

Bodak, A. and Hatt, P. Y. 1975. Myocardial lesions induced by rapeseed oil-rich diet in the rat: ultrastructural aspects. *Recent Adv. Stud. Cardiac Struct. Metab.* 6:479-486.

Bogdanov, M., Heacock, P. N. and Dowhan, W. 2002. A polytopic membrane protein displays a reversible topology dependent on membrane lipid composition. *EMBO J.* 21:2107-2116.

Bourgis, F., Kader, J.-C., Barret, P., Renard, M., Robinson, D., Robinson, C., Delseny, M. and Roscoe, T. J. 1999. A plastidial lysophosphatidic acid acyltransferase from oilseed rape. *Plant Physiol.* 120:913–921.

Bouvier-Navé, P. Benveniste, P., Oelkers, P., Sturley, S. L. and Schaller, H. 2000. Expression in yeast and tobacco of plant cDNAs encoding acyl-CoA:diacylglycerol acyltransferase. *Eur. J. Biochem.* 267:85-96.

Breuer-Katschinski, B., Nemes, K., Marr, A., Rump, B., Leiendecker, B., Breuer, N. and Goebell, H. 2001. Colorectal adenomas and diet: a case-control study. Colorectal Adenoma Study Group. *Digestive Diseases Sci.* 46:86-95.

Brock, D. J., Kass, L. R., and Bloch, K. 1967. β-hydroxydecanoyl thioester dehydrase. II. Mode of action. *J. Biol. Chem.* 242:4432-4440.

Brown, A. P., Schierer, T. P. and Slabas, A. K. 2000. Characterization of a putative diacylglycerol acyltransferase from *Brassica napus* embryo. (GenBank Accession No. AF251794).

Browse, J. A. 1998. Respiration and Lipid Metabolism. In L Taiz and E Zeiger, eds, Plant Physiology, Sinauer Associates, Inc. Publishers, Sunderland, Massachusetts.

Bungert, S., Molday, L. L. and Molday, R. S. 2001. Membrane topology of the ATP binding cassette transporter ABCR and its relationship to ABC1 and related ABCA transporters: identification of *N*-linked glycosylation sites. *J. Biol. Chem.* 276:23539–23546.

Byers, S. D., Laroche, A., Smith, K. C. and Weselake, R. J. 1999. Factors enhancing diacylglycerol acyltransferase activity in microsomes from cell-suspension cultures of oilseed rape. *Lipids* 34:1143-1149.

Cahoon, E. B., Shah, S., Shanklin, J. and Browse, J. 1998. A determinant of substrate specificity predicted from the acyl-acyl carrier protein desaturase of developing cat's claw seed. *Plant Physiol.* 117:593–598.

Cahoon, E. B., Marillia, E. F., Stecca, K. L., Hall, S. E., Taylor, D. C. and Kinney, A. J. 2000. Production of fatty acid components of meadowfoam oil in somatic soybean embryos. *Plant Physiol.* 124:243-251.

Carrere-Kremer, S., Montpellier-Pala, C., Cocquerel, L., Wychowski, C., Penin, F. and Dubuisson, J. 2002. Subcellular localization and topology of the p7 polypeptide of hepatitis C virus. *J. Virol.* 76:3720-3730.

Cases, S., Smith, S. J., Zheng, Y. W., Myers, H. M., Lear, S. R., Sande, E., Novak, S., Collins, C., Welch, C. B., Lusis, A. J., Erickson, S. K. and Farese, R. V. Jr. 1998. Identification of a gene encoding an acyl CoA:diacylglycerol acyltransferase, a key enzyme in triacylglycerol synthesis. *Proc. Natl. Acad. Sci. USA* 95:13018-13023.

Cases, S., Stone, S. J., Zhou, P., Yen, E., Tow, B., Lardizabal, K. D., Voelker, T. and Farese, R. V. Jr. 2001. Cloning of DGAT2, a second mammalian diacylglycerol acyltransferase, and related family members. *J. Biol. Chem.* 276:38870-38876.

Cheng, D., Meegalla, R. L., He, B., Cromley, D. A., Billheimer, J. T. and Young, P. R. 2001. Human acyl-CoA:diacylglycerol acyltransferase is a tetrameric protein. *Biochem. J.* 359:707-717.

Chen, H. C. and Farese, R. V. Jr. 2000. DGAT and triglyceride synthesis: a new target for obesity treatment. *Trends Cardio. Med.* 10:188-192.

Claros, M. G. and von Heijne, G. 1994. TopPred II: an improved software for membrane protein structure predictions. *Comput. Appl. Biosci.* 10:685-686.

Coleman, R. A. and Lee, D. P. 2004. Enzymes of triacylglycerol synthesis and their regulation. *Prog. Lipid Res.* 43:134-176.

Cronan, J. E. Jr., and Waldrop, G. L. 2002. Multi-subunit acetyl-CoA carboxylase. *Prog. Lipid Res.* 41:407-435.

Crowley, K. S., Liao, S., Worrell, V. E., Reinhart, G. D. and Johnson, A. E. 1994. Secretory proteins move through the endoplasmic reticulum membrane via an aqueous, gated pore. *Cell* 78:461-471.

Crystal, A. S., Morais, V. A., Pierson, T. C., Pijak, D. S., Carlin, D., Lee, V. M.-Y. and Doms, R. W. 2003. Membrane topology of γ-secretase component PEN-2. *J. Biol. Chem.* 278:20117-20123.

D'Agnolo, G., Rosenfeld, I. S. and Vagelos, P. R. 1975. Multiple forms of beta-ketoacyl-acyl carrier protein synthetase in *Escherichia coli*. *J. Biol. Chem.* 250:5289-5294.

Dahlqvist, A., Stahl, U., Lenman, A., Banas, M., Lee, L., Sandager, L., Ronne, H. and Styme, S. 2000. Phospholipid:diacylglycerol:acyltransferase: an enzyme that catalyzes the acyl-CoA-independent formation of triacylglycerol in yeast and plants. *Proc. Natl. Acad. Sci. USA* 97:6487-6492.

Dasso, M. C. and Jackson, R. J. 1989. On the fidelity of mRNA translation in the nuclease-treated rabbit reticulocyte lysate system. *Nucleic Acid Res.* 17:3129-3144.

Davies, H, M., Hawkins, D. J. and Nelsen, J. S. 1995. Lysophosphatidic acid acyltransferase from immature coconut endosperm having medium chain length substrate specificity. *Phytochemistry* 39:989-996

Davies, C., Heath, R. J., White, S. W. and Rock, C. 2000. The 1.8 Å crystal structure and active-site architecture of β-ketoacyl-acyl carrier protein synthase III (FabH) from *Escherichia coli*. *Structure* 8:185-195.

Declercq, P. E., Debeer, L. J. and Mannaerts, G. P. 1982. Role of glycerol-3-phosphate and glycerophosphate acyltransferase in the nutritional control of hepatic triacylglycerol synthesis. *Biochem J.* 204:247-256.

Dietrich, A., Souciet, G. and Weil, J. H. 1987. *In vitro* synthesis of bean (*Phaseolus vulgaris*) chloroplastic and cytoplasmic leucyl-tRNA synthetases. Characterization and processing of a precursor polypeptide for the chloroplast enzyme. *J. Biol. Chem.* 262:4248-4251.

Domergue, F., Chevalier, S., Santarelli, X., Cassagne, C. and Lessire, R. 1999. Evidence that oleoyl-CoA and ATP-dependent elongations coexist in rapeseed (Brassica napus L.). *Eur. J. Biochem.* 263:464-470.

Dupont, J., White, P. J., Johnston, K. M., Heggtveit, H. A., McDonald, B. E., Grundy S. M. and Bonanome, A. 1989. Food safety and health effects of canola oil. *J. Am. Coll. Nutr.* 8:360-375.

Dyers, J. M., Chapital, D. C., Kuan, J.-C. W., Mullen, R. T., Turner, C., McKeon, T. A. and Pepperman, A. B. 2002. Molecular analysis of a bifunctional fatty acid conjugase/desaturase from tung. Implications for the evolution of plant fatty acid diversity. *Plant Physiol.* 130:2027-2038.

Eberhardt, C., Gray, P. W. and Tjoelker, L. W. 1999. cDNA cloning, expression and chromosomal localization of two human lysophosphatidic acid acyltransferases. *Adv. Exp. Med. Biol.* 469:351-356.

Egea, P. F., Shan, S. O., Napetschnig, J, Savage, D. F., Walter, P. and Stroud, R. M. 2004. Substrate twinning activates the signal recognition particle and its receptor. *Nature.* 427:215-221.

Engfeldt, B. and Brunius, E. 1975a. Morphological effects of rapeseed oil in rats. I. Short-term studies. *Acta Med. Scand. Suppl.* 585:15-26.

Engfeldt, B. and Brunius, E. 1975b. Morphological effects of rapeseed oil in rats. II. Long-term studies. *Acta Med. Scand. Suppl.* 585:27-40.

Erickson, A. H. and Blobel, G. 1983. Cell-free translation of messenger RNA in a wheat germ system. *Methods Enzymol.* 96:38-50.

Faham, S. and Bowie, J. U. 2002. Bicelle crystallization: a new method for crystallizing membrane proteins yields a monomeric bacteriorhodopsin structure. *J. Mol. Biol.* 316:1-6.

Fehrmann, F., Jung, M., Zimmermann, R. and Krausslich, H. G. 2003. Transport of the intracisternal A-type particle Gag polyprotein to the endoplasmic reticulum is mediated by the signal recognition particle. *J. Virol.* 77:6293-6304.

Filling, C., Berndt, K. D., Benach, J., Knapp, S., Prozorovski, T., Nordling, E., Ladenstein, R., Jornvall, H. and Oppermann, U. 2002. Critical residues for structure and catalysis in short-chain dehydrogenases/reductases. *J. Biol. Chem.* 277:25677-25684.

Fisher, M., Kroon, J. T. M., Martindale, W., Stuije, A. R., Slabas, A. R., and Rafferty, J. B. 2000. The X-ray structure of *Brassica napus* β-keto acyl carrier protein reductase and its implications for substrate binding. *Structure* 8:339-347.

Fraser F, Corstorphine CG, Zammit VA. 1997. Topology of carnitine palmitoyltransferase I in the mitochondrial outer membrane. *Biochem. J.* 323:711-718.

Frentzen, M. 1993. Acyltransferases and Triacylglycerols. In TS Moore Jr., ed, Lipid Metabolism in Plants, CRC Press.

Frydman, J. 2001. Folding of newly translated proteins *in vivo*: the role of molecular chaperones. *Annu. Rev. Biochem.* 70:603–647.

Gafvelin, G., Sakaguchi, M., Andersson, H. and von Heijne, G. 1997. Topological rules for membrane protein assembly in eukaryotic cells. *J. Biol. Chem.* 272:6119-27.

Galili, G., Sengupta-Gopalan, C. and Ceriotti, A. 1998. The endoplasmic reticulum of plant cells and its role in protein maturation and biogenesis of oil bodies. *Plant Mol. Biol.* 38:1-29.

Ganesh Bhat, B., Wang, P., Kim, J. H., Black, T. M., Lewin, T. M., Fiedorek, F. T. Jr. and Coleman, R. A. 1999. Rat sn-glycerol-3-phosphate acyltransferase: molecular cloning and characterization of the cDNA and expressed protein. *Biochim. Biophys. Acta.* 1439:415-423.

Giannoulia, K. and Hatzopoulos, P. 2004. Olive DGAT1 cDNA. (GenBank Accession No. AY445635).

Giannoulia, K., Haralampidis, K., Poghosyan, Z., Murphy, D. J. and Hatzopoulos, P. 2000. Differential expression of diacylglycerol acyltransferase (DGAT) genes in olive tissues. *Biochem. Soc. Trans.* 28:695-697.

Gilstring, C. F. and Ljungdahl, P. O. 2000 A method for determining the in vivo topology of yeast polytopic membrane proteins demonstrates that Gap1p fully integrates into the membrane independently of Shr3p. *J. Biol. Chem.* 275:31488-31495.

Goder, V., Bieri, C. and Spiess, M. 1999. Glycosylation can influence topogenesis of membrane proteins and reveals dynamic reorientation of nascent polypeptides within the translocon. *J. Cell Biol.* 147:257-266.

Gorlich, D., Rapoport, T. A. 1993. Protein translocation into proteoliposomes reconstituted from purified components of the endoplasmic reticulum membrane. *Cell* 75:615-630.

Gonzalez-Baró, M. R., Granger, D. A. and Coleman, R. A. 2001. Mitochondrial glycerol phosphate acyltransferase contains two transmembrane domains with the active site in the N-terminal domain facing the cytosol. *J. Biol. Chem.* 276: 43182–43188.

Greenspan, M. D., Alberts, A. W. and Vagelos, P. R. 1969. Acyl carrier protein. 13. β-ketoacyl carrier protein synthase from *Escherichia coli*. *J. Biol. Chem.* 244:6477-6485.

Haagsman, H. P., de Haas, C. G., Geelen, M. J. and van Golde, L. M. 1981. Regulation of triacylglycerol synthesis in the liver: a decrease in diacylglycerol acyltransferase activity after treatment of isolated rat hepatocytes with glucagon. *Biochim. Biophys. Acta.* 664:74-81.

Haffar, O. K., Dowbenko, D. J. and Berman PW. 1988. Topogenic analysis of the human immunodeficiency virus type 1 envelope glycoprotein, gp160, in microsomal membranes. *J. Cell Biol.* 107:1677-1687.

Halic, M., Becker, T., Pool, M. R., Spahn, C. M., Grassucci, R. A., Frank, J. and Beckmann, R. 2004. Structure of the signal recognition particle interacting with the elongation-arrested ribosome. *Nature* 427:808-814.

Hamman, B. D., Hendershot, L. M. and Johnson, A. E. 1998. BiP maintains the permeability barrier of the ER membrane by sealing the lumenal end of the translocon pore before and early in translocation. *Cell* 92:747-758.

Harwood, J. 1996. Recent advances in the biosynthesis of plant fatty acids. *Biochim. Biophys. Acta* 1301:7-56.

He, X., Chen, G. Q., Lin, J. T. and McKeon, T. A. 2004a. Regulation of diacylglycerol acyltransferase in developing seeds of castor. *Lipids* 39:865-871.

He, X., Turner, C., Chen, G. Q., Lin, J. T. and McKeon, T. A. 2004b. Cloning and characterization of a cDNA encoding diacylglycerol acyltransferase from castor bean. *Lipids* 39:311-318.

Hesler, C. B., Carroll, M. A. and Haldar, D. 1985. The topography of glycerophosphate acyltransferase in the transverse plane of the mitochondrial outer membrane. *J. Biol. Chem.* 260:7452-7456.

Hobbs, D. H., Lu, C. and Hills, M. J. 1999. Cloning of a cDNA encoding diacylglycerol acyltransferase from Arabidopsis thaliana and its functional expression. *FEBS Lett.* 452:145-149.

Hofmann, K. and Stoffel, W. 1993. TMbase - A database of membrane spanning proteins segments *Biol. Chem. Hoppe-Seyler* 47:166.

Ikeda, M., Arai, M., Lao, D. M. and Shimizu, T. 2002. Transmembrane topology prediction methods: a re-assessment and improvement by a consensus method using a dataset of experimentally-characterized transmembrane topologies. *In Silico Biol.* 2:19-33.

Ishizaki, O., Nishida, I., Agata, K., Eguchi, G., and Murata, N. 1988. Cloning and nucleotide sequence of cDNA for the plastid glycerol-3-phosphate acyltransferase from squash. *FEBS Lett.* 238:424-430.

Jackowski, S. and Rock, C. O. 1987. Altered molecular form of acyl carrier protein associated with β-ketoacyl-acyl carrier protein synthase II *(fabF)* mutants. *J. Bacteriol.* 169:1469-1473.

Jackson, R. and Hunt, T. 1983. Preparation and use of nuclease-treated rabbit reticulocyte lysates for the translation of eukaryotic messenger RNA. *Methods Enzymol.* 96:50-74.

Jain, R. K. Coffey, M., Lai, K., Kumar, A. and MacKenzie, S. L. 2000. Enhancement of seed oil content by expression of glycerol-3-phosphate acyltransferase genes. *Biochem. Soc. Trans.* 28:958-961.

Jako, C., Kumar, A., Wei, Y., Zou, J., Barton, D. L., Giblin, E. M., Covello, P. S. and Taylor, D. C. 2001. Seed-specific over-expression of an *Arabidopsis* cDNA encoding a diacylglycerol acyltransferase enhances seed oil content and seed weight. *Plant Physiol.* 126:861–874.

Jezek, J., Haggett, B. G., Atkinson, A. and Rawson, D. M. 1999. Determination of glucosinolates using their alkaline degradation and reaction with ferricyanide. *J. Agric. Food Chem.* 47:4669-4674.

Jin, U., Lee, J., Chung, Y., Yi, Y., Kim, Y., Hyung, N., Pyee, J. and Chung, C. 2001. Characterization and temporal expression of ω-6 fatty acid desaturase cDNA from sesame (*Sesamum indicum* L.) seeds. *Plant Sci.* 161:515-517.

Jitrapakdee, S. and Wallace, J. C. 2003. The biotin enzyme family: conserved structural motifs and domain rearrangements. *Curr. Protein Pept. Sci.* 4:217-229.

Johnson, A. E. and van Waes, M. A. 1999. The translocon: a dynamic gateway at the ER membrane. *Annu. Rev. Cell Dev. Biol.* 15:799-842.

Johnson, P. E., Rawsthorne, S. and Hills, M. J. 2002. Export of acyl chains from the plastids isolated from embryos of *Brassica napus* (L). *Planta* 215:515-517.

Jörnvall, H., Persson, B., Krook, M., Atrian, S., Gonzalez-Duarte, R., Jeffery, J. and Ghosh, D. 1995. Short-chain dehydrogenases/reductases (SDR). *Biochemistry* 34:6003-6013.

Joyce, C. W., Shelness, G. S., Davis, M. A., Lee, R. G., Skinner, K., Anderson, R. A. and Rudel, L. L. 2000. ACAT1 and ACAT2 membrane topology segregates a serine residue essential for activity to opposite sides of the endoplasmic reticulum. *Mol. Biol. Cell* 11:3675-3687.

Kachroo, A., Lapchyk, L., Fukushige, H., Hildebrand, D., Klessig, D. and Kachroo, P. 2003. Plastidial fatty acid signaling modulates salicylic acid- and jasmonic acid-mediated defense pathways in the Arabidopsis ssi2 mutant. *Plant Cell.* 15:2952-2965

Kalies, K.-U. and Hartmann, E. 1998. Protein translocation into the endoplasmic reticulum (ER): two similar routes with different modes. *Eur. J. Biochem.* 254:1-5.

Kamisaka, Y., Mishra, S. and Nakahara, T. 1997. Purification and characterization of diacylglycerol acyltransferase from the lipid body fraction of an oleaginous fungus. *J. Biochem.* 121:1107-1114.

Kane, J. F. and Hartley, D. L. 1988. Formation of recombinant protein inclusion bodies in *Escherichia coli*. *Trends Biotechnol.* 6:95-101.

Katavic, V., Reed, D. W., Taylor, D. C., Giblin, E. M., Barton, Zou, J., Mackenzie, S. L., Covello, P. S. and Kunst, L. 1995. Alteration of seed fatty acid composition by an ethyl methanosulfonate-induced mutation in *Arabidopsis thaliana* affecting diacyglcyerol acyltransferase activity. *Plant Physiol.* 108:399-409.

Katavic, V., Mietkiewska, E., Barton, D. L., Giblin, E. M., Reed, D. W. and Taylor, D. C. 2002. Restoring enzyme activity in nonfunctional low erucic acid *Brassica napus* fatty acid elongase 1 by a single amino acid substitution. *Eur. J. Biochem.* 269:5625-5631.

Kaup, M. T., Froese, C. D. and Thompson, J. E. 2002. A role for diacylglycerol acyltransferase during leaf senescence. *Plant Physiol.* 129:1616–1626.

Keatinge-Clay, A. T., Shelat, A. A., Savage, D. F., Tsai, S. C., Miercke, L. J., O'Connell, J. D. 3rd, Khosla, C., Stroud, R. M. 2003. Catalysis, specificity, and ACP docking site of Streptomyces coelicolor malonyl-CoA:ACP transacylase. *Structure* 11:147-154.

Kennedy, E. P. 1961. Biosynthesis of complex lipids. *Fed. Proc.* 20:934-940.

Kim, H. U. and Huang, A. H. C. 2004. Plastid lysophosphatidyl acyltransferase is essential for embryo development in Arabidopsis. *Plant Physiol.* 134:1206–1216.

Knauf, V. C. and Facciotti, D. 1995. Genetic engineering of foods to reduce the risk of heard disease and cancer. *Adv. Exp. Med. Biol.* 369:221-228.

Knutzon, D. S., Lardizabal, K. D., Nelsen, J. S., Bleibaum, J. L., Davies, H. M. and Metz, J. C. 1995. Cloning of a coconut endosperm cDNA encoding a 1-acyl-*sn*-glycerol-3-phosphate acyltransferase that accepts medium-chain-length substrates. *Plant Physiol.* 109:999-1006.

Kornfeld, R. and Kornfeld, S. 1985. Assembly of asparagines-linked oligosaccharides. *Annu. Rev. Biochem.* 54:631-664.

Krogh, A., Larsson, B., von Heijne, G. and Sonnhammer, E. L. L. 2001. Predicting transmembrane protein topology with a hidden Markov model: application to complete genomes. *J. Mol. Biol.* 305:567-580.

Kwanyuen, P. and Wilson, R. F. 1986. Isolation and purification of diacylglycerol acyltransferase from germinating soybean cotyledons. *Biochim. Biophys. Acta.* 877:238-245.

Kyte, J. and Doolittle, R. F. 1982. A simple method for displaying the hydropathic character of a protein. *J. Mol. Biol.* 157:105-132.

Laemmli, U. K. 1970. Cleavage of structural proteins during the assembly of the head of bacteriophage T4. *Nature* 227:680-685.

Lai, C. Y. and Cronan, J. E. 2003. Beta-ketoacyl-acyl carrier protein synthase III (FabH) is essential for bacterial fatty acid synthesis. *J. Biol. Chem.* 278:51494-51503.

Lambert, C. and Prange, R. 2003. Chaperone action in the posttranslational topological reorientation of the hepatitis B virus large envelope protein: implications for translocational regulation. *Proc. Natl. Acad. Sci. USA* 100:5199-5204.

Landau, E. M. and Rosenbusch, J. P. 1996. Lipidic cubic phases: A novel concept for the crystallization of membrane proteins. *Proc. Natl. Acad. Sci. USA* 93:14532–14535.

Lardizabal, K. D., Mai, J. T., Wagner, N. W., Wyrick, A., Voelker, T. and Hawkins, D. J. 2001. DGAT2 is a new diacylglycerol acyltransferase gene family. *J. Biol. Chem.* 276:38862-38869.

Lassner, M. W., Levering, C. K., Davies, H. M. and Knutzon, D. S. 1995. Lysophosphatidic acid acyltransferase from meadowfoam mediates insertion of erucic acid at the *sn*-2 position of triacylglycerols in transgenic rapeseed oil. *Plant Physiol.* 109:1389-1394.

Lau, T. E. and Rodriguez, M. A. 1996. A protein tyrosine kinase associated with the ATP-dependent inactivation of adipose diacylglycerol acyltransferase. *Lipids* 31:277-283.

Leesong, M., Henderson, B. S., Gillig, J. R., Schwab, J. M. and Smith, J. L. 1996. Structure of a dehydratase–isomerase from the bacterial pathway for biosynthesis of unsaturated fatty acids: two catalytic activities in one active site. *Structure* 4:253-264.

Lehner, R. and Kuksis, A. 1993. Triacylglycerol synthesis by an *sn*- 1,2(2,3)-diacylglycerol transacylase from rat intestinal microsomes. *J. Biol. Chem.* 268:8781-8786.

Lewin, T. M. Schwerbrock, N. M. J., Lee, D. P. and Coleman, R. A. 2004. Identification of a new glycerol-3-phosphate acyltransferase isoenzyme, mtGPAT2, in mitochondria. *J. Biol. Chem.* 279:13488-13495.

Li, P., Gao, X-G., Arellano, R. O. and Renugopalakrishnan, V. 2001. Glycosylated and phosphorylated proteins—expression in yeast and oocytes if *Xenopus*: prospects and challenges—relevance to expression of thermostable proteins. *Protein Exp. Purif.* 22:369-380.

Lin, S., Lu, X., Chang, C. C. Y. and Chang, T. Y. 2003. Human acyl-coenzyme A:cholesterol acyltransferase expressed in Chinese hamster ovary cells: membrane topology and active site location. *Mol. Biol. Cell* 14:2447-2460.

Little, D., Weselake, R., Pomeroy, K., Furukawa, T. and Bagu, J. 1994. Solubilization and characterization of diacylglycerol acyltransferase from microspore-derived cultures of oilseed rape. *Biochem. J.* 304:951-958.

Lodish, H., Baltimore, D., Berk, A., Zipursky, S. L., Matsudaira, P. and Darnell, J. 1995. Membrane Structure: the Plasma Membrane. In Molecular Cell Biology, Ed 3. Scientific American Books, New York, New York.

Lommerse, P. H., Spaink, H. P. and Schmidt, T. 2004. *In vivo* plasma membrane organization: results of biophysical approaches. *Biochim. Biophys. Acta.* 1664:119-131.

Maldarelli, F., Chen, M. Y., Willey, R. L. and Strebel, K. 1993. Human immunodeficiency virus type 1 Vpu protein is an oligomeric type I integral membrane protein. *J. Virol.* 67:5056-5061.

Manaf, A. M. and Harwood, J. L. 2000. Purifcation and characterisation of acyl-CoA:glycerol 3-phosphate acyltransferase from oil palm (*Elaeis guineensis*) tissues. *Planta* 210: 318-328.

Mandon, E. C., Jiang, Y. and Gilmore, R. 2003. Dual recognition of the ribosome and the signal recognition particle by the SRP receptor during protein targeting to the endoplasmic reticulum. *J. Cell Biol.* 162:575-585.

Marston, F. A. and Hartley, D. L. 1990. Solubilization of protein aggregates. *Methods Enzymol.* 182:264-276.

Martelli, A. M., Fala, F., Faenza, I., Billi, A. M., Cappellini, A., Manzoli, L. and Cocco, L. 2004. Metabolism and signaling activities of nuclear lipids. *Cell. Mol. Life Sci.* 61:1143-1156.

Martin, B. A. and Wilson, R. F. 1983. Properties of diacylglycerol acyltransferase from spinach leaves. *Lipids* 18:1-6.

Martin, B. A. and Wilson, R. F. 1984. Subcellular localization of TAG synthesis in spinach leaves. *Lipids* 19:117-121.

Martínez-Rivas, J. M., Sperling, P., Lühs, W. and Heinz, E. 2001. Spatial and temporal regulation of three different microsomal oleate desaturase genes (*FAD2*) from normal – type and high-oleic varieties of sunflower (*Helianthus annus* L.). *Mol. Breed.* 8:159-168.

Mathews, C. K. and van Holde, K. E. 1996. Lipid Metabolism I: Fatty Acids, Triacylglycerols, and Lipoproteins. In Biochemistry, Ed 2. The Benjamin Cummings Publishing Company, Inc. Menlo Park.

Mayorek, N., Grinstein, I. and Bar-Tana, J. 1989. Triacylglycerol synthesis in cultured rat hepatocytes. The rate limiting role of diacylglycerol acyltransferase. *Eur. J. Biochem.* 182:395-400.

McCartney, A. W., Dyer, J. M., Dhanoa, P. K., Kim, P. K., Andrews, D. W., McNew, J. A. and Mullen, R. T. 2004. Membrane-bound fatty acid desaturases are inserted co-translationally into the ER and contain different ER retrieval motifs at their carboxy termini. *Plant J.* 37:156-173.

Menetret, J. F., Neuhof, A., Morgan, D. G., Plath, K., Radermacher, M., Rapoport, T. A. and Akey, C. W. 2000. The structure of ribosome-channel complexes engaged in protein translocation. *Moll. Cell.* 6:1219-1232.

Meyer, D. I., Krause, E. and Dobberstein, B. 1982. Secretory protein translocation across membranes—the role of the "docking protein". *Nature* 297:647-650.

Miao, G.-H., Hong, Z. and Verma, D. P. S. 1992. Topology and phosphorylation of soybean nodulin-26, an intrinsic protein of the peribacteroid membrane. *J. Cell Biol.* 118:481-490.

Miller, L. K. 1988. Baculoviruses as gene expression vectors. *Ann. Rev. Microbiol.* 47:177-199.

Mishra, S. and Kamisaka, Y. 2001. Purification and characterization of thiol-reagent-sensitive glycerol-3-phosphate acyltransferase from the membrane fraction of an oleaginous fungus. *Biochem. J.* 355:315-322.

Mistry, D. H. and Medrano, J. F. 2002. Cloning and localization of the bovine and ovine *lysophosphatidic acid acyltransferase (LPAAT)* genes that codes for an enzyme involved in triglyceride biosynthesis. *J. Dairy Sci.* 85:28-35.

Miyazaki, A., Sakai, M., Sakamoto, Y. and Horiuchi, S. 2003. Acyl-coenzyme A:cholesterol acyltransferase inhibitors for controlling hypercholesterolemia and atherosclerosis. *Curr. Opin. Investig. Drugs.* 4:1095-1099.

Morimoto, T., Arpin, M. and Gaetani, S. 1983. Use of proteases for the study of membrane insertion. *Methods Enzymol.* 96:121-150.

Murata, N. and Tasaka, Y. 1997. Glycerol-3-phosphate acyltransferase in plants. *Biochim. Biophys. Acta* 1348:10-16.

Murthy, M. S. and Pande, S. V. 1987. Malonyl-CoA binding site and the overt carnitine palmitoyltransferase activity reside on the opposite sides of the outer mitochondrial membrane. *Proc. Natl. Acad. Sci. USA* 84:378-382.

Nagai, K., Oubridge, C., Kuglstatter, A., Menichelli, E., Isel, C. and Jovine, L. 2003. Structure, function and evolution of the signal recognition particle. *EMBO J.* 22:3479-3485.

Nicolosi, R. J. and Rogers, E. J. 1997. Regulation of plasma lipoprotein levels by dietary triglycerides enriched with different fatty acids. *Med. Sci. Sports Exerc.* 29:1422-1428.

Nilsson, J., Pearson, B. and von Heijne, G. 2002. Prediction of partial membrane protein topologies using a consensus approach. *Protein Sci.* 11:2974-2980.

Nishida, I., Frentzen, M., Ishizaki, O. and Murata, N. 1987. Purifcation of isomeric forms of acyl-[acyl-carrier-protein]:glycerol-3-phosphate acyltransferase from greening squash cotyledons. *Plant Cell Physiol.* 28:1071-1079.

Nykiforuk, C. L., Furukawa-Stoffer, T. L., Huff, P. W., Sarna, M., Laroche, A., Moloney, M. M. and Weselake, R. J. 2002. Characterization of cDNAs encoding diacylglycerol ayltransferase from cultures of *Brassica* napus and sucrose-mediated induction of enzyme biosynthesis. *Biochimi. Biophysi. Acta.* 1580:95-109.

Nykiforuk, C. L., Laroche, A. and Weselake, R. J. 1999a. Isolation and analysis of a novel cDNA encoding a putative diacylglycerol ayltransferase from a microspore-derived cell suspension culture of *Brassica* napus L. cv Jet Neuf (Accession No. AF155224). (PGR99-123) *Plant Physiol.* 120:1207.

Nykiforuk, C. L., Laroche, A. and Weselake, R. J. 1999b. Isolation and characterization of a novel cDNA encoding a second putative diacylglycerol ayltransferase from a microspore-derived cell suspension culture of *Brassica* napus L. cv Jet Neuf (Accession No. AF164434). (PGR99-153) *Plant Physiol.* 121:1057.

Oker-Blom, C., Airenne, K. J. and Grabherr, R. 2003. Baculovirus display strategies: emerging tools for eukaryotic libraries and gene delivery. *Brief Funct. Genomic. Proteomic.* 2:244-253.

Ohlrogge, J. and Browse, J. 1995. Lipid biosynthesis. *Plant Cell* 7:957-970.

Oppermann, U., Filling, C., Hult, M., Shafqat, N., Wu, X., Lindh, M., Shafqat, J., Nordling, E., Kallberg, Y., Persson, B. and Jörnvall, H. 2003. Short-chain dehydrogenases/reductases (SDR): the 2002 update. Chem. Biol. Interact. 143-144:247-253.

Orr, W., Keller, W. A. and Singh, J. 1986. Induction of freezing tolerance in an embryogenic cell suspension culture of *Brassica napus* by abscisic acid at room temperature. *J. Plant Physiol.* 126:23-32.

Owen, M. R. Corstorphine, C. C. and Zammit, V. A. 1997. Overt and latent activities of diacylglycerol acytransferase in rat liver microsomes: possible roles in very-low-density lipoprotein triacylglycerol secretion. *Biochem. J.* 323:17-21.

Pan, C. J., Lei, K. J., Annabi, B., Hemrika, W. and Chou, J. Y. 1998. Transmembrane topology of glucose-6-phosphate. *J. Biol. Chem.* 274:13865-13869.

Pelham, H. R. B. and Jackson, R. J. 1975. An efficient mRNA-dependent translation system from reticulocyte lysate. *Eur. J. Biochem.* 67:247-256.

Pirtle, I. L., Kongcharoensuntorn, W., Nampaisansuk, M., Knesek, J. E., Chapman, K. D. and Pirtle, R. M. 2001. Molecular cloning and functional expression of the gene for a cotton Δ-12 fatty acid desaturase (FAD2). *Biochim. Biophys. Acta* 1522:122-129.

Polokoff, M. A. and Bell, R. M. 1980. Solubilization, partial purification and characterization of rat liver microsomal diacylglycerol acyltransferase. *Biochim. Biophys. Acta* 618:129-142.

Post-Beittenmiller, D. 1996. Biochemistry and molecular biology of wax production in plants. *Annu. Rev. Plant Physiol. Mol. Biol.* 47:405-430.

Puyaubert, J., Garbay, B., Costaglioli, P., Dieryck, W., Roscoe, T. J., Renard, M., Cassagne, C. and Lessire, R. 2001. Acyl-CoA elongase expression during seed development in Brassica napus. *Biochim. Biophys. Acta* 1533:141-152.

Qiu, X., Janson, C. A., Konstantinidis, A. K., Nwagwu, S., Silverman, C., Smith, W. W.,

Khandekar, S., Lonsdale, J. and Abdel-Meguid, S. S. 1999. Crystal structure of β-ketoacyl-acyl carrier protein synthase III. A key condensing enzyme in bacterial fatty acid biosynthesis. *J. Biol. Chem.* 274:36465-36471.

Rafferty, J. B., Simon, J. W., Baldock, C., Artymiuk, P. J., Stuitje, A. R., Slabas, A. R. and Rice, D. W. 1995. Common themes in redox chemistry emerge from the X-ray structure of oilseed rape (*Brassica napus*) enoyl acyl carrier protein reductase. *Structure* 3:927-938.

Renfrew, C. A. and Hubbard, A. L. 1991. Degradation of Epidermal Growth Factor Receptor in Rat Liver: membrane topology through the lysosomal pathway. *J. Biol. Chem.* 266: 21265-21273.

Rodriguez, M. A., Dias, C. and Lau, T. E. 1992. Reversible ATP-dependent inactivation of adipose diacylglycerol acyltransferase. *Lipids* 27:577-581.

Rothman, R. E., Andrews, D. W., Calayag, M. C. and Lingappa, V. R. 1988. Construction of defined polytopic integral transmembrane proteins: the role of signal and stop transfer sequence permutations. *J. Biol. Chem.* 263:10470-10480.

Royant, A., Nollert, P., Edmani, K., Neutze, R., Landau, E. M., Pebay-Peyroula, E. and Navarro, J. 2001. X-ray structure of sensory rhodopsin II at 2.1-Å resolution. *Proc. Natl. Acad. Sci. USA* 98:10131–10136.

Ruch, F. E. and Vagelos, P. R. 1973. The isolation and general properties of *Escherichia coli* malonyl Coenzyme A-acyl carrier protein transacylase *J. Biol. Chem.* 248:8086-8094.

Rusinol, A. E., Jamil, H. and Vance, J. E. 1997. In vitro reconstitution of assembly of apolipoprotein B48-containing lipoproteins. *J. Biol. Chem.* 272:8019-8025.

Sambrook, J. and Russell, D. W. 2001. Expression of cloned genes in *Escherichia coli*. In: Molecular cloning, a laboratory manual, 3rd Ed. Cold Spring Harbor Laboratory Press. Cold Spring Harbour, New York.

Sato, M., Hresko, R. and Mueckler, M. 1998. Testing the charge difference hypothesis for the assembly of a eucaryotic multispanning membrane protein. *J. Biol. Chem.* 273:25203-25208.

Schägger, H. and von Jagow, G. 1987. Tricine-sodium dodecyl sulfate-polyacrylamide gel electrophoresis for the separation of proteins in the range from 1 to 100 kDa. *Anal. Biochem.* 166:368-379.

Shin, D.-H., Paulauskis, J. D., Moustaid, N. and Sul, H. S. 1991. Transcriptional regulation of p90 with sequence homology to *Escherichia coli* glycerol-3-phosphate acyltransferase. *J. Biol. Chem.* 266:23834-23839.

Simon, J. W. and Slabas, A. R. 1998. cDNA cloning of *Brassica napus* malonyl-CoA:ACP transacylase (MCAT)(fabD) and complementation of an *E. coli* MCAT mutant. *FEBS Lett.* 435:204-206.

Sipos, L. and von Heijne, G. 1993. Predicting the topology of eukaryotic membrane proteins. *Eur. J. Biochem.* 213:1333-1340.

Slabas, A. R., Kroon, J. T., Scheirer, T. P., Gilroy, J. S., Hayman, M., Rice, D. W., Turnbull, A. P., Rafferty, J. B., Fawcett, T. and Simon, W. J. 2002. Squash glycerol-3-phosphate (1)-acyltransferase. Alteration of substrate selectivity and identification of arginine and lysine residues important in catalytic activity. *J. Biol. Chem.* 277: 43918-43923.

Sonnhammer, E. L. L., von Heijne, G. and Krogh, A. 1998. A hidden Markov model for predicting transmembrane helices in protein sequences. In J Glasgow, T Littlejohn, F Major, R Lathrop, D Sankoff and C Sensen, eds. Proceedings of the Sixth International Conference on Intelligent Systems for Molecular Biology. Menlo Park, CA. AAAI Press. p. 175-182.

Spiess, M., Handschin, C. and Baker, K. P. 1989. Stop-transfer activity of hydrophobic sequences depends on the translation system. *J. Biol. Chem.* 264:19117-19124.

Stals, H. K., Mannaerts, G. P. and Declercq, P. E. 1992. Factors influencing triacylglycerol synthesis in permeabilized rat hepatocytes. *Biochem J.* 283:719-725.

Stals, H. K., Top, W. and Declercq, P. E. 1994. Regulation of triacylglycerol synthesis in permeabilized rat hepatocytes: role of fatty acid concentration and diacylglycerol acyltransferase. *FEBS Lett.* 343:99-102.

Stefansson, B. R., Hougen, F. W. and Downey, R. K. 1961. Note on the isolation of rape plants with seed oil free from erucic acid. *Can. J. Plant Sci.* 41:218-219.

Stobart, K., Mancha, M., Lenman, M., Dahlqvist, A. and Stymne, S. 1997. Triacylglycerols are synthesized and utilized by transacylation reactions in microsomal preparations of developing safflower (*Carthamus tinctorius* L.) seeds. *Planta* 203:58-66.

Stymne, S. and Stobart, A. K. 1987. Triacylglycerol Biosynthesis *In* PK Stumpf, ed, The Biochmistry of Plants, Vol 9. Academic Press, New York, pp. 175-214.

Thoden, J. B., Blanchard, C. Z., Holden, H. M. and Waldrop, G. L. 2000. Movement of the biotin carboxylase B-domain as a result of ATP binding. *J. Biol. Chem.* 275:16183-16190.

Thompson, L. K., McDermott, A. E., Raap, J. J., van der Wielen, C. M., Lugtenburg, J., Herzfeld, J. and Griffin, R. G. 1992 Rotational resonance NMR study of the active site structure in bacteriorhodopsin: conformation of the Schiff base linkage? *Biochemistry* 31:793 1-7938.

Towbin, H., Staehelin, T. and Gordon, J. 1979. Electrophoretic transfer of proteins from polyacrylamide gels to nitrocellulose sheets: procedure and some applications. *Proc. Natl. Acad. Sci. USA* 76:4350-4354.

Trombetta, E. S. and Helenius, A. 1998. Lectins as chaperones in glycoprotein folding. *Curr. Opin. Struct. Biol.* 8:587–592.

Turnbull, A. P., Rafferty, J. B., Sedelnikova, S. E., Slabas, A. R., Schierer, T. P., Kroon, J. T. M., Simon, J. W., Fawcett, T., Nishida, I., Murata, N. and Rice, D. W. 2001. Analysis of structure substrate specificity and mechanism of squash glycerol-3-phosphate (1)-acyltransferase. *Structure* 9:347-353.

Tusnády, G. E. and Simon, I. 1998. Principles governing amino acid composition of integral membrane proteins: applications to topology prediction. *J. Mol. Biol.* 283:489-506.

Tusnády, G. E. and Simon, I. 2001. The HMMTOP transmembrane topology prediction server. *Bioinformatics* 17:849-850.

Vancura, A. and Haldar, D. 1994. Purification and characterization of glycerophosphate acyltransferase from rat liver mitochondria. *J. Biol. Chem.* 269:27209-27215.

van der Leij, F., Kram, A. M., Bartelds, B., Roelofsen, H., Smid, G. B., Takens, J., Zammit, V. A. and Kuipers, J. R. G. 1999. Cytological evidence that the C-terminus of carnitine palmitoyltransferase I is on the cytosolic face of the mitochondrial outer membrane. *Biochem. J.* 341:777-784.

von Heijne, G. 1992. Membrane protein structure prediction, hydrophobicity analysis and the positive-inside rule. *J. Mol. Biol.* 225:487-494.

Walter, P. and Blobel, G. 1981a Translocation of proteins across the endoplasmic reticulum. II. Signal recognition protein (SRP) mediates the selective binding to microsomal membranes of *in vitro* assembled polysomes synthesizing secretory proteins. *J. Cell Biol.* 91:551-556.

Walter, P. and Blobel, G. 1981b Translocation of proteins across the endoplasmic reticulum. III. The signal recognition protein (SRP) causes signal sequence dependent and site-specific arrest of chain elongation that is released by microsomal membranes. *J. Cell Biol.* 91:557-561.

Walter, P. and Blobel, G. 1983. Preparation of microsomal membranes for cotranslational protein translocation. *Methods Enzymol.* 96:84-93.

Walter, P. and Lingappa, V. R 1986. Mechanism of protein translocation across the endoplasmic reticulum membrane. *Annu. Rev. Cell Biol.* 2:499-516.

Walter, P., Ibrahimi, I. and Blobel, G. 1981 Translocation of proteins across the endoplasmic reticulum. I. Signal recognition protein (SRP) binds to *in vitro* assembled polysomes synthesizing secretory proteins. *J. Cell Biol.* 91:545-550.

Waterman, I. J., Price, N. T. and Zammit, V. A. 2002. Distinct ontogenic patterns of overt and latent DGAT activities of rat liver microsomes. *J. Lipid Res.* 43:1555-15562.

Watts, A., Straus, S. K., Grage, S. L., Kamihira, M., Lam, Y. H. and Zhao, X. 2004. Membrane protein structure determination using solid-state NMR. *Methods Mol. Biol.* 278:403-473.

Weber, S., Wolter, F. P., Buck, F., Frentzen, M. and Heinz, E. 1991. Purification and cDNA sequencing of an oleate-selective acyl-ACP:sn-glycerol-3-phosphate acyltransferase from pea chloroplasts. *Plant Mol. Biol.* 17:1067-1076.

Weselake, R. J. 2002. Biochemistry and Biotechnology of Triacylglycerol Accumulation in Plants *In* TM Kuo, HW Gardner, eds, Lipid Biotechnology. Marcel Dekker, Inc., New York, p.27-56.

Weselake, R. J. 2005. Storage lipids. In: Plant Lipids - Biology, Utilization and Manipulation. eds. D.J. Murphy Blackwell Publishing, Sheffield, UK. p. 162-225.

Weselake, R. J. and Taylor, D. C. 1999. The study of storage lipid biosynthesis using microspore-derived cultures of oil seed rape. *Prog. Lipid Res.* 38:401-460.

Weselake, R. J., Madhavji, M., Foroud, N., Szarka, S., Patterson, N., Wiehler, W., Nykiforuk, C., Burton, T., Boora, P., Mosimann, S., Moloney, M. and Laroche, A. 2004. Probing the structure/function of diacylglycerol acyltransferase-1 from *Brassica napus*. *Proceedings of the 16th International Plant Lipid Symposium.* Budapest, Hungary., June 1-4, published online in November (www.mete.mtesz.hu/pls). p.38-41.

Weselake, R. J., Pomeroy, M. K., Furukawa, T. L., Golden, J. L., Little, D. B. and Laroche, A. 1993. Developmental profile of diacylglycerol acyltransferase in maturing seeds of oilseed rape and safflower and microspore-derived cultures of oilseed rape. *Plant Physiol.* 102:565-571.

Wessels, H. P. and Spiess, M. 1988. Insertion of a multispanning membrane protein occurs sequentially and requires only one signal sequence. *Cell* 55:61-70.

Wiedmann, M., Kurzchalia, T. V., Hartmann, E. and Rapoport, T. A. 1987. A signal sequence receptor in the endoplasmic reticulum membrane. *Nature* 328:830-833.

Yu, Y.-H., Zhang, Y., Oelkers, P., Sturley, S. L., Rader, D. J. and Ginsberg, H. N. 2002. Posttranscriptional control of the expression and function of diacylglycerol acyltransferase-1 in mouse adipocytes. *J. Biol. Chem.* 277:50876-50884.

Zhang, M., Hu, P. and Napoli, J. L. 2004. Elements in the N-terminal signaling sequence that determines cytosolic topology of short-chain dehydrogenases/reductases: studies with retinol dehydrogenase type 1 and *cis*-retinol/androgen dehydrogenase type 1. *J. Biol. Chem.* 279:51482-51489.

Zhang, F., Yang, M. and Xu, Y. 2004. Cloning and functional analysis of soybean diacylglycerol-O-acyltransferase gen by RNAi. (GenBank Accession No. AY652765).

Zheng, Z., Xia, Q., Dauk, M., Shen, W., Selvaraj, G. and Zou, J. 2003. Arabidopsis AtGPAT1, a member of the membrane-bound glycerol-3-phosphate acyltransferase gene family, is essential for tapetum differentiation and male fertility. *Plant Cell.* 15:1872-1887.

Zock, P. L. 2001. Dietary fats and cancer. *Curr. Opin. Lipid.* 12:5-10.

Zou, J., Katavic, V., Giblin, E. M., Barton, D. L., MacKenzie, S. L., Keller, W. A., Hu, X. and Taylor, D. C. 1997. Modification of seed oil content and acyl composition in the brassicaceae by expression of a yeast *sn*-2 acyltransferase gene. *Plant Cell* 9:909-923.